

Autonomous Agent-Based Modelling of Resistance Frequencies in Pathogenic Bacteria

James T. Murphy

B.Sc. in Cell & Molecular Biology, M.Sc. in Bioinformatics

A thesis submitted in fulfilment of the
requirements for the award of
Doctor of Philosophy (Ph.D.)

to the



Dublin City University

Faculty of Engineering and Computing

School of Computing

Supervisors: Ray Walshe and Marc Devocelle

September, 2008

Declaration

I hereby certify that this material, which I now submit for assessment on the programme of study leading to the award of Doctor of Philosophy is entirely my own work, that I have exercised reasonable care to ensure that the work is original, and does not to the best of my knowledge breach any law of copyright, and has not been taken from the work of others save and to the extent that such work has been cited and acknowledged within the text of my work.

Signed: _____

(James T. Murphy)

Student ID:

98534564

Date:

22nd September 2008

CONTENTS

Abstract	7
Acknowledgements	9
List of Tables	10
Glossary	14
1 Introduction	15
1.1 Motivation	15
1.2 Objectives	17
1.3 Outline of Thesis	18
2 Literature Review	20
2.1 Computational Modelling of Bacteria	20
2.1.1 Mathematical Approaches	21
2.1.2 Petri Nets	22
2.1.3 Cellular Automata	23
2.1.4 Agent-Based Approach	24
2.2 Examples of Agent-Based Models of Bacteria	26
2.2.1 BacSim Model	26
2.2.2 INDISIM Model	27

2.2.3	Other Agent-Based Bacterial Models	28
2.2.4	BAIT & Micro-Gen Bacterial Simulator	30
2.3	Methicillin-Resistant <i>Staphylococcus aureus</i>	32
2.3.1	Overview	32
2.3.2	Antibiotic Resistance Mechanisms	33
2.3.3	Pharmacokinetics and Pharmacodynamics	37
3	Model Description	40
3.1	Overview	40
3.1.1	Environment	40
3.2	Principal Model Entities	43
3.2.1	Bacterial Agents	43
3.2.1.1	Growth Parameters	44
3.2.1.2	Antibiotic Resistance Mechanisms	46
3.2.1.3	Movement and Chemotaxis	48
3.2.1.4	Overcrowding Algorithm	48
3.2.2	Antibiotics	51
3.2.3	β -lactamase Enzymes	55
3.2.4	Pro-Drugs	57
3.3	Program Structure	58
3.3.1	Program Flow Structure	58
3.3.2	Graphical Output	61
3.3.3	Parallelisation	62
3.3.3.1	Parallel Performance	67
4	Population Dynamics	69
4.1	Overview	69

4.2	System Dynamics	69
4.2.1	Standard Bacterial Growth Curve	70
4.2.2	Antibiotic Intake Rate	73
4.2.3	Antibiotic Half-Life	74
4.2.4	Diffusion Rate	75
4.2.5	Population Size (Inoculum Effect)	79
4.2.6	β -lactamase Production Rate	81
4.3	Conclusions	82
5	Kinetic Studies	86
5.1	Overview	86
5.2	Minimum Inhibitory Concentration	87
5.2.1	Overview	87
5.2.2	Predicted MICs	89
5.2.3	Discussion	93
5.3	Kinetic Parameters	96
5.3.1	Catalytic Efficiency of β -lactamase	100
5.3.2	PBP2a Interactions	101
5.3.3	Discussion	102
5.4	Conclusions and Future Work	103
6	Pro-Drug Delivery System	111
6.1	Overview	111
6.2	System Dynamics of Pro-Drug Delivery System	112
6.2.1	Kinetics Studies	115
6.2.2	Half-Life	118
6.2.3	Diffusion Rate	119

6.2.4	<i>β</i> -lactamase Production Rate	122
6.3	Case Study: NB2001 & NB2030	125
6.3.1	MIC Test Results	128
6.3.2	Sensitivity Analyses	130
6.4	Conclusions	134
7	Conclusions and Future Work	137
7.1	Summary and Conclusions	137
7.2	Future Work	139
	Bibliography	142

Abstract

In recent years there has been a rapid growth in the understanding of the basic cellular processes of individual bacterial cells through advances in molecular biological research. However, this has introduced a demand to understand how the interactions between the individual system components contribute to the overall population dynamics. A useful theoretical approach for relating information at the individual cellular/molecular level with emergent population characteristics is the agent-based (or individual-based) modelling approach. The agent-based modelling approach involves assigning pre-defined rules and parameters to each individual component (e.g. the bacterial cell) of the population. Therefore, the emergent behaviour of the population as a whole can be examined without the need for population-level laws.

An agent-based model of bacterial population growth, called the Micro-Gen Bacterial Simulator, has been developed to provide a theoretical framework for investigating the interactions between antibiotics and bacterial cells in culture. Parameters are inputted at the cellular level in order to replicate the life cycle of bacteria grown in batch culture. The individual bacteria of a colony are represented by software agents, which store the physical traits such as energy state or antibiotic damage and the behavioural rules of the bacteria. The interactions of antibiotic molecules with the bacterial cells and extra-cellular enzymes (e.g. β -lactamases) are governed by defined kinetic rules derived from the biological literature.

The Minimum Inhibitory Concentration (MIC) was calculated from the model for a number of common antibiotics, against methicillin-resistant *S. aureus* (MRSA), and compared with real-world results. The predicted values from these initial tests matched closely those recorded from *in vitro* experimental studies of MRSA in the literature. The model was also used to examine the system dynamics of the enzyme-catalysed therapeutic activation (ECTA) pro-drug delivery system, a novel approach for achieving β -lactamase-mediated selective release of antimicrobial agents. It is thought that this strategy might be a promising approach for treating β -lactamase over-expressing strains of bacteria that are resistant to traditional β -lactam antibiotics. The model provides a suitable theoretical framework for comparing and contrasting different drug treatment strategies from a system's perspective in order to assess their potential efficacy.

Acknowledgements

Firstly, I would like to thank my family for supporting me during the process of completing this work and throughout my education.

I would also like to thank my supervisors Ray Walshe and Marc Devocelle for their invaluable guidance and help throughout the PhD. I'd also like to acknowledge the help and support I received from Heather Ruskin and Martin Crane as well as my fellow members in the Modelling and Scientific Computing Group in DCU.

I would like to acknowledge the contribution of Mathieu Joubert, Gráinne Kerr, Chris Pender, Marian Duggan, and Ronan Winters for developing the original BAIT software tool on which the Micro-Gen project was based.

I would like to take this opportunity to thank all those I met at the University of Southern Mississippi during my research visit there in 2008. In particular, I'd like to thank Ras B. Pandey for hosting me in his lab at the Department of Physics and Astronomy. I'd also like to thank Ray Seyfarth, author of the 3D visualization software Animp which I used in my work.

Before finishing, I'd like to acknowledge all those public figures in science who I've never met but inspired me to enter the world of scientific research (particular mention goes to the naturalists David Attenborough and Steve Irwin).

Finally, I'd like to thank my undergraduate course director Martin Steer (Professor of Botany, University College Dublin) for supporting and encouraging me to pursue a scientific career.

LIST OF TABLES

3.1	Input Parameters for Bacterial Agents in Micro-Gen model. Sample values for <i>S. aureus</i> species included. b.u. = biomass units	44
3.2	Kinetic Parameters of β -lactam Antibiotics versus Type A and Type C β -lactamase-producing MRSA. Pen G = Penicillin G; Amp = Ampicillin; Ceph = Cephalothin.	57
3.3	Parallel Efficiency of Micro-Gen When Run on a 16 Node (Intel Xeon 2.8 GHz) Computing Cluster	67
5.1	Results from comparison of predicted versus experimentally determined MICs of penicillin G, ampicillin and cephalothin antibiotics (Ab) against three different types of MRSA. Geometric mean MIC \pm SEM ($\mu\text{g/ml}$) given. Experimentally determined MICs are from Norris <i>et al.</i> (1994) and Malouin <i>et al.</i> (2003) [1, 2].	91
5.2	Results from comparison of predicted MICs and experimentally determined MICs for eleven common β -lactam antibiotics versus β -lactamase-negative MRSA bacteria. The minimum and maximum MIC values found in a review of a subset of the experimental literature are recorded [1, 2, 3, 4, 5, 6, 7, 8].	94
5.3	Inputted parameter values for simulations of antibiotic interactions with MRSA bacteria in Micro-Gen model. <i>b.u.</i> = biomass units; <i>loop</i> = program loop (~ 2 s in real time)	107

5.4	Inputted kinetic parameter values (k_2 , K_d), molecular weight (M_R) and half-life parameters for simulations of antibiotic interactions with penicillin-binding protein 2a (PBP2a) in MRSA bacteria [1 - 8]. For diagrams of the chemical structures of these antibiotics see figures 5.10 & 5.11	108
6.1	Comparison of predicted MICs (with and without contamination with free triclosan) from Micro-Gen model and experimentally determined MICs for the pro-drugs NB2001 and NB2030, as well as triclosan and cephalothin, versus Type A β -lactamase-producing MRSA bacteria. Percentage contamination with free triclosan: NB2001 = 4 %, NB2030 = 1 %.	128
6.2	Inputted parameter values for simulations of pro-drug interactions with β -lactamase-producing <i>S. aureus</i> bacteria in Micro-Gen model. <i>b.u.</i> = biomass units; <i>loop</i> = program loop (~ 2 s in real time)	136

GLOSSARY

β -lactam Antibiotics

Common class of antibiotics, characterised by the presence of a β -lactam ring structure which facilitates binding to the penicillin-binding proteins in cell membrane of bacteria and disrupting cell wall synthesis. Examples include penicillin G, ampicillin and cephalothin, 15

β -lactamase

Enzyme produced by bacterial cells which degrades β -lactam antibiotic molecules by cleaving their β -lactam ring structure., 31

Staphylococcus aureus

Non-motile species of bacteria that generally exist as part of the normal flora found on nasal passages, skin and mucous membranes in humans. Have the potential to cause a variety of infections from superficial skin lesions such as boils, to more serious conditions such as pneumonia, 15

Agent-Based Model	Computational modelling approach which simulates the actions and interactions of autonomous individuals/agents. Rules and parameters are defined at the individual-level rather than for the population as a whole., 17
Antibiotic Resistance	Refers to the ability of a microorganism to resist the effects of an antibiotic. Examples of mechanisms of antibiotic resistance include the synthesis of antibiotic-degrading enzymes (e.g. β -lactamase), and modifications to drug targets such as the penicillin-binding proteins (PBPs) in bacterial cell membranes, 33
BAIT	Bacteria-Antibiotic Interaction Tool - precursor to Micro-Gen, which implemented a simple model of bacterial growth and interactions with antibiotic molecules in discrete, 2D environment, 30
Chemotaxis	The movement/orientation of a cell/organism either towards (positive) or away from (negative) a chemical stimulus, along a chemical concentration gradient, 48

MIC	Minimum Inhibitory Concentration is the minimum concentration of an antibiotic that results in inhibition of bacterial growth <i>in vitro</i> for a specified period of time, 38
Micro-Gen Bacterial Simulator	Agent-based model of bacteria-antibiotic interactions <i>in vitro</i> . Uses basic cellular and kinetic parameters to explore the emergent population dynamics of antibiotic resistance, 7
Model	A mathematical or computational model is a purposeful representation of an entity or system whose purpose is to capture the essence of a problem and explore different solutions of it, 20
MRSA	Methicillin-Resistant <i>S. aureus</i> - multi-drug resistant form of <i>S. aureus</i> which was first isolated in 1961. Resistance conferred by expression of penicillin-binding protein 2a which has reduced binding to β -lactam antibiotics, 32
Pro-drug	A drug that is administered in a pharmacologically inactive (or significantly less active) form and is then metabolised <i>in vivo</i> into an active metabolite., 111

CHAPTER 1

INTRODUCTION

1.1 Motivation

The emergence of multi-drug resistance in *Staphylococcus aureus* bacteria has become a major healthcare problem in recent years. Prior to the introduction of antibiotics, patients with *S. aureus* bacteraemia had a mortality rate of over 80% [9]. This situation improved dramatically when the first β -lactam antibiotic, penicillin, was introduced into clinical use during the early 1940s [10]. However, today greater than 95% of all *S. aureus* isolates possess resistance to penicillin, and 40-60% of clinical isolates in the United States of America and the United Kingdom express methicillin resistance (MRSA) [11, 12].

There has been a rapid increase in information about the basic cellular processes that lead to antibiotic resistance due to advances in cell and molecular biology. This development has allowed a finer-grained approach to investigating the spread of resistance in populations of bacteria. However, the overall population response to antibiotic treatment is often a function of a diverse range of interacting components. In order to develop strategies to minimize the spread of antibiotic resistance, a sound theoretical understanding of the systems of interactions taking place must

be developed. For example, there has been a rapid development in the field of pharmacokinetic/pharmacodynamic studies in the last few decades that has led to a better understanding of the complex dynamics that contribute to the bacterial response to drug treatment [13]

There are a number of different approaches that have been taken to analyse how populations of bacteria grow and interact. The most common approach is to develop mathematical, or state variable, models that describe the population as a whole. This can give important insights into parameters at the population-level that influence the development of the colony [14]. These approaches are appropriate for developing an integrated view of colony development and benefit from the fact that they are often less parameter-rich than other approaches. However, the use of global parameters requires the implicit assumption that the population is in a homogeneous, mixed environment. However, in nature, bacteria often form highly heterogeneous colonies where there can be significant localised variations in the chemical environment such as ion concentrations, pH, temperature and nutrient availability [15].

The approach taken here is to implement an agent-based (or individual-based) model where the individual bacterial cells represent the fundamental units of the simulation. This bottom-up approach means that parameters are defined for the bacterial cells rather than for the population as a whole. The properties of a colony thus emerge from the set of interactions of a population of heterogeneous bacterial agents. Therefore, the inherent heterogeneity that exists in a bacterial colony is explicitly modelled. Some of the drawbacks of this approach include the fact that it can sometimes require more parameters than a state variable approach since the individual entities are explicitly modelled and it also may become too open to empirical knowledge [13]. However, by using appropriate aggregation of parame-

ters in order to simplify the model, and cognisant of its limitations, the agent-based approach can be used as a powerful tool for tracing back system behaviour to that of its individual components.

A model has been developed called Micro-Gen that implements the agent-based approach to simulate the life cycle of bacteria grown in culture and their interactions with antibiotic molecules [16, 17, 18]. This model can be adapted to represent different species and strains of bacteria using basic cellular information. For this study, simulations were carried out using parameters applicable to MRSA. Micro-Gen has been designed to incorporate the two main antibiotic resistance strategies characteristic of MRSA. It is possible to produce a quantitative model of the interactions between antibiotics and MRSA bacteria because the kinetic rules for these reactions have been well characterized experimentally [19, 20]. The ability to simulate the individual molecular interactions of antibiotic molecules and bacteria, and scale this up to large population sizes using the agent-based approach, is a powerful tool for exploring the emergent dynamics that contribute to antibiotic resistance in bacterial populations.

1.2 Objectives

The objective of the research is to develop an agent-based model of MRSA that incorporates the main antibiotic resistance mechanisms found used by these pathogenic bacteria. The model will be used to study the effects of changes at the molecular level on the overall efficacy of existing antibiotics.

Our key objectives for attaining this goal were as follows:

1. Develop a robust, adaptable model of bacterial cellular growth in culture which replicates the standard life cycle of bacteria. Validate the model for

the clinically important gram-positive bacterial species *S. aureus*.

2. Expand the model to include a detailed representation of the interactions between antibiotics and MRSA that incorporates the principal kinetic rules governing these interactions.
3. Use the model to examine the relationship between low-level cellular/biochemical properties of individual bacteria/antibiotics and high-level treatment response at the population level. Assess the impact of the different kinetic parameters on antibiotic treatment outcome.
4. Explore potential, novel drug delivery systems such as the pro-drug technology and predict their efficacy using theoretical studies.

1.3 Outline of Thesis

The second chapter of the thesis gives an overview of existing approaches taken to model bacterial growth and development, and compares the agent-based approach to more traditional population-based mathematical models. Following this, a more detailed overview of MRSA will be given and the antibiotic resistance strategies that have been identified in it. The next chapter contains a detailed description of the agent-based model Micro-Gen, which was developed to simulate the interactions of anti-microbial drugs with bacteria in culture.

In chapters four and five, a detailed analysis of the system dynamics involved in the interactions between anti-microbial drugs and MRSA is carried out. The effects of key cellular parameters associated with antibiotic-resistance mechanisms on treatment outcome are also explored. The cellular and molecular parameters for this model were derived from the biological literature for three different strains of

MRSA, and the model was used to predict the Minimum Inhibitory Concentration (MIC, which is a key clinical measure of antibiotic efficacy) of each antibiotic versus the three strains. When the predicted MICs from the model were compared with experimentally derived MICs for MRSA, they were found to be in close quantitative agreement.

Chapter six details simulations to explore a novel drug delivery system called the enzyme-catalysed therapeutic activation (ECTA) pro-drug delivery system and illustrate the value of Micro-Gen in supporting drug discovery efforts. The final sections of the thesis include the conclusions from the present research along with future directions that may be taken, followed by a bibliography of relevant papers in the field. Full copies of publications that have arisen out of the current research are attached at the end of the thesis.

CHAPTER 2

LITERATURE REVIEW

2.1 Computational Modelling of Bacteria

Computational systems biology is a swiftly developing field in biological simulation that attempts to model complex biological processes as integrated systems of interacting components, using data from genomic, proteomic, metabolomic and cellular studies [21]. This often involves collecting large datasets of experimental data to develop predictive computational models which are then assessed and compared with newly derived experimental data in order to further improve the model and give insights into the biological processes being observed.

The power of the computational modelling approaches is not so much in their ability to make predictions (some degree of experimental validation will always be needed to confirm any predictions) but in their ability to give new insights into the underlying mechanistic basis for the observed biological phenomena. A computational model may be defined as a ‘purposeful representation’ of an entity or system whose “purpose is to capture the essence of a problem and explore different solutions of it” [22]. The most important role of a model is therefore to aid in our understanding of a particular process. From this perspective, all the different

modelling approaches share the same principal aim, though they may differ in the assumptions and tools that are used.

There have been many different modelling approaches developed in computational systems biology that encompass many different temporal and spatial scales. Complex biological processes can range from microscopic sub-cellular processes such as cell metabolic pathways to large-scale ecological questions involving the development of populations of organisms over long periods of time. For this reason, many different modelling approaches, with differing granularity in their temporal/spatial scales, have been developed to approach these problems. However, many of them are adaptations of particular modelling strategies that use common techniques such as ordinary differential equations or agent-based modelling techniques to address their specific modelling questions.

2.1.1 Mathematical Approaches

A number of the most common simulation techniques used include mathematical approaches such as ordinary differential equations (ODEs) and partial differential equations (PDEs). ODE models are probably the most common modelling approach used in systems biology since they are computationally efficient and mathematically robust, and can be used to develop an integrated view of biological systems. Basic ordinary differential equation methods are limited in their ability to model situations such as discontinuous state-changes, stochasticity, diffusion, compartmentalization and cell migration [23]. However, in order to address some of these limitations extensions to the basic ODE methods have been developed such as stochastic ODEs and compartmentalised ODE models. Basic ODEs are limited to temporal modelling, but partial differential equations (PDEs) can be used to

model processes that have spatial as well temporal dependencies.

Mathematical population models are commonly used to describe the growth and development of a bacterial colony as a unit, using global parameters or state variables [24, 14]. These “top-down” approaches have the advantage that they are computationally efficient and less parameter-rich than more low-level approaches. However, an important limitation of the state variable approach is that it does not allow the user to trace back the system behaviour to the behaviour of the individual agents. For example, this approach cannot explain the underlying factors that lead to the population exhibiting a particular growth rate or carrying capacity [22]. However, they are important to provide an appropriate integrated view of the population behaviour.

2.1.2 Petri Nets

Other techniques used in computational systems biology include Petri nets, cellular automata, and finally, the approach used in this project, the agent-based approach. Petri nets are an alternative approach to modelling time-dependent processes [23]. Petri nets consist of two types of node: a ‘place’ which can be used to represent, for example, a particular species of molecule, and a ‘transition’ node, which might represent reactions (Fig. 2.1). Petri nets are a discrete system which is driven by implicit time increments where a transition ‘fires’ when the markings (or tokens) at all of its ‘input’ places exceed the ‘weights’ on its input arcs, producing product on its output arcs. This correlates with a reaction occurring when there are enough reactant molecules, resulting in the generation of reaction products.

The Petri nets approach has been expanded to address more complex modelling questions involving either discrete or continuous values (Hybrid Petri nets

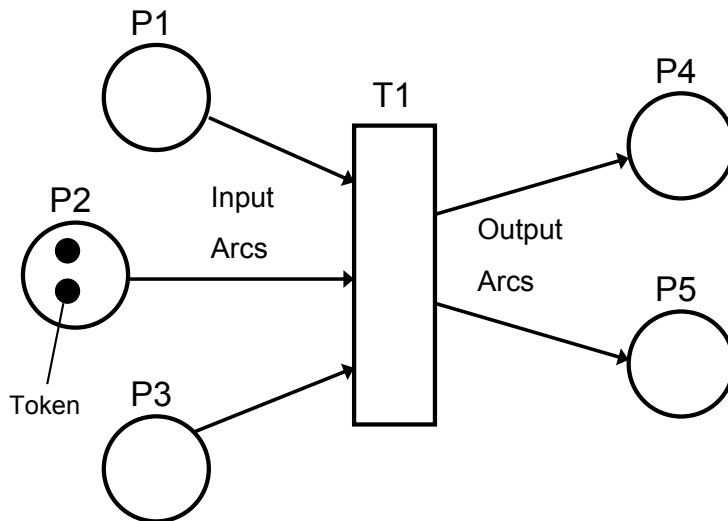


Figure 2.1: An example of a simple Petri net, consisting of input places (P1-P3), output places (P4-P5), transition (T1), and arcs (input and output). Places can contain tokens, and when there are enough tokens in the input places the transition ‘fires’, removing tokens from its input places and adding them to the output places.

and Functional Hybrid Petri nets). Coloured Petri nets have also been developed that allow mathematical relationships to be incorporated in transitions to govern the rate of firing. Petri nets can also be used to build compartmental models by having different ‘places’ to represent the same chemical species in different compartments. For this reason, the Petri nets formalism represents a powerful tool for qualitative and quantitative modelling of many biological processes [25]. However, this approach is not as amenable to modelling spatially dependent processes such as diffusion, growth or cell chemotaxis.

2.1.3 Cellular Automata

The Cellular Automata (CA) approach to modelling biological systems is a powerful tool for modelling both temporal and spatiotemporal processes. In CA models the environment of the models is represented by a discrete lattice/grid where the

states of the components evolve synchronously in discrete time steps according to a set of rules [23]. The CA simulation Conways Game of Life was one of the first computer applications in biology [26]. This model consisted of randomly placed cells on a square lattice and simulated birth, death and interactions according to pairwise interaction rules which used Boolean logic conditions.

In basic CA models, the objects of the model do not strictly move, but rather their properties or attributes are updated each time step, allowing movement to be represented indirectly. A variation on this technique is the dynamic cellular automata (DCA) approach, which allows for the explicit modelling of movement and is conceptually similar to the agent-based modelling approach [27]. Cellular automata approaches are particularly amenable to modelling stochastic spatial and temporal processes such as transport processes, cell migration, diffusion or viral infection. They can also be useful for visualising processes such as chemotaxis, drug diffusion or pattern formation.

The robustness and adaptability of the cellular automata modelling approach has made it amenable to simulating a wide range of biological process, from enzyme-kinetics and hydrodynamics studies to the progression of HIV/AIDS [28, 29]. Cellular automata theory has also been used successfully to explain pattern formation in bacterial colonies [30].

2.1.4 Agent-Based Approach

An alternative approach to modelling bacterial growth and development is the agent-based (or individual-based) modelling approach [31, 32]. The distinguishing characteristic of the agent-based approach is that the properties of the individual cells, rather than the colony as a whole, are modelled. This “bottom-up” approach

allows a finer-grained analysis, connecting local changes at the cellular level to the overall patterns of population growth. The agent-based approach shares some of the strengths of the cellular automata modelling approach, in that it is able to explicitly model both temporal and spatiotemporal processes. For this reason, it is particularly amenable to modelling processes such as chemotaxis, diffusion and pattern formation in bacterial colonies. However, it represents an even finer grained approach in that the individual biological entities being modelled are explicitly represented by unique software objects.

It must be noted that the agent-based approach and higher-level mathematical approaches are not mutually exclusive but rather complement each other in studies of population dynamics. The latter approach allows a general conceptual framework to be developed for a population which can lead to theories at the systems level. The agent-based approach meanwhile allows important features of the individuals to be taken into account and related to the overall system's properties. The agent-based approach can suffer from being more computationally intensive and dependent on empirical data than high-level mathematical approaches such as ODEs because each individual of a population is explicitly modelled. However, in cases where the population being modelled expresses a high degree of heterogeneity, both spatially and between individuals, the agent-based approach represents a powerful tool for exploring how this heterogeneity contributes to the system dynamics.

The next section contains an overview of existing agent-based models that have been used to explore bacterial population development. Following this, the Micro-Gen Bacterial Simulator which was developed over the course of this Ph.D project is introduced.

2.2 Examples of Agent-Based Models of Bacteria

2.2.1 BacSim Model

One of the most significant examples of an agent-based (or individual-based) modelling approach to modelling microbial colonies is the ‘BacSim’ simulator [32]. It is an individual-based model that uses the known physiology of individual cells to produce a quantitative model of microbial colony development. When it was introduced, it differed from previous models of microbial colony growth which depended on mathematical and cellular automaton approaches to address this problem [33, 24, 30].

BacSim had an advantage over the previous approaches in that it explicitly allowed for spatial differences in the environment and between the individual bacterial cells. It demonstrated the power of this modelling technique for exploring the heterogeneous population dynamics occurring within a microbial colony. For example, it was used to explore the effects of growth asynchrony and random variation of cell parameters on population development [32].

BacSim was further developed into a two-dimensional multi-substrate, multi-species model of microbial biofilms [34]. Biofilms are multi-species communities of surface-attached micro-organisms characterised by their genetic diversity, structural heterogeneity and complex cellular interactions. Although the model allowed a continuous 3D space for bacterial movement, the extra dimension for bacterial movement was restricted to about two cell diameters and the substrate diffusion-reaction was restricted to 2D space, so therefore it was described as essentially a 2D model.

The model was compared to an established biomass-based model (BbM) of biofilm growth where the spreading of biomass was dictated by cellular automata

rules [35]. Biomass-based models are spatially structured population models where the interactions of the biomass units lead to the emergent development of the community. The comparison between the individual-based and biomass-based approaches showed qualitative agreement in terms of the overall growth of the simulated biofilms. However, it must be noted that the study did not take into account the different phenotypic characteristics of cells in biofilms or the complex three-dimensional structure of biofilms.

BacSim has continued to be developed since then and used to address questions such as the migration of *Salmonella enteridis* in hen's eggs, and the population dynamics during the lag phase of bacterial growth [36, 37, 38]. It was used as a basis for studying cell division at the individual-level in order to understand better the mechanistic principles underlying the lag phase. These different applications of the agent-based modelling paradigm illustrate the power of this approach for investigating many factors of microbial population development and connecting them with information obtained at the cellular level.

2.2.2 INDISIM Model

Another important model developed to investigate microbial population dynamics using an agent-based approach is INDISIM, which stands for Individual Discrete Simulations [31]. INDISIM differs from BacSim in that whereas the latter treated bacterial cells in continuous space (with discrete time) INDISIM is discrete in both space and time. However, they both share in common the fact that they represent bacterial colonies with respect to their individual cells allowing for spatial heterogeneity in the environment and individual variability between the different cells. INDISIM has been used to study biomass distributions, growth rates and metabolic

oscillations in simulated batch culture bacterial colonies [31].

The environment of INDISIM is represented as a discrete grid with each lattice point containing variables storing the concentrations of different types of particles, for example nutrients, reaction products or residual products. The diffusion of particles through the environment is calculated using a discretized implementation of Fick's First Law of diffusion. Like BacSim, individual rules are applied to the bacterial cells for motion, uptake, metabolism, reproduction and viability.

Simulations with INIDISIM have shown that it can be used to reproduce qualitatively the growth patterns of *Bacillus subtilis* bacteria on an agar plate [39]. It was also used in studies of the lag phase, where it was demonstrated that the evolution of the mean mass and biomass distribution of a colony was a determining factor for entering the exponential phase of bacterial growth and the rate of enzyme synthesis also had a direct effect on lag duration [40, 41].

Finally, an extended version of INDISIM, INDISIM-SOM has been applied in studies of the dynamics of soil organic matter (SOM) and the evolution of carbon and nitrogen sources in the soil and their effect on microbial growth [42]. The agent-based approach is particularly suitable for modelling an environment such as soil since it is a heterogeneous, discontinuous environment with discrete microhabitats where the chemical and biological properties vary greatly over small distances.

2.2.3 Other Agent-Based Bacterial Models

A number of different agent-based simulators were developed in the lab of R. Paton to approach the problem of modelling bacterial cells. These were built on previous work using the agent-based approach to model ecological systems involving learning herbivore animals in a world populated by plants [43]. The COSMIC system

was an agent-based model of evolution in bacterial cells involving four levels of interaction in the system (Environment - Individual Cells - Gene Products - Genes) [44, 45]. The BacSim model, described above, was used for representing cell growth and division. COSMIC introduced an extra level of complexity by incorporating a genetic component into the bacterial cells, and a parallel implementation was created to take advantage of parallel computing resources.

COSMIC incorporated a gene transcription network that outputted a ‘flagella activation protein’ which was a generic gene product responsible for bacterial movement. This gene product triggered motility and chemotaxis towards areas of higher nutrient concentration, creating a positive feedback loop for the gene transcription network. The goal of COSMIC was to evolve a genome that maximised cell growth as a result of this feedback loop. Although COSMIC represented a somewhat limited implementation of a genetic component, it demonstrated the strength of the agent-based modelling approach for investigating questions such as the evolution of bacterial agents over time to produce different phenotypes that affect cell survival.

A simpler model of bacterial growth, which did not include a gene component, was also developed in the same laboratory, called RUBAM [44]. The bacterial agents incorporated a Learning Classifier System (LCS) based on fuzzy logic for implementing chemotaxis. The LCS was the decision making component of a feedback loop that included the environment, sensors to detect the environment and directed swimming of the bacterial cell. This resulted in the evolution of survival strategies from an initial pool of bacterial agents initialized with random rules. With this approach it took a long time to find good solutions, but the bacteria would eventually evolve to a point where they could adapt to prevailing conditions and respond to environmental stimuli.

The most recent project from the lab of R. Paton, COSMIC-Rules, attempts to combine the experiences from COSMIC and RUBAM to develop an agent-based model consisting of three levels: the genome, bacterial cell, and environment [43]. Each individual bacterium has a unique location, size, state of cell division and genome. The model expands on the genetic component of the original COSMIC model to incorporate representations of plasmids and bacteriophages which add to the complexity of the population dynamics. This means that horizontal transfer of genetic information within a population can occur as well as vertical transmission between generations.

The agent-based modelling approach has also been applied to understand the mechanisms that affect microcolony and biofilm formation in bacteria by L.R. Johnson in the University of California [46]. A model was developed there to infer how the patterns observed in the early stages of biofilm formation are affected by the behaviour of the individual bacterial cells. The formation of groups was modelled as a function of the doubling rates, stopping rates and the strength of the interactions between the cells. This could be used to make predictions about how the inter-cellular interactions affect the mean colony size and maximum colony size for example.

2.2.4 BAIT & Micro-Gen Bacterial Simulator

The ‘Micro-Gen Bacterial Simulator’ was developed to model the growth and interactions of bacterial cells with antibiotics *in vitro* using the agent-based approach [17, 18]. It was built on existing work in the laboratory to develop an agent-based model of bacterial growth in culture called the Bacteria-Antibiotic Interaction Tool (BAIT) [16]. BAIT incorporated a simple model of bacterial growth and interactions with antibiotic molecules in a discrete two-dimensional grid environment

using the Java programming language. Mathieu Joubert, as part of an internship project in the laboratory, developed a C++ version of BAIT which formed the basis for the Micro-Gen project. Micro-Gen represents a significant expansion and re-design of the original BAIT tool, in order to build a more realistic representation of bacterial growth and development in culture and their kinetic interactions with antibiotics.

The theory of autonomous agents is a useful approach for the modelling of bacterial cell colonies as it allows large-scale population models to be derived from simple rules dictating the growth and interactions of the individual bacterial cells of the population. The Micro-Gen Bacterial Simulator uses information about the cell biology of bacteria to produce global information about population growth in different environmental conditions.

An agent-based approach was chosen over a simpler mass action model in order to explicitly model the heterogeneity in environmental conditions, for example between the interior and exterior of the colony, and between individual bacterial cells. In complex microbial communities, such as biofilms, there can be highly heterogeneous localised niches where the chemistry varies dramatically over small distances.

A key component of the model is the ability to quantitatively model antibiotic molecules and their interactions with the bacterial cells. These interactions are governed by defined kinetic parameters specific to the type of antibiotic and bacterial strain being modelled. This allows a quantitative model of antibiotic interactions with bacteria to be built up and their pharmacokinetic properties to be investigated.

The model also incorporates two important antibiotic resistance mechanisms employed by bacterial cells against antimicrobial agents which form the cornerstone of the antibiotic arsenal: special enzymes released by bacteria, called β -lactamases,

which degrade the antibiotic molecules, and reduced binding affinities between the antibiotics and receptors in the bacterial cells. These antibiotic resistance mechanisms are of great clinical concern as their development and spread across many species of bacteria has led to the erosion of the efficacy of many commonly prescribed antibiotics, in particular penicillin and its derivatives. Moreover, the production of these β -lactamases persists in multidrug resistant strains, which can be resistant to more than ten different antibiotics.

2.3 Methicillin-Resistant *Staphylococcus aureus*

2.3.1 Overview

The emergence of multi-drug resistance in *Staphylococcus aureus* bacteria has become a major healthcare problem in recent years. Prior to the introduction of antibiotics, patients with *S. aureus* bacteraemia had a mortality rate of over 80% [9]. This situation improved dramatically when the first β -lactam antibiotic, penicillin, was introduced into clinical use during the early 1940s [10]. However, the widespread therapeutic use of penicillin resulted in selection for strains of *S. aureus* carrying antibiotic resistance mechanisms [47]. By 1950, penicillin resistance was recorded in over 50% of all staphylococcal isolates [48]. Today greater than 95% of all *S. aureus* isolates possess resistance to penicillin, and 40-60% of clinical isolates in the United States of America and the United Kingdom express methicillin resistance [11, 12].

Members of the *Staphylococcus aureus* species are gram-positive bacteria with spherical-shaped cells (cocci) approximately 0.5 - 1 μm in diameter [49]. They divide in three planes, with a generation time of approximately 30 minutes, result-

ing in three-dimensional, cuboidal packets of cells [49]. They are non-motile and generally exist as part of the normal flora found on nasal passages, skin and mucous membranes in humans. However, *S. aureus* strains have the potential to cause a variety of infections from superficial skin lesions such as boils, to more serious conditions such as pneumonia. *S. aureus* is also a major cause of nosocomial (hospital-acquired) and community-acquired infections [50, 51].

2.3.2 Antibiotic Resistance Mechanisms

Antibiotic resistance refers to the ability of a microorganism to resist the effects of an antibiotic. The development and spread of antibiotic resistance in pathogenic bacteria is affected by a complex range of interacting factors. The appearance of resistant strains of bacteria is thought to be an ancient evolutionary event, however the fitness cost associated with resistance mechanisms previously limited their proliferation [52]. In recent years, the widespread use of antibiotics has resulted in a significant positive selective pressure for resistant strains, particularly in the clinical setting [11].

There are several responses that have been observed in bacteria in response to selective pressure by the widespread use of β -lactam antibiotics. These include the deletion of porin proteins in gram-negative bacteria to block the passage of antibiotic molecules through the bacterium's outer membrane, and also the activation of efflux exporter proteins [53, 54]. However, perhaps the most important resistance mechanisms in gram-positive pathogens such as *S. aureus* bacteria are the expression of enzymes called β -lactamases, and alterations to the molecular targets (Penicillin-Binding Proteins) of the antibiotics (see Fig. 2.2).

The mediator of penicillin resistance in *S. aureus* is a β -lactamase enzyme

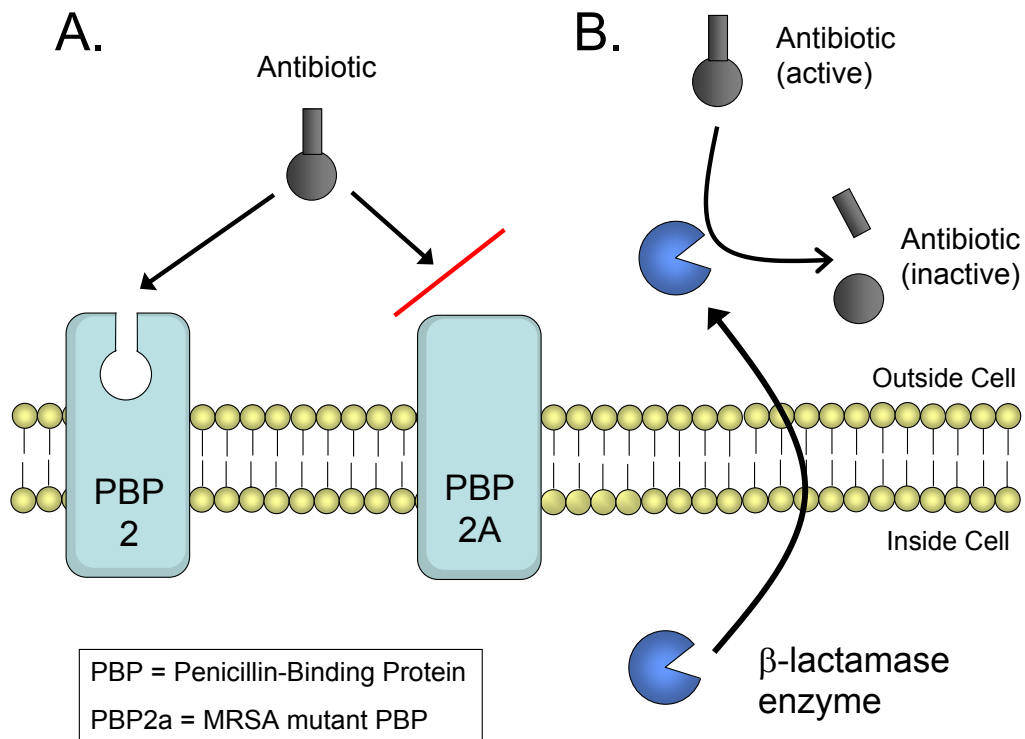


Figure 2.2: Schematic representation of main antibiotic resistance strategies in MRSA bacteria. **A.** Expression of alternate form of PBP2, called PBP2a, with reduced binding affinity for antibiotic. **B.** Production of β -lactamase enzyme which cleaves antibiotic molecules.

which hydrolytically cleaves the β -lactam ring present in penicillin and other β -lactam antibiotics (Fig. 2.3). β -lactamase was first discovered in *Escherichia coli* bacteria in 1940, and β -lactamase-expressing *S. aureus* bacteria were isolated soon afterwards [55, 56, 47]. The appearance of β -lactamases is thought to be an ancient evolutionary event. However their broadened distribution across many bacterial species, under selective pressure from antibiotic usage, has become a serious health concern [54].

Four variants of *S. aureus* β -lactamase have been identified by immunologic methods (types A-D) [19]. The most well studied β -lactamase is the class A β -lactamase characteristic of *S. aureus* strain PC1 [58]. This is encoded by the *blaZ*

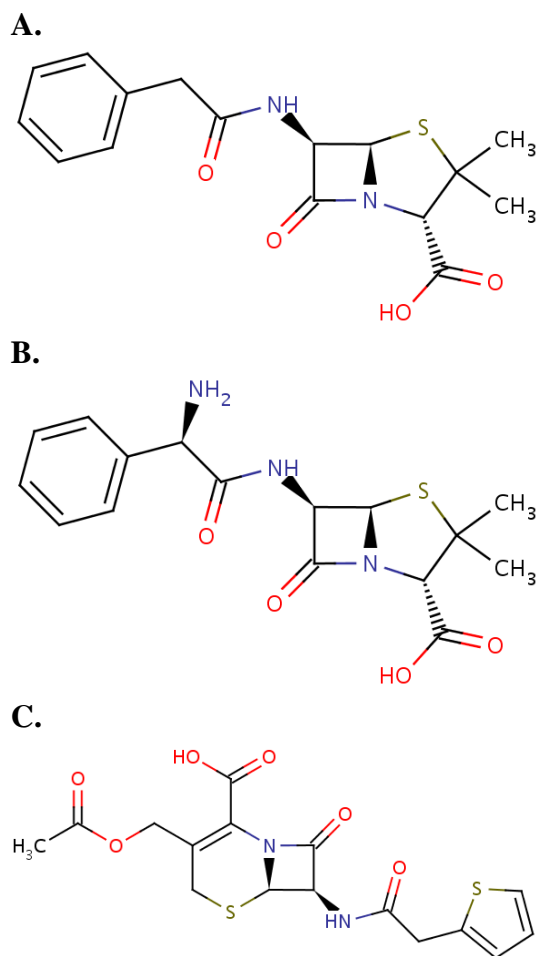


Figure 2.3: Examples of the chemical structures of three common β -lactam antibiotics: **A.** Penicillin G. **B.** Ampicillin. **C.** Cephalothin. They are characterised by the presence of a β -lactam ring structure (square at the centre of each structure above). Chemical structures were derived from the on-line DrugBank cheminformatics database [57].

gene which is carried on a transposable element of a large plasmid. Expression of β -lactamase is regulated by the interaction between β -lactams in the environment and a cell surface signal-transducer protein BlaR1 [48, 59]. After induction of expression, most of the β -lactamase enzyme is secreted into the extracellular milieu, while some remains bound to the cytoplasmic membrane of the cell [60]. When the antibiotic concentration in the environment decreases, re-repression of β -lactamase

expression occurs because BlaR1 is no longer auto-activated [61]. A study by Norris *et al.* (1994) found that among 50 β -lactamase-producing MRSA isolates taken from nine locations across the U.S.A., 80% expressed type A β -lactamase and the remainder expressed type C. Type B and type D β -lactamases are thought to be less common among MRSA strains [1].

Despite fifty years of selective pressure from continued use of β -lactam antibiotics, *S. aureus* has not acquired any new or modified β -lactamases [48]. This differs considerably from other species, such as *Escherichia coli* where over a hundred TEM β -lactamase variants have arisen from the ancestral TEM-1 gene [62]. However, some *S. aureus* strains have developed another mechanism that confers resistance to β -lactam drugs, including methicillin. This is based on alterations to the penicillin-binding proteins, which are the main molecular targets of β -lactam antibiotics in bacteria.

The introduction of methicillin in 1959 to treat infections of penicillin-resistant *Staphylococcus aureus* resulted in the selection of MRSA strains [48]. As early as 1961, MRSA strains were isolated and there has been a steady increase in incidences since then [63]. Normal *S. aureus* cells produce four types of membrane-bound transpeptidase proteins called penicillin-binding proteins (PBPs 1-4), which assemble and regulate the final stages of cell wall biosynthesis. The mode of action of the β -lactam antibiotics involves the acylation of a catalytic residue in the transpeptidase active site of PBPs which results in the inhibition of the corresponding catalytic activity (cell-wall cross-linking). However, MRSA bacteria contain a gene called *mecA*, which encodes an extra penicillin-binding protein, PBP2a.

The *mecA* gene is located on the staphylococcal cassette chromosome *mec* (SCC*mec*), which is a mobile genetic element capable of transferral across different bacterial species [64]. At present, there are five known types of SCC*mec*

(types I - V) distinguished by their genetic composition and size [65]. It is not known at what frequency *SCCmec* is acquired in nature, however Robinson & Enright estimated that methicillin resistance in *S. aureus* may have been acquired on over 20 separate occasions during evolutionary history, with *SCCmec* Type IV the most frequently acquired [66]. *SCCmec* Type IV has been associated with a recent increase in community-acquired MRSA. This may be due to its smaller size and lower fitness cost compared to the *SCCmec* types I-III [67].

The product of the *mecA* gene, PBP2a, does not bind the β -lactam moiety readily because the approach to the active site is sterically encumbered. When an MRSA organism is subjected to β -lactam stress, PBP2a confers resistance by supplementing its transpeptidase activity (cell-wall cross-linking) to the transglycosylase function of native PBPs during cell wall synthesis [48].

2.3.3 Pharmacokinetics and Pharmacodynamics

The term pharmacokinetics refers to the absorption, distribution and decay of drugs in patients, which determines the time course of drug concentrations in serum [68]. The complementary field of pharmacodynamics, in the context of antibiotic therapies, deals with investigating the functional relationship between the concentration of drug and the rate of growth/death of the bacteria in its presence [69]. The most common pharmacodynamic parameter used in the clinical setting has traditionally been the minimum inhibitory concentration (MIC) of a drug. This is the concentration of antibiotic that ensures a net rate of bacterial growth equal to zero. However, this parameter on its own does not give insights into the time course of antimicrobial activity, or persistent effects of the drugs such as the post-antibiotic effect (PAE), which is the length of time that bacterial growth continues to be inhibited after re-

removal of the antibiotic [68]. For this reason, in recent decades there has been extensive research into developing detailed pharmacokinetic-pharmacodynamic models that can be used to optimize treatment regimens of antimicrobial drugs and aid in rational drug design strategies.

The pharmacodynamics of antibiotics are usually studied *in vitro* by developing time-kill curves of exponentially growing bacteria exposed to different concentrations of antibiotics [69]. Pharmacodynamic functions are a means of formally describing the relationship between bacterial growth/death and the antibiotic concentration. This functional description can range from a very simple form, like the MIC, to more complex mathematical models such as the sigmoid E_{max} models which quantitatively describe the net growth rate of the bacterial colony as a function of the antibiotic concentration [69].

The sigmoid E_{max} model is a highly flexible, non-linear model which is used to capture many concentration-effect relationships. It takes into account a minimum threshold drug concentration below which little or no effect is observed, a log-linear drug concentration versus effect intensity relationship, and a plateau at relatively high drug concentrations [70]. Simpler models of the concentration-effect relationship, such as linear or log-linear models, have been used when data are available over a limited effect intensity range [71]. However, the E_{max} model is more commonly used because it can take into account the leveling of drug effect at higher drug concentrations and appears to be more physiologically relevant [70].

Mechanism-based mathematical pharmacokinetic-pharmacodynamic (PK-PD) models generally incorporate equations or sub-models describing microbial growth, the effects of the antimicrobial drugs, and the changing drug concentrations. A recent review by Czock & Keller (2007) showed that most published mathematical mechanism-based PK-PD models can be derived from a common model of anti-

microbial drug effects based on cell growth and cell killing processes [72]. In this common model, two pharmacodynamic functions are incorporated which determine the replication and death rates of the bacterial colony respectively in relation to the drug concentration. The relationship between the rate of bacterial growth inhibition and the drug concentration is described using a sigmoid E_{max} model. The second pharmacodynamic equation, which relates the increase in the rate of bacterial death to drug concentration, is also based on a sigmoid E_{max} model. This commonality among the apparently different models allowed their parameters to be related to the MIC and to a common set of PK-PD indices [72].

Even the most inclusive pharmacodynamics functions assume a global (population based) killing function that changes according to the changes in antibiotic concentration. However, the approach followed in the current work documented in this thesis involves the explicit incorporation of the kinetics of the interaction between antibiotics and the macromolecules involved in resistance and derives from it those concentrations of antibiotic that lead to inhibition of bacterial growth. This approach is complementary to the pharmacokinetic-pharmacodynamic modelling approach generally used to assess and model drug efficacy. It approaches the understanding of drug function and efficacy from the perspective of the underlying biochemical mechanisms that lead to the observed outcome. This, in conjunction with PK-PD studies, would allow a computational framework of analysis for relating molecular/biochemical data with more high level pharmacological studies.

CHAPTER 3

MODEL DESCRIPTION

3.1 Overview

The Micro-Gen Bacterial Simulator is an extended and modified version of an agent-based Java software tool called BAIT (Bacteria-Antibiotic Interaction Tool) [16]. Micro-Gen is coded in the C++ object oriented programming language. The individual microorganisms are represented by software agents which store physical traits of the bacterial cells as well as behavioural rules associated with them. The modular nature of the program means that functionalities/characteristics specific to particular bacterial species can be readily incorporated into the basic cellular model. This research describes work carried out to simulate the antibiotic resistance mechanisms specific to MRSA bacteria. However, to illustrate the capacity of Micro-Gen to simulate various bacterial populations, some test results simulating *Escherichia coli* are also included to demonstrate the effect of motility on bacterial behaviour.

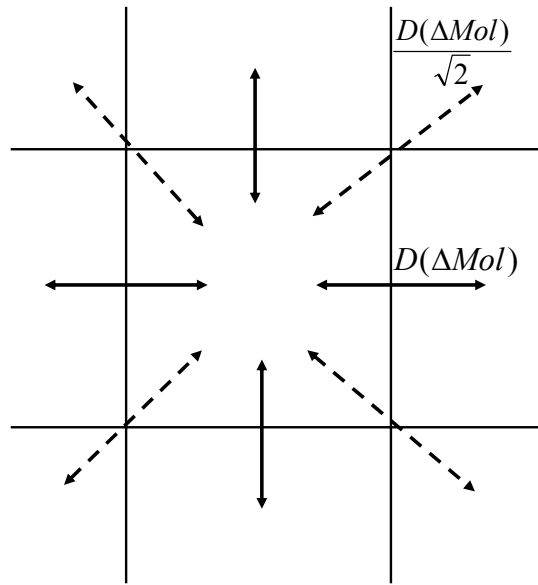
3.1.1 Environment

The culture environment is represented by a discrete, two-dimensional grid containing diffusible elements such as nutrients (glucose), enzymes and antibiotics. Each

discrete grid position (called a “patch”) in the environment contains variables to record the levels of nutrients, antibiotics and bacterial enzymes in it. It also includes pointers to bacterial agents that currently occupy the patch. The movement of molecules in the environment is assumed to occur according to the process of random diffusion down local concentration gradients. A discretized implementation of Fick’s first law of diffusion is used to calculate the movement of molecules between adjacent patches [31]. According to the diffusion algorithm, the amount of substance exchanged between two adjacent patches is proportional to the concentration difference (ΔMol) multiplied by a user-defined diffusion coefficient, D (Fig. 3.1A). The diffusion coefficient determines the proportion of molecules that are exchanged between two patches during each time step. When patches are diagonally adjacent to one another a diffusion rate modifier ($1/\sqrt{2}$) is applied.

There is also another higher-level diffusion rate modifier to take into account the relative differences in the molecular mass (M_r) of the various molecules (glucose, antibiotics, β -lactamases). The rate modifier of glucose is 1.0, i.e. the user-defined diffusion co-efficient D directly determines the rate of diffusion of glucose. The rates of diffusion of the other molecules are expressed relative to glucose. Glucose was chosen as the benchmark since it is the smallest molecule that is simulated in the model. The diffusion rate modifiers for the other molecules are calculated by dividing the M_r of glucose by the M_r of the diffusing molecule. The rate of diffusion is not influenced by the density of bacterial cells in the current patch, but this will be included in future work to develop a more detailed model of particle diffusion within a colony.

A.



B.

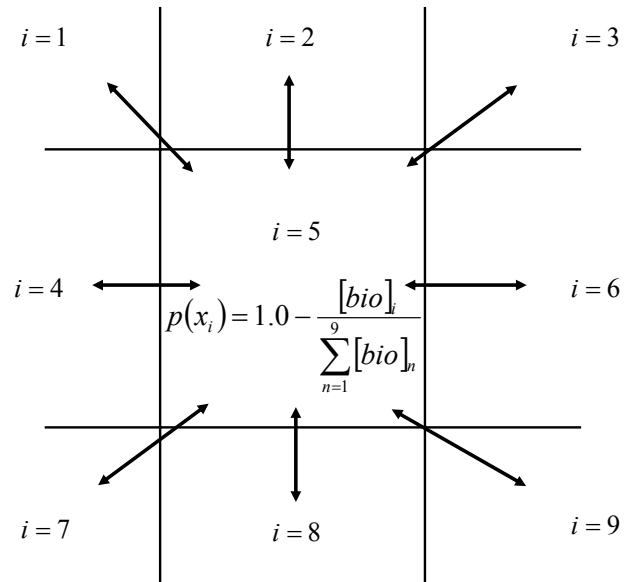


Figure 3.1: **A.** Diffusion algorithm applied to molecules. D = diffusion coefficient, ΔMol = concentration difference. **B.** Overcrowding algorithm applied to bacterial cells. $p(x_i)$ = probability of bacterial agent moving to patch i ; $[bio]_i$ = bacterial biomass in patch i .

3.2 Principal Model Entities

3.2.1 Bacterial Agents

The bacterial agents have a number of parameters associated with them along with a set of behavioural rules that dictate how they interact with the environment. The agents are an abstract representation of bacterial cells with the internal subcellular processes not explicitly modelled. This is done in order to minimize the number of parameters associated with each agent, because of the principle that each new parameter makes it more difficult to understand what a model does [13]. The agent-based approach can result in more parameter-rich models than with mathematical state variable modelling, but this problem can be alleviated somewhat by the aggregation of details into a single parameter. However, it is a challenge to determine the appropriate level of aggregation since there is often a trade-off between ‘realism’ and keeping the model as simple as possible. The main input parameters for the bacterial agents are listed in Table 3.1.

The bacterial software agents are stored in a “fabric” (array) data structure which is initialized with a pool of bacterial agents at the start of the simulation. Bacterial agents in the fabric only become active in the simulation when they are flagged as “alive”. When reproduction occurs and a new daughter agent is added to the environment, one of the non-active agents in the fabric is switched to active status and its variables updated. The pre-initialization of a pool of non-active agents in a fabric at the start of the simulation means that new software objects do not have to be created or destroyed in memory every time a bacterium is born or dies. This results in significant performance gains when dealing with large populations of agents. Furthermore, algorithms are used to maintain the bacterial fabric in a non-fragmented state with active agents stored in contiguous blocks of memory.

This is done to minimize the memory access times which otherwise could lead to a significant performance bottleneck when running large numbers of agents.

Table 3.1: Input Parameters for Bacterial Agents in Micro-Gen model. Sample values for *S. aureus* species included. b.u. = biomass units

<i>Input Parameter</i>	<i>Input Value</i>
Biomass threshold for division	10000
Nutrient Intake (b.u. loop ⁻¹)	10.0
Survival cost (b.u. loop ⁻¹)	0.2
Stationary phase relative metabolic rate	0.2
Lag phase length (min)	66
β -lactamase production rate ($\mu\text{M s}^{-1}$)	3.28×10^{-7}
β -lactamase production cost (b.u.)	0.1
Antibiotic Intake (μM)	6.0×10^{-8}
Kinetic Parameters (k_2, K_d, k_{cat}, K_M),	see Table 3.2

3.2.1.1 Growth Parameters

The biomass of the cell is tracked within the simulation by using simulation units called “biomass units”. Bacterial agents increase their biomass by absorbing nutrient from the immediate environment. The rate of nutrient absorption is determined by the “nutrient intake” parameter specified by the user. There is also a “survival cost” associated with normal metabolic activities of the cell and this is subtracted from the cell biomass each time step. As the agent accumulates nutrient, its biomass increases until it reaches a certain threshold (“biomass threshold for division”) when reproduction is triggered. Bacterial cells reproduce asexually by the process of binary fission, whereby a cell divides into two identical daughters cells approximately half the size of the original cell.

The nutrient intake rate and biomass threshold for division were determined

by fitting to an experimentally determined bacterial doubling time of 29 minutes, which is the estimated generation time of *S. aureus* strain BB255 [73]. The survival cost parameter influences the length of the stationary phase of the growth cycle. A higher survival cost results in a shorter stationary phase because cells enter the death phase more quickly. A survival cost of 2% of the rate of nutrient intake was chosen for the test simulations recorded here. This represents a level which does not limit the exponential phase of bacterial growth (see Chapter 4). However, in nature this would vary considerably between different strains and for a more detailed quantitative representation of the growth curve of a particular strain this would need to be estimated from experimental studies.

Some other parameters associated with the bacterial agents are the “stationary phase relative metabolic rate” and the “lag phase length”. The first parameter refers to a state of reduced metabolic activity that bacterial cells enter when they are subjected to severe stress such as nutrient deprivation. The “survival cost” parameter is multiplied by the proportion specified. The principal effect of this parameter is to modify the length of the stationary phase (see Chapter 4). It represents the bacterium’s ability to preserve itself in hostile, nutrient-deprived conditions by shutting down non-essential metabolic activities. A sample value of 0.2 is used in our test simulations for illustrative purposes, however as with the “survival cost” parameter, this would need to be experimentally estimated in order to give a quantitatively accurate representation of the length of the stationary phase. It is not a significant factor in the simulations for predicting the Minimum Inhibitory Concentration (MIC) of an antibiotic (Chapter 5) since the drug is added during the exponential phase of growth prior to the bacteria entering the stationary phase.

The “lag phase length” parameter specifies the length of time it takes for the bacteria to adapt to their new environment at the start of the simulation. During this

phase, bacterial cells synthesise the required cellular components to adapt to their conditions. Their rate of nutrient intake increases from an initial low level until the maximum intake rate is achieved. This represents the accumulation of proteins required to process the nutrients available in the bacterium's new environment. The underlying dynamics that determine the length of the lag phase are not explicitly modelled, however there is a random element introduced by the fact that the bacteria are initialized with different energy states at the start of the simulation. Prats *et al.* (2008) describe a more detailed model of the underlying population dynamics occurring within the lag phase using an agent-based approach [41].

3.2.1.2 Antibiotic Resistance Mechanisms

If the bacteria are exposed to antibiotics, this triggers the synthesis and release of an enzyme called β -lactamase into the extracellular milieu (Fig. 3.2). The β -lactamase enzyme is an important defensive protein that bacterial cells secrete to destroy any β -lactam antibiotics (e.g penicillin) in their vicinity. The rate of β -lactamase production and the extra metabolic cost associated with it can be specified by the user. For our simulations, the β -lactamase production rate was estimated by varying it over a range of values and calculating the minimum inhibitory concentration (MIC) of penicillin G at each value (using kinetic parameters for penicillin G described below). The β -lactamase production rate was chosen as that which resulted in a simulated MIC equal to the experimentally determined MIC for penicillin G versus the particular bacterial strain being modelled.

For the test simulations, Type A and Type C β -lactamase-producing MRSA strains were modelled and calibrated with the experimental results of Norris *et al.* (1993) for penicillin G (Type A MIC = 72.1 $\mu\text{g/ml}$; Type C = 47.9 $\mu\text{g/ml}$) [1]. Based on this, the β -lactamase production rates were es-

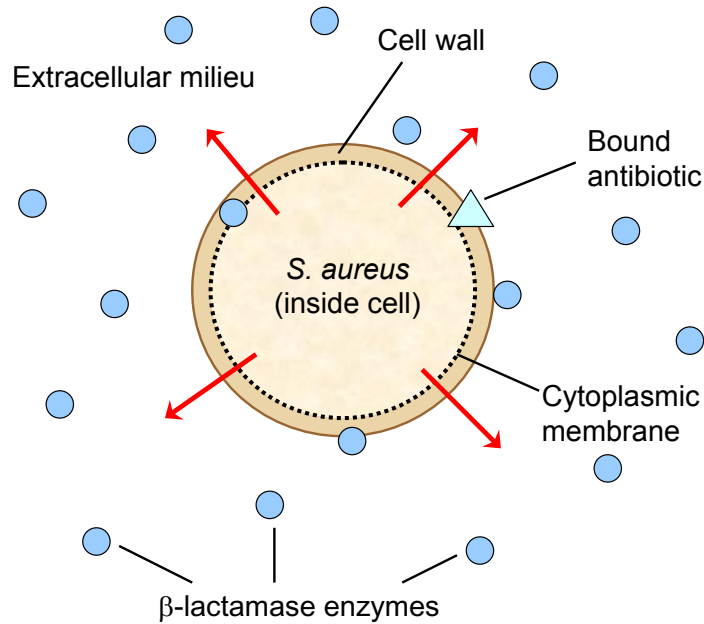


Figure 3.2: Schematic representation of release of β -lactamase enzymes from *S. aureus* cell. Production of β -lactamase is induced by binding of β -lactam antibiotics to a cell surface signal transducer protein (BlaR1). Most of the β -lactamase enzyme is secreted into the extracellular milieu while some remains bound to the cytoplasmic membrane of the cell.

estimated to be $3.28 \times 10^{-7} \mu\text{M s}^{-1} \text{agent}^{-1}$ for the type A simulated strain and $1.62 \times 10^{-7} \mu\text{M s}^{-1} \text{agent}^{-1}$ for the type C simulated strain.

There are a number of parameters listed in Table 1 dealing with the interactions between the bacterial agent and antibiotic molecules. The antibiotic intake parameter determines the rate at which free antibiotic is depleted in the patch by absorption across the cell wall of the bacteria. There are two kinetic parameters (k_2 , K_d) which determine the rate at which the antibiotic molecules bind to penicillin-binding proteins (PBPs) in the cytoplasmic membrane, underneath the cell wall. There are also two kinetic parameters (k_{cat} , K_M) that describe the interactions between antibiotic molecules and β -lactamase enzymes in the environment. Values for these kinetic parameters were taken directly from experimental literature and are explained in

the sections on antibiotics and β -lactamases below.

3.2.1.3 Movement and Chemotaxis

The bacterial agents in Micro-Gen, for motile bacteria, can implement a “run and tumble” mode of movement characteristic of species with flagella, such as *Escherichia coli* [74]. They move forward smoothly during the “run” phases and reorient to a random direction during the alternating “tumble” phases (Fig. 3.3). They also display positive chemotaxis when exposed to nutrient concentration gradients. This is facilitated by a temporal sensing system whereby the bacteria periodically compare nutrient concentrations as they move from patch to patch through the environment [75]. When a bacterium encounters a positive nutrient gradient it lengthens the time of its “run” phase, and the relative duration of runs and tumbles determines if the cell moves towards or away from a chemical environment.

The impact of positive chemotaxis by the bacterial agents in the presence of nutrient gradients is illustrated in Figure 3.4. The bacteria possess a temporal sensing system to detect nutrient gradients and move towards areas of higher nutrient concentration. In Figure 3.4, two localised areas with higher nutrient concentrations were created in the upper-left and lower-right corners of the environment. As the nutrient diffuses into the rest of the environment it produces a gradient and the bacteria respond by moving up this gradient. In Figure 3.4D (taken at the 2 hour time point), the bacterial cells, marked in yellow, can be seen clustered around the areas of high nutrient concentration, represented by lighter shades of grey.

3.2.1.4 Overcrowding Algorithm

In the case of *S. aureus* bacteria, which are non-motile, an overcrowding algorithm is applied to take into account the physical size constraints of a single patch in

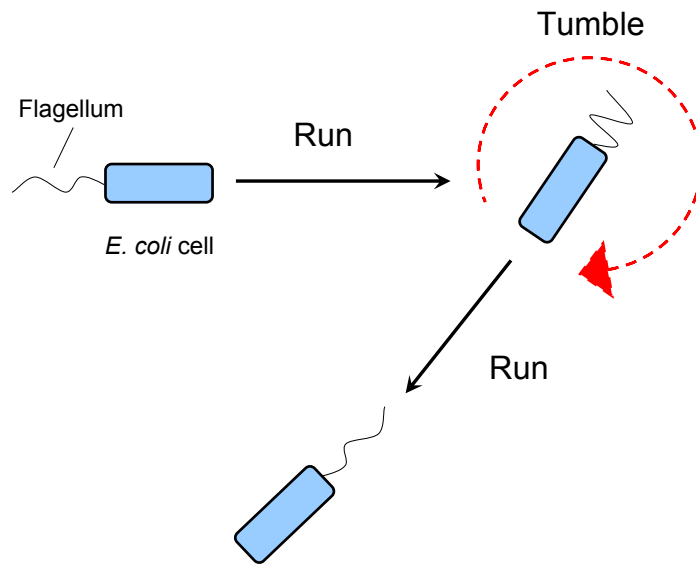


Figure 3.3: Diagram of “run and tumble” mode of movement characteristic of bacteria with flagella (e.g. *E. coli*). During the run phase, bacteria swim forward by active propulsion from the flagellum. This is punctuated by tumbles, where the cell randomly reorients to a new direction. Decreased frequency of tumbles in response to a chemical attractant gradient (e.g. nutrient) results in migration of the cell up the gradient in an analogous way to a biased random walk (chemotaxis).

the environment. The area of each patch is configured to represent approximately $1 \mu\text{m}^2$ of medium. Depending on the size of the bacterial species being simulated, overcrowding will come into effect when more bacteria occupy the patch than can be accommodated. For example, the estimated cell diameter of a newly divided *S. aureus* cell is $0.5 \mu\text{m}$ [49]. Therefore, when more than four such cells occupy a single patch an overcrowding algorithm is applied (Fig. 3.1B). According to this, the probability, $p(x_i)$, of a bacterial cell in an overcrowded patch being moved to an adjacent patch i is inversely proportional to the relative bacterial biomass in the adjacent patch. The direction a cell is moved is determined by sampling from the resultant probability distribution of the surrounding patches.

A ‘*bacOvercrowd*’ input parameter may be specified by the user to control the rate of spreading of the bacterial colony across the surface of the environment. If

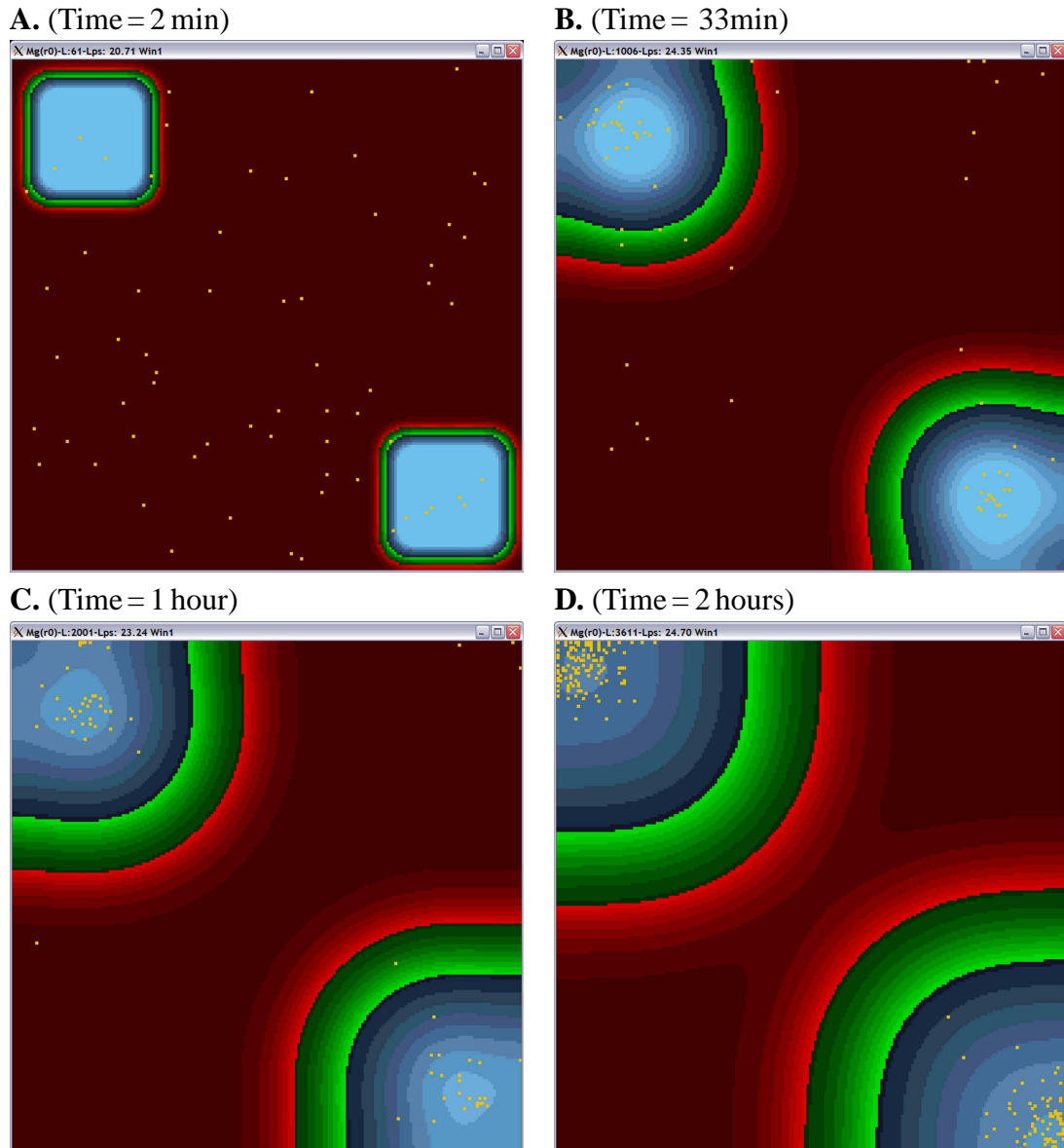


Figure 3.4: Screenshots from Micro-Gen illustrating positive chemotaxis of motile bacterial agents towards areas of higher nutrient concentration: (A) Bacteria (yellow) initially randomly distributed, with localised areas of high nutrient concentration initialised in upper-left and lower-right corners of the environment. (B - D) As nutrient diffuses into the environment, the bacteria detect the nutrient concentration gradient and move towards areas of higher nutrient concentration. Nutrient levels in environment are represented by colour-coded gradient (lighter shade = higher conc.) with blue, green and red colours representing high, medium and low nutrient concentrations, respectively.

the bacterial biomass in the current patch is greater than *bacOvercrowd* multiplied by the lowest bacterial biomass in an adjacent patch then the bacterial overcrowding algorithm is applied. For example, with a *bacOvercrowd* value of 1.0 there must be at least one adjacent patch with a bacterial biomass less than or equal to the current patch for there to be a chance of a bacterial cell being moved. On the other hand with a value of 2.0, the bacterial biomass must be twice the level of all the surrounding patches. A higher value results in more densely packed cells and less radial expansion of the colony (Fig. 3.5).

The *bacOvercrowd* parameter may be thought of as a crude “aggregation” constraint. However, a more sophisticated model of cell aggregation would need to be implemented to recreate the complex cell assemblages found, for example, in biofilm communities. However, the bacterial overcrowding algorithm suffices to represent the gradual spreading of non-motile *S. aureus* cells across the surface of an agar plate. The parameter is used to ensure that movement of bacterial cells is always down a bacterial biomass concentration gradient ($bacOvercrowd > 1.0$). Increasing the *bacOvercrowd* input value affects the transition from the exponential to the stationary phases of the bacterial population growth curve (Fig. 3.6). For the test simulations documented in this report, a *bacOvercrowd* value of 1.3 was used. This represents a relatively unconstrained expansion of the colony (down the bacterial biomass concentration gradient), i.e. only minimal cell aggregation is assumed.

3.2.2 Antibiotics

The quantities of antibiotics in the environment are stored as variables in each patch and subject to diffusion as described above. Each molecule has a distinct half-life derived from the biological literature which determines its rate of degradation

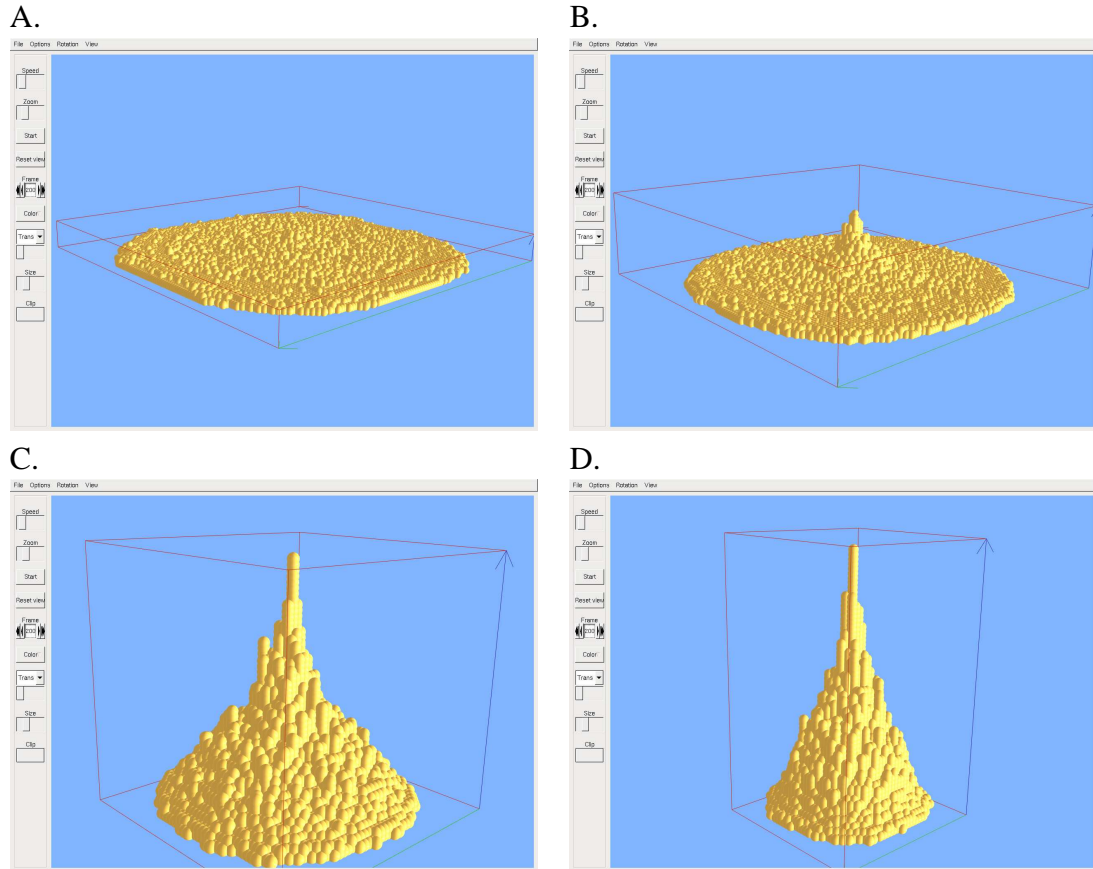


Figure 3.5: Effect of ‘bacOvercrowd’ parameter on the radial expansion of bacterial colonies. Four different simulations were carried out with different input values for bacOvercrowd: **A.** bacOvercrowd = 1.0; **B.** bacOvercrowd = 1.3; **C.** bacOvercrowd = 1.6; **D.** bacOvercrowd = 2.0. Higher values of bacOvercrowd result in more aggregation of bacterial cells and less radial expansion. Images were produced using the open-source ‘Animp’ 3D visualisation software (developed by Ray Seyfarth, University of Southern Mississippi, USA).

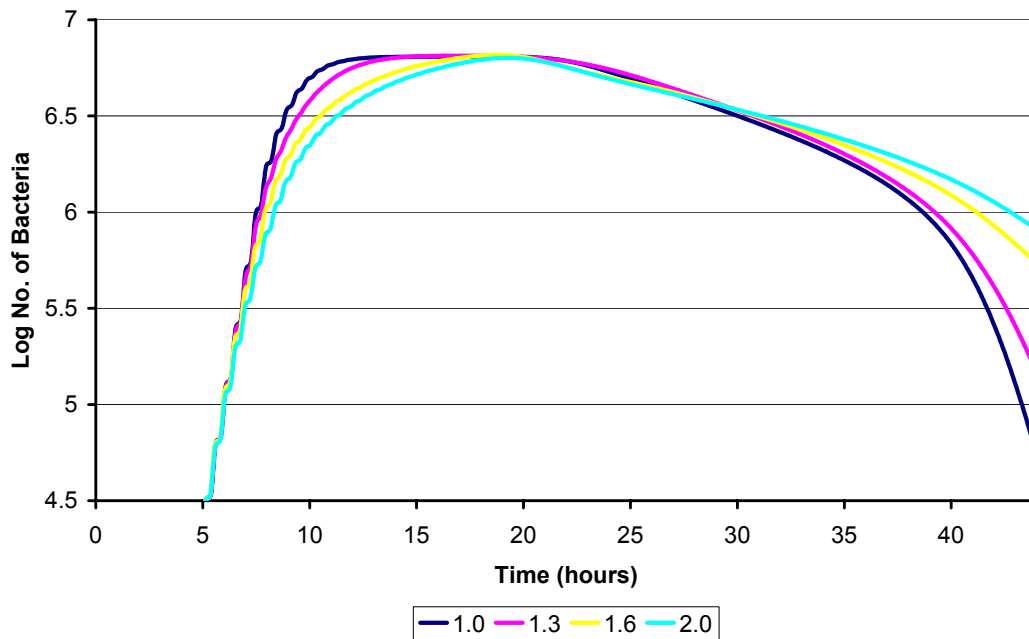


Figure 3.6: Log growth curves of simulated MRSA bacterial agents grown under *in vitro* culture conditions with different ‘bacOvercrowd’ input parameter values (1.0 - 2.0) Initial inoculum = 64 bacterial agents.

over time (Table 5.3) [57]. If there are bacterial agents in the patch they will absorb antibiotic according to their specified rate of intake. The ability of β -lactam antibiotics to inhibit bacterial cell division is based on the fact that they bind to proteins in the cell membrane called penicillin-binding proteins (PBP) which are necessary for cell division (Fig. 3.7). Upon binding to PBP the antibiotic inactivates it and if a significant proportion of PBPs in the cell are inactivated the bacteria will be unable to reproduce and cell death may occur [49].

The interactions between the β -lactam antibiotic molecules and PBP2a are explicitly represented in the simulation. However, the interactions with the other PBPs present in the bacterial cell membrane (PBPs 1 - 4) are not explicitly modelled for the MRSA bacterial agents. This is sufficient for representing MRSA because the limiting reaction for antibiotic efficacy is that with PBP2a, which has a binding

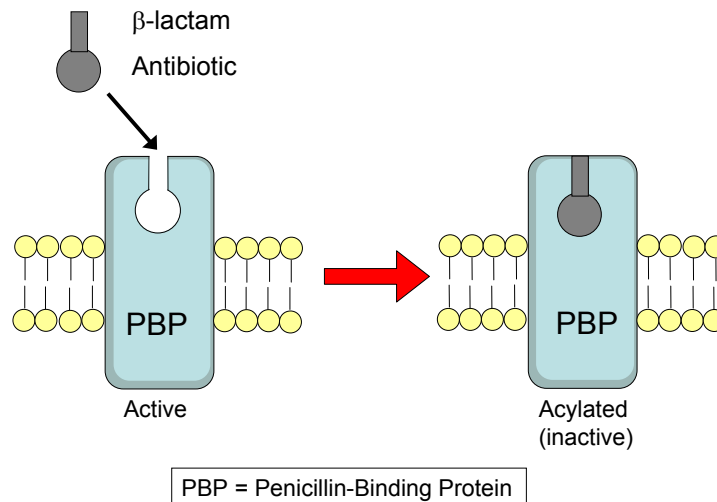


Figure 3.7: Schematic representation of β -lactam antibiotic (e.g. penicillin or cephalothin) binding to penicillin-binding protein (PBP) in cell membrane of bacterial cell. PBP is required for normal cell wall synthesis to occur during cell division. However, binding and acylation of the PBP by antibiotic results in inhibition of this function.

affinity for β -lactams that is reduced compared to the other PBPs. This reduces the level of complexity caused by introducing more empirical parameters into the model.

There is an internal counter associated with each bacterial agent which represents the proportion of PBP2a molecules that have been acylated (or bound) by antibiotics. When this value reaches 100%, then death of the bacterial agent occurs. Reproduction will only occur successfully when the percentage of bound PBP2a in the bacterial agent is $<10\%$. When the percentage of bound PBP2a is between 10% and 100%, cell division is assumed to be disrupted until normal turnover of protein in the cell reduces this percentage below the threshold again. The threshold values are maintained constant across all the simulations documented here in order to be able to compare the relative efficacies of the antibiotics against a single hypothetical MRSA strain. In nature, however, the relative values for these thresholds might

vary considerably between different strains [76].

In order to quantify the efficacy of the antibiotic at inhibiting cell division, kinetic parameters describing the reaction between antibiotic and PBP2a in the cell are used. This is a pre-steady state reaction, with the parameters k_2 (rate of inactivation of PBP2a), and K_d (dissociation constant) used to describe it. The ratio of these values (k_2/K_d), or the second order rate constant, is a convenient measure of the antibiotic efficacy at inhibiting PBP2a function. The proportion of PBP2a that is inactivated per second, k_a (the apparent first order rate constant), at a given drug concentration can be calculated as a function of these parameters (equation 3.1) [76].

$$k_a = \frac{k_2[Ab]}{K_d + [Ab]} \quad (3.1)$$

Values for the kinetic parameters, k_2 and K_d , of PBP2a were derived from the biological literature (Table 3.2) [77, 78, 20]. By inputting these parameters it was possible to estimate the proportion of PBP2a de-activated by antibiotic each time step. Once the proportion of acylated PBP2a crosses a certain threshold, then cell division is inhibited (see above).

3.2.3 β -lactamase Enzymes

β -lactamase enzymes are proteins produced by resistant bacteria that attack a common type of antibiotic, called β -lactams, which includes penicillins, such as penicillin G and ampicillin, and cephalosporins such as cephalothin. In the case of MRSA bacteria, most of the enzyme is released into the extracellular milieu where it binds to and cleaves antibiotic molecules (Fig. 2.2B).

When a β -lactamase-producing bacterium comes into contact with antibiotic, an intracellular signal is sent to activate expression of the β -lactamase gene. A true/false flag for β -lactamase expression is associated with each bacterial agent. After the first interaction (when the flag is changed to true), there is an exponential increase in the β -lactamase production rate until the maximum rate is reached after approximately eighty minutes [59]. This corresponds to the activation of gene expression mediated by antibiotic binding to the signal-transducer protein BlaR1, as described in chapter 3.

β -lactamase is released into the local patch where it is subject to diffusion according to Fick's First law of diffusion, as described above. It also has a defined half-life parameter determining its rate of degradation over time in the environment. When antibiotic has been removed from the environment, re-repression of β -lactamase expression occurs (BlaR1 is no longer auto-activated - software flag changed to false).

The interactions between β -lactamase enzymes and antibiotic molecules in the same patch are governed by defined kinetic rules. Michaelis-Menten kinetics are used to describe the reaction, with the reaction rate, V , calculated as the rate at which antibiotic is cleaved (or de-activated) by the enzyme (equation 3.2):

$$V = \frac{k_{cat}[E]_t[Ab]}{K_M + [Ab]} \quad (3.2)$$

The kinetic parameters required as input to the model are the turnover rate, k_{cat} , and the Michaelis constant, K_M , the ratio of which (k_{cat}/K_M) is often used as a measure of enzyme efficiency [19]. These were derived from the biological literature for MRSA (Table 3.2) [19]. $[E]_t$ and $[Ab]$ refer to the concentrations of

Table 3.2: Kinetic Parameters of β -lactam Antibiotics versus Type A and Type C β -lactamase-producing MRSA. Pen G = Penicillin G; Amp = Ampicillin; Ceph = Cephalothin.

<i>Parameter</i>	<i>Type A MRSA</i>			<i>Type C MRSA</i>		
	<i>Pen G</i>	<i>Amp</i>	<i>Ceph</i>	<i>Pen G</i>	<i>Amp</i>	<i>Ceph</i>
k_{cat} (s^{-1})	171.0	308.0	0.015	210.0	355.0	0.095
K_M (μM)	51.1	255.0	6.8	55.9	122.0	5.2
k_2 (s^{-1})	0.185	0.0047	0.00115	0.185	0.0047	0.00115
K_d (μM)	15400	495	586	15400	495	586

β -lactamase enzyme (sum of both free and occupied enzyme) and antibiotic in the local patch respectively.

3.2.4 Pro-Drugs

The basic premise of the enzyme-catalysed therapeutic activation (ECTA) pro-drug treatment strategy is that a substrate-like pro-drug molecule containing a β -lactam structure is administered to treat an infection. When it comes into contact with β -lactamase producing bacteria, it undergoes therapeutic activation by cleavage of its β -lactam ring which causes selective release of a cytotoxic anti-microbial agent [79, 80]. More details about this approach are included in chapter 6.

From a conceptual standpoint, the pro-drugs are represented as antimicrobial agents that start the simulation in an inactive form, but become flagged to ‘active’ status when they come into contact with β -lactamase enzymes in the environment. The reaction between pro-drug and β -lactamase is defined by the same reaction kinetics that were used to represent the antibiotic- β -lactamase reaction (equation 3.2). This is because it is essentially the same reaction between a β -lactam ring structure in the pro-drug molecule and the β -lactamase enzyme. However, the outcome of the interaction is reversed, whereby the pro-drug molecule is activated

after cleavage of its β -lactam ring structure, rather than inactivated as is the case with traditional antibiotic molecules.

The active component of a pro-drug may be any type of antimicrobial agent depending on how it was designed. Therefore, in order to represent specific pro-drugs, the Micro-Gen model would have to be adapted to take into account the specific mode of action of the particular active agent released. For the purposes of this study, the aim was to assess the pro-drug delivery system from a general perspective so the emphasis was placed on analysing the effects of the β -lactamase mediated activation step.

For the case study described in chapter 6, the active component of the pro-drugs NB2001 and NB2030 was triclosan. The mode of action of this drug is not fully understood, although it is thought that an important component is the binding to the enoyl-[acyl-carrier-protein] reductase (FabI) enzyme involved in the bacterial fatty acid synthesis cycle [81]. The interaction between the activated component of the pro-drug and the bacterial cell was modelled using the pre-steady state reaction kinetics described above for the β -lactam antibiotics (equation 3.1).

3.3 Program Structure

3.3.1 Program Flow Structure

Micro-Gen is coded in the C++ object-oriented programming language with individual components of the simulation represented by software objects. At the start of a simulation, the main components of the environment, the patches, are initialized, along with the bacterial fabric containing the pool of pre-initialized bacterial agents.

The principle activities of the simulation are carried out during the main program loop which represents a discrete time step of the model (Fig. 3.8). The loop is configured to represent approximately two seconds of real-time, although this is modifiable by the user to apply a different temporal granularity. The various time-dependent input parameters (e.g. nutrient intake rate, antibiotic kinetic parameters) must be configured to the specified timescale.

The program loop is divided into six distinct steps during which different aspects of the simulation are implemented. The first step (diffusion) is to update the levels of the various molecular constituents (nutrients, antibiotics and enzymes) of the environment. Fick's first law of diffusion is applied at this point to model the movement of free molecules between patches.

Step two (metabolism) is when the basic metabolic processes of the bacterial cells are modelled. This includes subtracting a survival cost from the bacterium's energy stock, representing energy expended on basic housekeeping duties in the cell. If β -lactamase gene expression is active then the enzyme is produced and secreted into the environment, with an associated energy cost.

The third step is to update the positions of the bacterial agents by applying a movement algorithm. In the case of bacteria capable of propelled locomotion, such as *Escherichia coli*, the model implements their characteristic "run and tumble" motion [17]. *E. coli* cells can respond to a chemical stimulus (chemotaxis) such as a positive nutrient gradient by extending the length of their run phase relative to the tumble phase. This results in movement of the cells towards regions of higher nutrient content. *S. aureus* cells are immotile so there is no active movement algorithm associated with them. However, if a patch becomes overcrowded then it is possible for cells to be shunted into an adjacent patch, in which case an overcrowding algorithm is applied at this step (Fig. 3.1B).

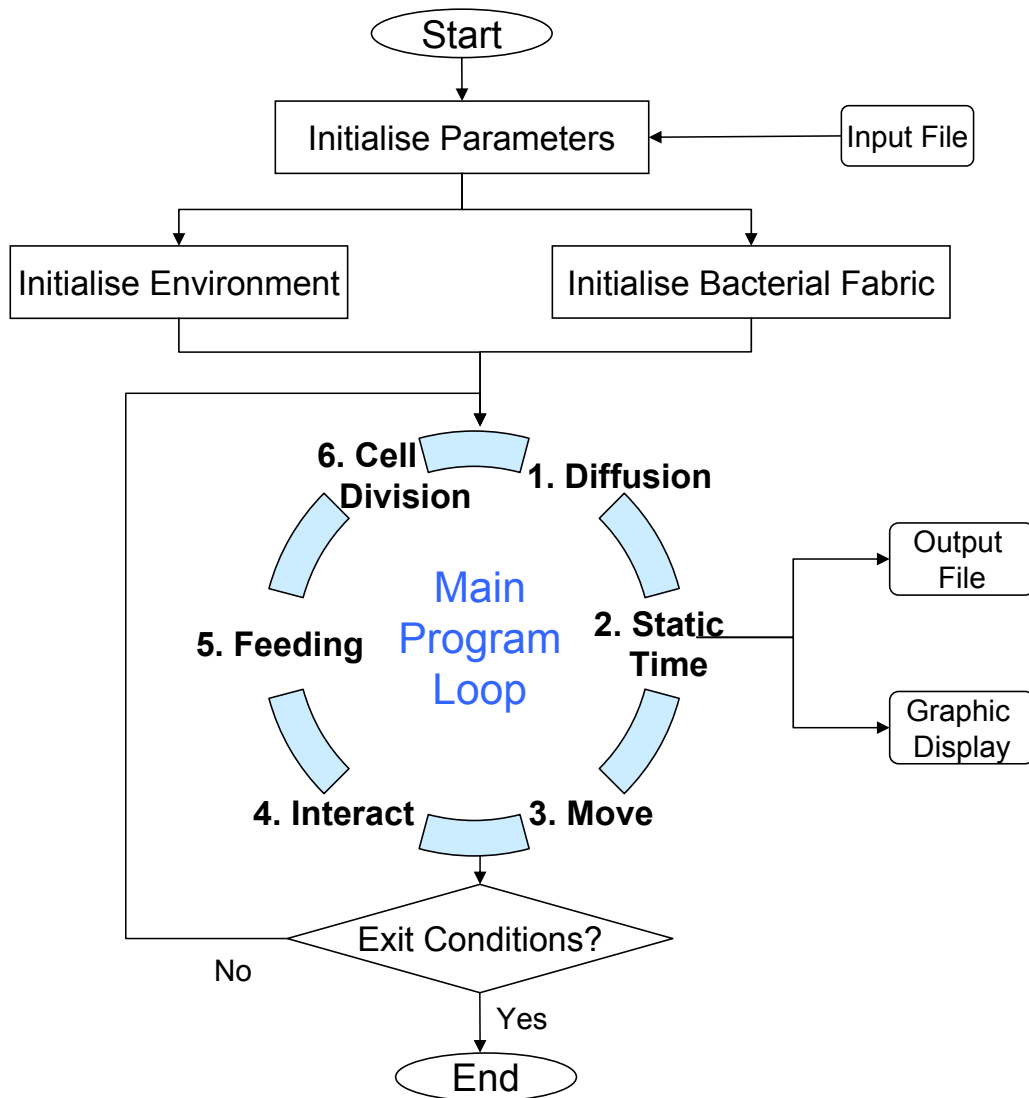


Figure 3.8: Diagram of program flow structure in Micro-Gen Bacterial Simulator, including the main stages of program loop.

Step 4 (agent interactions) of the program loop is when the kinetic rules for bacteria-antibiotic and β -lactamase-antibiotic interactions are applied. These reactions are governed by defined kinetic rules, with parameters derived from biochemical studies used to determine the reaction rates (Eqs. 3.1, 3.2). During the following step (feeding), the bacterial agents take up nutrient from the environment at a defined rate. In the case of the simulations carried out for this study, the rate is

that which will result in a generation time of 29 minutes [73].

The final stage of the loop is when bacterial agents reproduce according to the process of binary fission, producing two identical daughter cells. Reproduction is dependent on the fact that the bacterial cell's energy store has exceeded a defined threshold for replication, and the level of antibiotic damage (proportion of inactivated PBP) is below a critical level. The exit conditions for the simulation are if there are no longer any bacterial agents alive or a specified number of loops have been completed.

3.3.2 Graphical Output

The simulation may be run with an optional dynamic graphical display that shows the positions of bacteria in the environment and the levels of various molecular components such as nutrients or antibiotics in real-time. This can be useful for studying pattern formation in colonies. For example, in Figure 3.9, the characteristic circular colonies of *S. aureus* bacteria can be seen.

The model also outputs a movie file compatible with the open-source 3D visualisation software 'Animp' (Animated Particles) developed by Ray Seyfarth (University of Southern Mississippi, Hattiesburg, MS 39406, USA). Animp is an OpenGL-based 3D renderer that takes advantage of modern 3D graphics cards for visualising particles in three-dimensional space. Although Micro-Gen is a two dimensional model (X and Y dimensions), it produces a pseudo-3D output (for visualisation purposes) by assigning the Z dimension to represent the number of bacterial cells in a patch (Fig. 3.10). This 3D visualisation is useful, for example, for assessing the effect of the bacterial overcrowding algorithm on cell densities within a colony (Fig. 3.5). However, it will become more important when Micro-Gen is expanded to

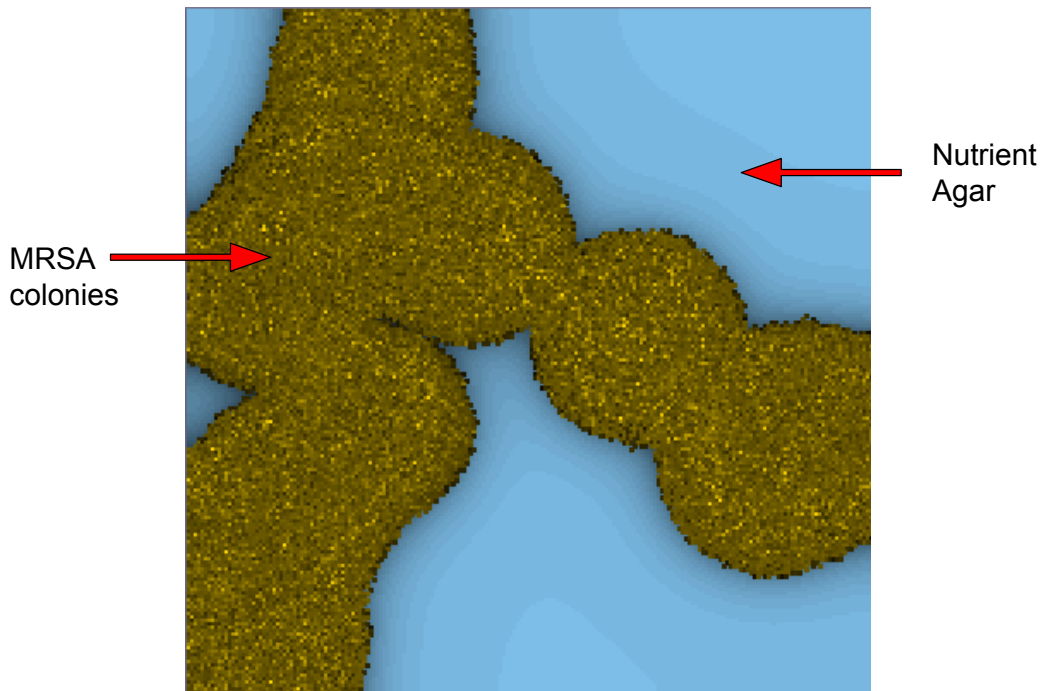


Figure 3.9: Screenshot of Micro-Gen simulation showing growing *S. aureus* colonies (yellow-brown, lighter = higher bacterial biomass) on simulated nutrient agar medium. Shaded blue contours represent nutrient gradient (lighter blue = higher nutrient concentration).

represent three-dimensional space, which is an important future aim of the project.

3.3.3 Parallelisation

A challenge of modelling from the individual cellular level up is that it requires a significant amount of computing resources in order to scale up to biologically realistic numbers of cells. For example, the concentration of bacterial cells in nature can range from 10^6 - 10^{10} cells per millilitre of seawater [82]. Despite rapid advances in traditional desktop computers, due to their memory and performance limitations it is currently not practically feasible to model the numbers of agents typically found in nature using only a single processor. Therefore, it is important to be able to take advantage of parallel high performance computing resources in

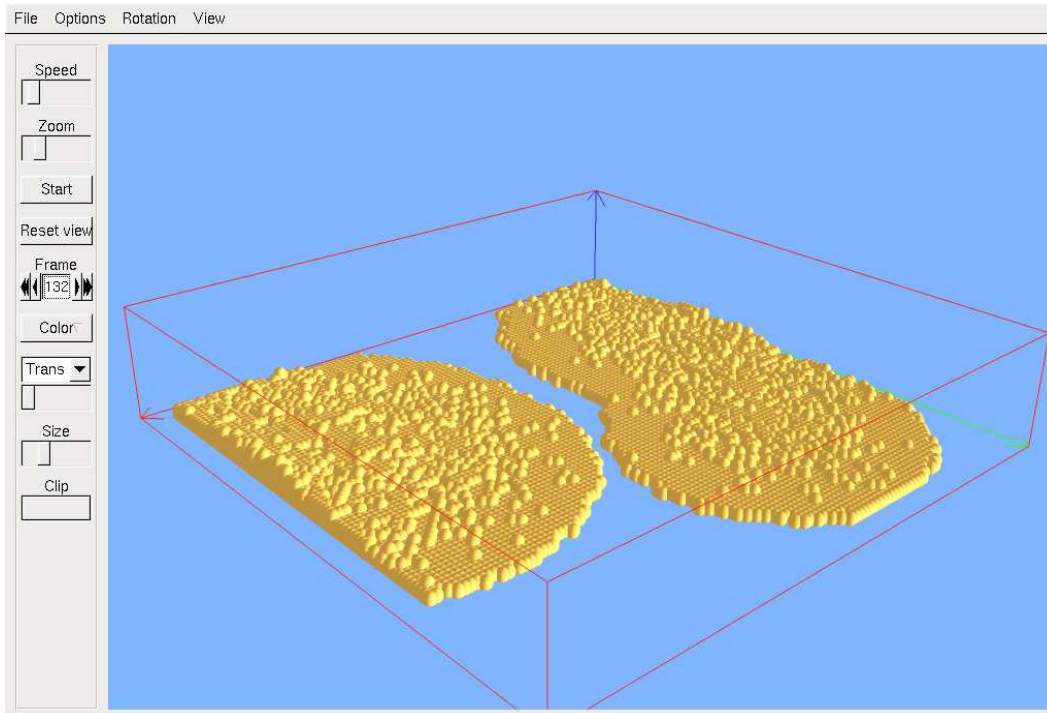


Figure 3.10: Screenshot of Animp 3D movie file generated by Micro-Gen simulation showing growing *S. aureus* colonies (yellow spheres). Images were produced using the open-source ‘Animp’ 3D visualisation software (developed by Ray Seyfarth, University of Southern Mississippi, USA).

order to tackle problem at a more realistic scale.

Micro-Gen is designed to take advantage of high performance computing resources by incorporating an implementation of the Message Passing Interface (MPI) for running in parallel on multiple computers. The strategy of domain decomposition is used for parallelisation, whereby the simulation environment is divided equally among the computing nodes (Fig. 3.12). Each node processes its section of the environment independently of the other nodes. Communication between adjacent nodes occurs at overlapping boundary conditions where quantities such as nutrient, antibiotic and enzyme levels are exchanged during each time step (Fig. 3.13). For example, when a bacterial cell crosses over the border separating parts of the environment controlled by two different processors/computers then the bacterium

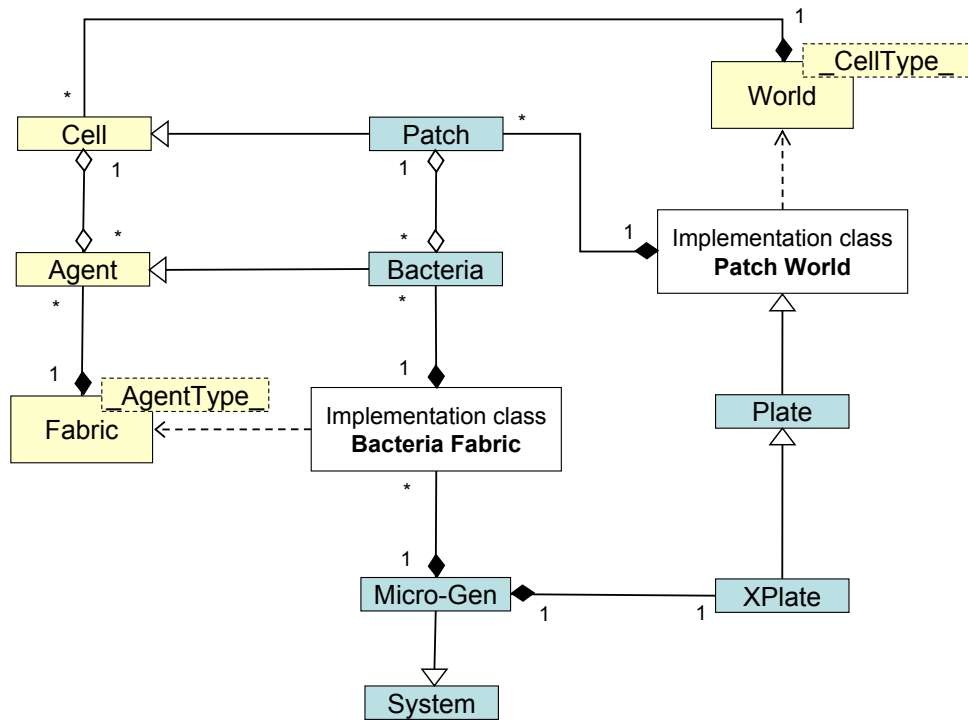


Figure 3.11: Diagram of principal classes of Micro-Gen model using standard UML notation. Yellow shaded components represent base classes of a generalised agent-based model. Derived classes specific to Micro-Gen, which contain functionality for representing bacterial cells and antibiotics, are shaded in blue-green.

is sent across to the other computer in an analogous way to sending a letter between two postal addresses.

By being able to run the simulation in tandem across multiple processors/computers, it frees up the traditional limitations of computing resources found in the desktop space. The model can be scaled up to as many processors/computers as there are available in order to increase the environment size from the microscopic level up to a visible scale. However, it is important to optimize parallel algorithms to avoid the process of diminishing returns as the numbers of processors are increased. This is because with more processors there is more traffic/communication between them and this can result in significant bottlenecks.

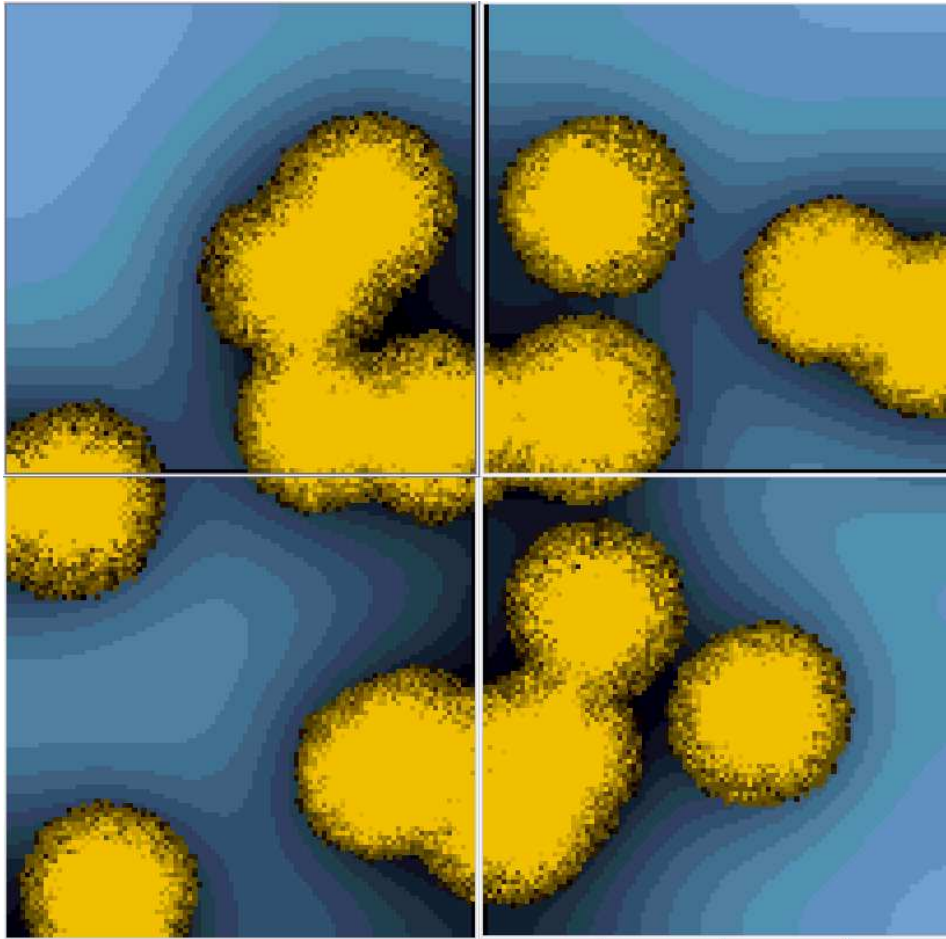


Figure 3.12: Screenshot of Micro-Gen simulation running in parallel on four computing nodes, with bacterial colonies (yellow) growing on nutrient agar medium (blue). Lighter shade of blue represents higher nutrient concentration, and lighter shade of yellow represent higher bacterial biomass in patch.

For this reason, particular emphasis has been placed on optimizing the communication strategy for sending bacterial agents between different computer nodes in Micro-Gen, while ensuring the integrity of the information in transit. At each iteration of the main program loop, data of the same type that has to be transferred between nodes is collected into communication buffers and then sent as a single large message, rather than a series of smaller individual messages in order to minimize the latencies associated with multiple message calls. Advances in communication

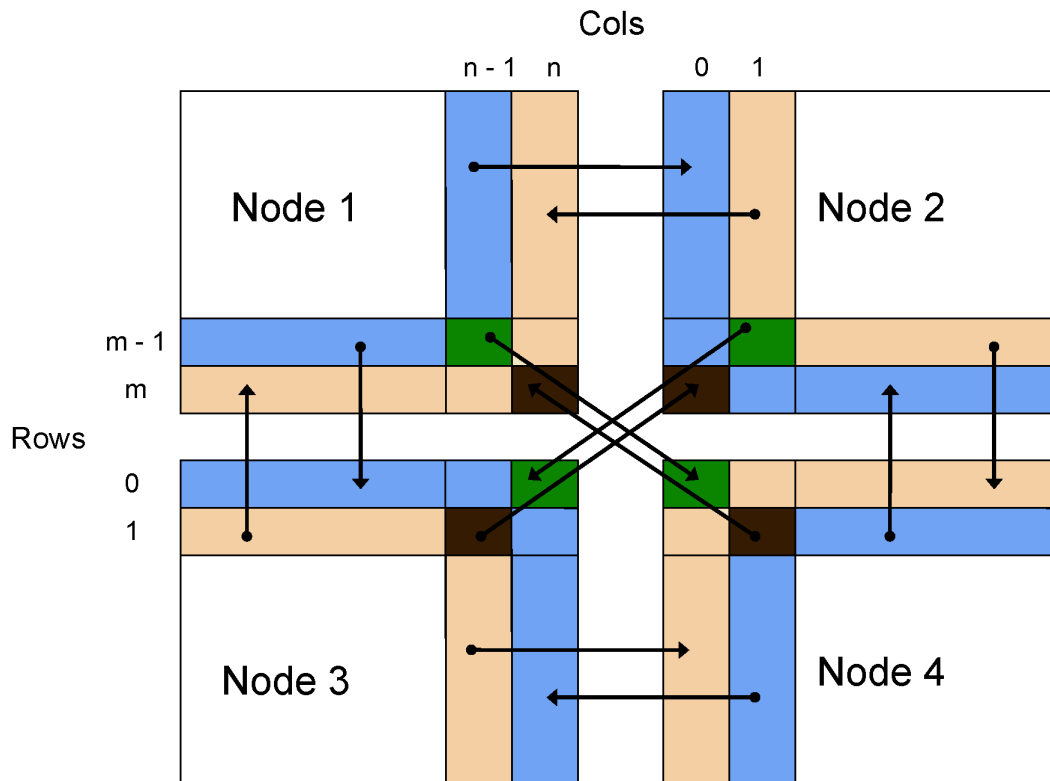


Figure 3.13: Schematic representation of communication between adjacent nodes when Micro-Gen is run in a parallel configuration. Overlapping boundary conditions are shaded.

technology for connecting computer nodes within clusters have also minimized the overheads associated with communication traffic.

The movement of bacteria between nodes is complicated by the fact that MPI has no in-built mechanisms for communicating software objects between nodes. Therefore, the constituent cell traits of the bacterial agents are communicated as basic variables. When these variables are received, pre-initialized bacterial agents from the fabric data structure are used to make a copy of the bacteria on the receiving node. The availability of a pool of pre-initialized bacterial agents minimizes the performance penalty associated with this step, since new bacterial objects do not have to be created/destroyed in memory each time a bacterial agent is sent to a

new node. This means that a simulation can be seamlessly divided among multiple processors/computers to obtain an efficient speed-up on parallel architectures.

3.3.3.1 Parallel Performance

It is important to be able to scale up the simulation to represent biologically realistic numbers of agents in order to correctly predict emergent population behaviour. The model is scalable to represent population sizes of $>10^7$ bacterial agents, so as to represent more closely the numbers found in nature. For example, when simulating the standard growth curve of a bacterial population with a maximum size of 0.5×10^7 bacteria (environment size = 1000^2 patches) it takes 158 minutes to simulate 33 hours of real-time on a local 16 x 2.8 GHz Pentium 4 computing cluster (Dell PowerEdge 1750), with the total memory footprint of the program across all nodes <512 MB. The parallel efficiency of the algorithm was found to be $>90\%$ when tested in parallel across the 16 nodes (Table 3.3) [18].

Table 3.3: Parallel Efficiency of Micro-Gen When Run on a 16 Node (Intel Xeon 2.8 GHz) Computing Cluster

<i>No. of Nodes</i>	<i>Parallel Efficiency (%)</i>
4	97.6
9	97.2
16	91.1

The communication overheads associated with sending agents between nodes are minimized by the use of the ‘fabric’ data structure containing a pool of pre-initialized bacterial agents (see above). A defragmentation routine is applied to the bacterial fabric to prevent efficiency losses accumulating as agents are interchanged between nodes. Without this defragmentation step, the overall execution time would increase by over four-fold for the test conditions above due to gradual fragmentation

of the fabric data structure.

CHAPTER 4

POPULATION DYNAMICS

4.1 Overview

Micro-Gen is a highly scalable, parallel model that can be used to test theoretical assumptions about bacterial cell biology and how it affects overall population dynamics. A number of test simulations were carried out to explore the mechanistic basis of the model and how changes in the input parameters affect the model output. This involved testing situations or parameter values that may not occur in nature (so-called ‘strong cues’) in order to gain insight into the mechanisms important for the model output. Examining extreme or hypothetical scenarios is an important step in developing an agent-based model, due to its inherent complexity, in order to understand how the model works and identify potential limitations [13].

4.2 System Dynamics

For the test simulations, the effect of one parameter was investigated while all other parameters were kept constant in order to isolate the influence of the particular parameter under investigation. For the same reason, the test simulations involved

a phenotypically homogeneous bacterial population growing in a heterogeneous environment. This is to avoid any ambiguity in the output resulting from random factors related to different competing sub-populations. However, the strength of the agent-based approach exists in being able to easily introduce this heterogeneity into the model in order to study more complex situations, which will be the topic of future work.

The strain of bacteria modelled in these simulations was MRSA, a clinically important pathogenic strain (see Chap. 3). The dimensions of the environment were 1000 x 1000 patches or grid elements (approximately 1 mm^2 in real-world) with each patch containing 80000 simulation units (called “biomass units”) of nutrient. Biomass units are used to express the amount of nutrient available relative to the bacterial nutrient intake rate ($10 \text{ b.u. loop}^{-1}$).

4.2.1 Standard Bacterial Growth Curve

Populations of bacteria follow a standard growth curve consisting of lag, log, stationary and death phases, when grown in nutrient limited culture conditions. During the initial lag phase, there is no net increase in cell numbers as the cells adapt to their new conditions. The log phase is when the bacterial numbers increase exponentially until nutrient or space constraints limit their growth and they enter the stationary phase. The final death phase occurs when the available nutrient reserves have been exhausted. This behaviour is reproduced in the model by incorporating five key parameters: lag phase length; nutrient intake rate/biomass threshold for division; survival cost; and relative stationary phase metabolic rate (see Chap. 3).

The lag phase is the initial period after inoculation in fresh culture medium when cell division has not begun to occur [83]. During this phase, the bacteria

begin to synthesize macromolecules required to transport and process the nutrients from their new environment. Once they have adapted to their environment, cell division begins to occur and the bacteria enter the logarithmic phase of growth. This is typified by an exponential rate of increase in cell numbers until nutrient availability or accumulation of waste products begins to limit growth.

When the nutrient content of the medium has been exhausted, the bacteria typically enter the stationary phase where no net increase/decrease in cell numbers is observed. Bacteria in this phase are characterised by a metabolically less active and more resistant state [84, 85]. A low level of endogenous metabolism is maintained and the rate of protein turnover by the cell increases. However, as nutrient starvation persists, eventually most of the cells enter the death phase, characterised by an exponential decrease in viable cell counts.

The length of the lag phase is influenced by the energy state of the cells when they are added to the environment and the lag phase length parameter. Each cell is randomly set with a particular energy state (in biomass units) at the start of the simulation. The maximum rate of growth during the exponential phase is determined by the nutrient intake rate relative to the biomass threshold for division (see Chap. 3). The effect of the survival cost parameter can be seen in Figure 4.1A by varying over a range of 1 - 64% (relative to nutrient intake rate), i.e. with a value of 1%, the bacterial cell burns up approximately 1% of the nutrient it absorbs in normal metabolic activities per loop. A survival cost input value of 8% or more results in no apparent stationary phase for the simulated population as a whole, but instead the population immediately enters the death phase following the exponential phase. Also, the relative stationary phase metabolic rate parameter is important for determining the length of the stationary phase (Fig. 4.1B). However, it has no influence on the exponential phase or entry into the stationary phase.

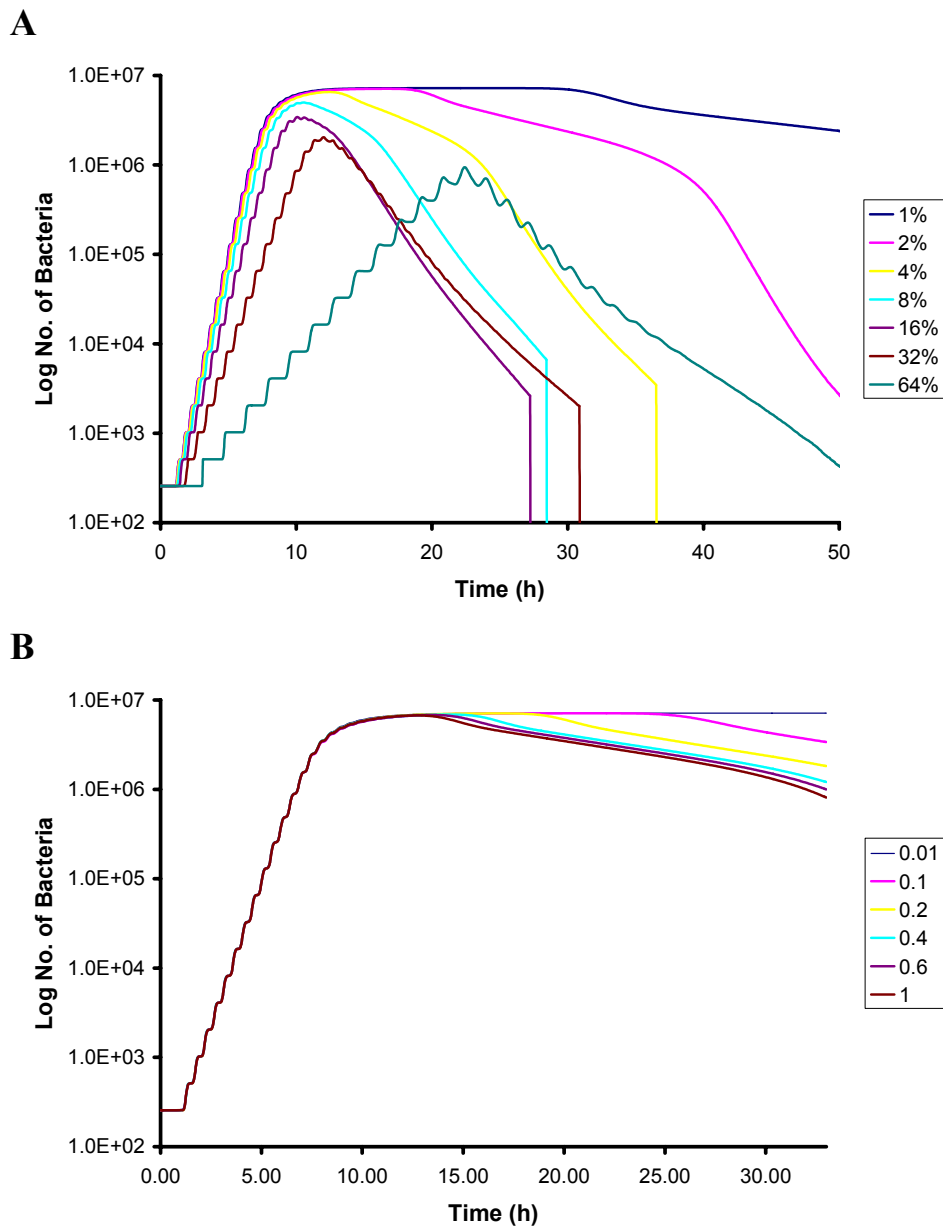


Figure 4.1: Log growth curves of simulated MRSA bacterial agents grown under simulated *in vitro* culture conditions with different input values for: **(A)** “Survival Cost” parameter (1% - 64%) - values represented as a percentage of the bacterial nutrient intake rate ($10.0 \text{ b.u. loop}^{-1}$ - see Chap. 3); **(B)** “Stationary Phase Relative Metabolic Rate” (0.01 - 1.0) - representing the relative survival cost during the stationary phase when the bacterial cells enter a state of reduced metabolic activity induced by severe stress such as nutrient deprivation.

4.2.2 Antibiotic Intake Rate

Figure 4.5 shows results from varying the antibiotic intake rates for penicillin G, ampicillin and cephalothin on the length of time bacterial growth is inhibited by the antibiotics. The antibiotic intake rate is proportional to the amount of PBP proteins in the cell membrane of *S. aureus*. As this parameter is increased, more antibiotic is bound per time step, thus depleting the available reserve in the local environment more quickly. A range of values was explored in order to assess the impact of this parameter on the model.

The intake rate parameter was varied in the range 10^{-10} to $10^{-5} \mu\text{M loop}^{-1}$ to investigate how this influences the output of the simulation. For cephalothin, the rate of antibiotic intake does not have any significant effect on the inhibition time of the drug over the wide range of values tested. For penicillin G and ampicillin, the antibiotic intake rate directly influences the inhibition time up to a certain point. However, interestingly, in the range 10^{-8} - 10^{-5} there is no significant change in the inhibition times. Therefore, there seems to be an upper limit (10^{-8}), in the context of this model, above which a higher number of PBPs in the cell membrane does not affect the efficacy of the antibiotics.

For all further test simulations, an antibiotic intake rate of 6.0×10^{-8} was chosen which represents a comparatively high number of PBP proteins in the cell membrane. This was chosen in order to represent the worst case scenario in terms of drug treatment success, i.e. an MRSA bacterial cell that expresses a high number of PBP proteins will be inherently more resistant to β -lactam antibiotics. However, future work will include expanding the model to include a more detailed quantitative representation of the interactions of the antibiotic molecules not only with PBP2a, but also with the other PBPs (1 - 4) characteristic of *S. aureus* bacteria, using exper-

imentally estimated data about the total number of PBP copies per cell [86]. Then a better quantitative estimation of the antibiotic intake rate would be able to be made.

4.2.3 Antibiotic Half-Life

In order to explore the effects of antibiotic half-life on the outcome of treatment of MRSA, this parameter was varied over a range of 5 minutes to 8 hours for the antibiotics penicillin G and cephalothin (Fig. 4.2). These two antibiotics were chosen in order to illustrate the different responses that can occur to changes in half-life depending on the type of antibiotic used. Cephalothin is predicted to be strongly sensitive to changes in half-life. For example, increasing the half-life from 30 minutes to 480 minutes results in a ten-fold increase in the length of time MRSA growth is inhibited by the antibiotic. However, for penicillin a similar change in half-life results in less than a 10% increase in inhibition time.

The half-life of an antibiotic can be an important determinant of treatment success. It varies considerable depending on environmental conditions, and in particular the half-life of an antibiotic *in vivo* (i.e. in a patient) is often considerably reduced compared to *in vitro* laboratory conditions. Therefore, it is useful to understand the impact of the half-life parameter on our predicted results for antibiotic efficacy.

It is interesting to note from the results that penicillin G is not as sensitive to half-life changes as cephalothin is. A possible explanation for this is that it is due to the different reaction profiles of cephalothin and penicillin G with MRSA. As will be discussed further in the next chapter, cephalothin is relatively resistant to β -lactamase enzymes (low k_{cat}/K_M) secreted by the MRSA bacteria. Cephalothin binds slowly to penicillin-binding protein 2a (PBP 2a) in the bacterial cell mem-

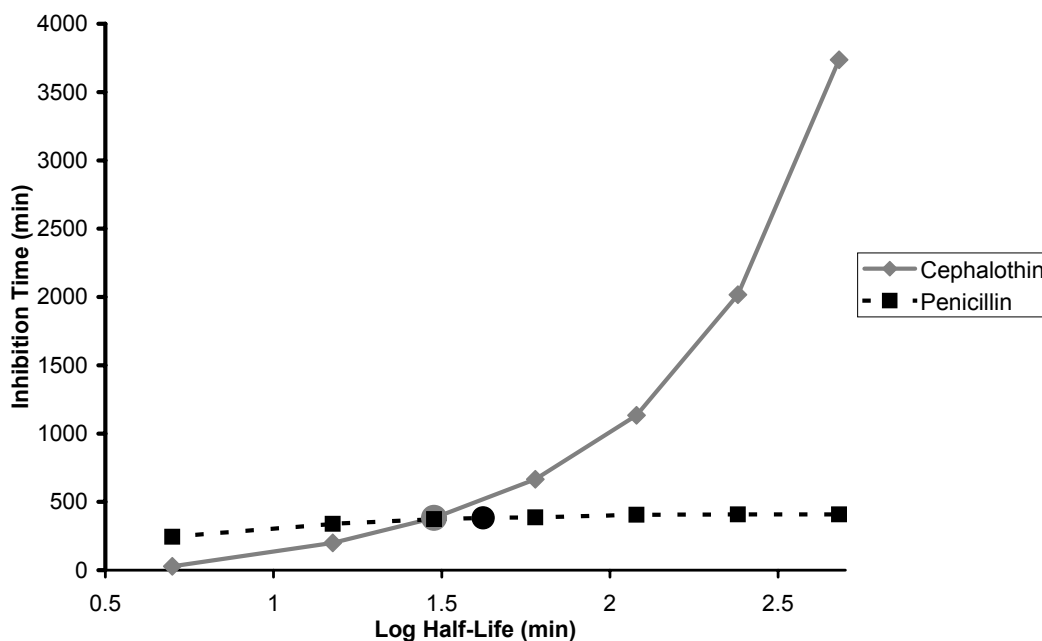


Figure 4.2: Predicted effect of half-life parameter of antibiotic molecules on length of time bacterial growth is inhibited. Antibiotic added after 4.4 hours of simulated time, during exponential phase of growth. Cephalothin = 103.1 $\mu\text{g/ml}$; Penicillin G = 72.1 $\mu\text{g/ml}$. Round points represent default input values for half-life parameters (Ceph, = 30 min; Pen G = 42 min) [57].

brane, and increasing the half-life directly improves efficacy by allowing more antibiotic to survive for a longer time to bind to the MRSA. Penicillin G on the other hand is cleaved more rapidly by β -lactamase enzymes in the environment and therefore, increasing its half-life does not improve the efficacy since it is rapidly destroyed by the β -lactamases.

4.2.4 Diffusion Rate

In order to investigate the effects of nutrient availability on the growth and development of bacterial colonies the user-defined diffusion coefficient for Fick's First Law of diffusion was varied over the range 0.0 - 0.2, where a larger co-efficient means a higher rate of diffusion (Fig. 4.3). The rate of diffusion is an important param-

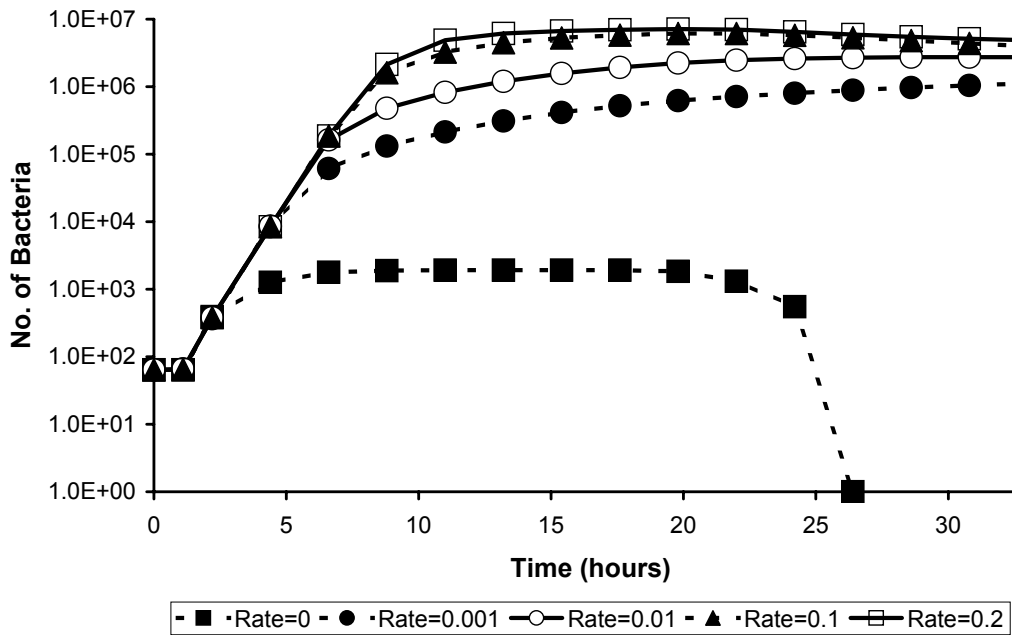


Figure 4.3: Effect of rate of diffusion on log growth curves of simulated MRSA bacterial agents grown under simulated *in vitro* culture conditions. The diffusion co-efficient for Fick's First Law of diffusion was varied between 0.0 - 0.2. The characteristic phases of the standard bacterial growth curve (lag, log, stationary and death phases) are observable. Environment size = 1000^2 patches. Cellular input parameters listed in Chapter 3.

eter dictating population development as it limits the transfer of nutrients towards the interior of a bacterial colony. The diffusion co-efficient for Fick's First Law of diffusion may be configured to represent different environments by calibrating with experimental results. However, for the tests here the aim was to give a more generalised assessment of the mechanistic influences of the diffusion algorithm on model output. It must be noted that the diffusion algorithm applies to molecular movement between patches, not within a patch. Each discrete patch, or grid element, is assumed to have a homogeneous concentration of molecules.

As can be seen in figure 4.3, in the absence of diffusion (rate=0.0) the bacterial growth curve still follows the four standard stages expected under *in vitro* culture conditions. However, the maximum population size is severely limited due

to the lack of nutrient transport between patches. This could explain why bacterial colonies tend to thrive better in conditions of water availability where nutrients are more readily transported by diffusion. In arid conditions, the lack of nutrient diffusion would be a significant growth-limiting factor, aside from problems associated with desiccation.

When a trace amount of diffusion (rate = 0.001) is applied, the maximum bacterial population size increases by 2 - 3 orders of magnitude over conditions where diffusion is absent. However, as the diffusion rate is increased the maximum bacterial population size is limited by the total nutrient content (carrying capacity of the environment). Higher diffusion rates result in the population peaking in a shorter time, but the carrying capacity remains similar. It can be concluded from this that environments with high rates of diffusion do not confer an advantage to bacterial colonies in terms of the overall population sizes they support. However, these conditions may allow the colony to gain a foothold more quickly allowing a critical mass to be developed which is more resistant to external stresses.

When antibiotic is added to the bacterial cultures, the rate of diffusion in the environment can have a significant impact on the efficacy of the antibiotic. To investigate this, the length of time bacterial growth was inhibited (which is a measure of antibiotic efficacy) was recorded over the range of diffusion coefficient values 0.001 - 0.2, using kinetic parameters for three common antibiotics: penicillin G, ampicillin and cephalothin (Fig. 4.4). The results show a significant positive correlation (Pen G: $r > 0.992$, $p < 0.01$; Amp: $r = 0.993$, $p < 0.01$) between the rate of diffusion and the inhibition times for penicillin G and ampicillin. However, for cephalothin the diffusion rate has no effect on the length of time growth is inhibited ($r = 0.0$).

The effect of environmental conditions such as the rate of diffusion can have an

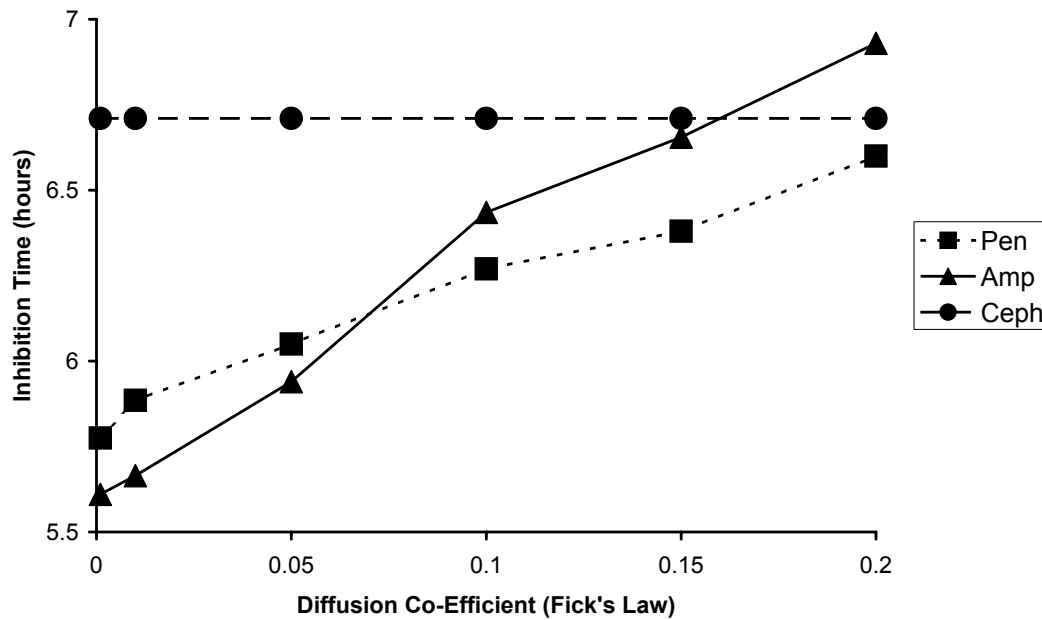


Figure 4.4: Effect of varying diffusion co-efficient of Fick's First Law of diffusion (0.001 - 0.2) on the length of time bacterial growth is inhibited after addition of antibiotic to the environment. The antibiotic was added (time = 4.4 hours) during the exponential phase of growth of a population of Type A β -lactamase-producing MRSA. Population size = $\sim 10^5$ agents; environment size = 1000^2 patches. The concentration of each antibiotic was: penicillin G (Pen) = $66.9 \mu\text{g/ml}$, ampicillin (Amp) = $69.9 \mu\text{g/ml}$, and cephalothin (Ceph) = $118.9 \mu\text{g/ml}$. Cellular and kinetic input parameters listed in Chapter 3.

important impact on antibiotic treatment outcome. For example, it has been found that some bacteria can form structured communities of cells such as biofilms, where the rate of diffusion within the colony is significantly reduced [87]. The results from this computational analysis clearly indicate that a decreased rate of diffusion can result in reduced antibiotic efficacy, depending on the type of antibiotic, and therefore increase the bacteria's survival chances.

Cephalothin, which is unaffected by variations in the diffusion rate, differs from penicillin G and ampicillin in that it is a poor substrate for the β -lactamase enzyme produced by MRSA bacteria. Penicillin G and ampicillin are both rapidly cleaved by β -lactamase enzymes secreted into the immediate environment of the bacterial

cells, and the diffusion rate limits the rate at which the antibiotic is replenished. For cephalothin, it is more resistant to cleavage by β -lactamase enzyme and as a result the local concentration of antibiotic does not decrease significantly. Instead, the factor that limits the efficacy of cephalothin is the rate of binding to the bacterial cells, which is not influenced by the diffusion rate. This situation indicates how the specific biochemical profile of the antibiotic and its interactions with local environmental factors can have a significant impact on its reaction to changing environmental conditions.

Knowledge of how antibiotics react under different conditions could inform the rational development of drug treatment regimens. For example, when treating bacterial infections where there is poor transport of antibiotic by diffusion (e.g. biofilms), the model indicates that the susceptibility of the antibiotic to β -lactamase plays a larger role than under normal free-diffusing conditions. This may result in deviations between the expected behaviour as determined from laboratory experiments and the actual real-world outcome.

4.2.5 Population Size (Inoculum Effect)

The Minimum Inhibitory Concentration (MIC) of an antibiotic is defined as the minimum concentration of an antibiotic required to inhibit growth of a bacterial culture *in vitro*. Micro-Gen has been used previously to predict the MICs of antibiotics by inputting relevant kinetic parameters for them [18, 88]. The present manuscript provides a detailed overview of the model structure and parameters used to describe the bacterial cells and focuses on the effects of changing environmental conditions and population size on the development of an MRSA colony.

The MIC is an emergent property of the population that results from the in-

teractions of the individual bacterial agents and antibiotics. However, it is sometimes difficult to relate information from cellular and molecular studies with this high-level population parameter. The Micro-Gen model provides a good theoretical framework for bridging this gap of knowledge between fundamental studies at the individual level and high-level population parameters such as the MIC.

Figure 4.6 shows results from simulations investigating the effect of population size (inoculum effect) on the MICs of a number of common β -lactam antibiotics against MRSA. Three types of MRSA bacteria were tested: Type-A (Fig. 4.6A) and Type-C (Fig. 4.6B) β -lactamase producing strains, and a β -lactamase-negative strain (control). The strains are differentiated by their unique kinetic parameters and β -lactamase production rates (see Chap. 3). The β -lactamase production rates were estimated as described in chapter 3, and the antibiotic intake rate was chosen as described above. The diffusion rate for the environment was set to 0.1 to ensure that bacterial growth was not diffusion-limited (see Fig. 4.3).

When the population size is varied by several orders of magnitude the results indicate that the β -lactamase status of the bacterial cells is an important contributor to the inoculum effect on the MIC (Fig. 4.6A, B). There is no clear inoculum effect associated with cephalothin against either Type-A or Type-C β -lactamase producing MRSA strains over the range of population sizes tested. This is consistent with the fact that cephalothin is a poor substrate for either type of β -lactamase. In the case of larger population sizes, the total concentration of β -lactamase available to bind and de-activate antibiotic is increased. However, since cephalothin is a poor substrate for the β -lactamase, the increased enzyme concentration does not have a significant impact on the MIC. Rather the binding reaction between cephalothin and PBP2a in the cell membrane of MRSA is the limiting factor for cephalothin's efficacy. It binds poorly to PBP2a, relative to penicillin G and ampicillin, which

results in a high MIC that remains unchanged over the range of population sizes tested.

Penicillin G and ampicillin are better substrates for cleavage by β -lactamase enzyme. As a result, the MIC increases in response to higher concentrations of enzyme in the environment. So even though penicillin G is shown to be more effective than cephalothin at low population sizes, in the case of larger sizes ($>10^6$ bacterial agents) the advantage is negated. Experimental studies of various strains of β -lactamase producing *S. aureus* have also shown a significantly larger inoculum effect for penicillin G compared to cephalothin [89, 90].

The variation in the MIC of an antibiotic with different bacterial population sizes is an important factor to consider when determining drug treatment regimens. The stage of development of a bacterial infection and the number of bacteria present at any given time can vary from patient to patient and over the course of a treatment course. Therefore, it is useful to be able to quantify the impact of these changes on the response of bacterial colonies to treatment.

4.2.6 β -lactamase Production Rate

Another important parameter that influences the MIC of a β -lactam drug is the β -lactamase production rate. This can vary by several orders of magnitude between different strains of MRSA. Therefore, it is important to assess the impact of this parameter on model output. In order to do this, simulations were carried out over a range of production rate values in order to illustrate the different effects it has depending on the type of drug used (Fig. 4.7).

The results clearly show that for antibiotics that are sensitive to cleavage by β -lactamase, such as penicillin G and ampicillin, there is a strong positive correlation

between the enzyme production rate and the MIC of the drug (Pen G: $r=0.999$, $p < 0.01$; Amp: $r=0.998$, $p < 0.01$). On the other hand, cephalothin, which is relatively resistant to cleavage by the enzymes has no correlation between its MIC and the β -lactamase production rate ($r=0.0$). A more detailed discussion about the effects of the kinetic parameters on cleavage of antibiotics molecules by β -lactamase is presented in the next chapter.

4.3 Conclusions

These initial results indicate that the emergent effects from the population dynamics can have a dramatic impact on the efficacy of antibiotics. This must be taken into account in the rational development of drug treatment regimens, as differences in environmental conditions and bacterial phenotypes may result in varied responses between individual patients. Micro-Gen provides a good theoretical framework for investigating these effects in the context of a simulated environment. The agent-based modelling approach can be used to understand the relationships and complex sets of interactions taking place between the individual components of the system and how they contribute to the high-level population dynamics. The value of the model in making quantitative predictions depends on the availability of good experimental data about individual bacterial cells. However, it can also be used as tool for developing a better mechanistic understanding of population dynamics by varying key parameters and observing how they determine the model output.

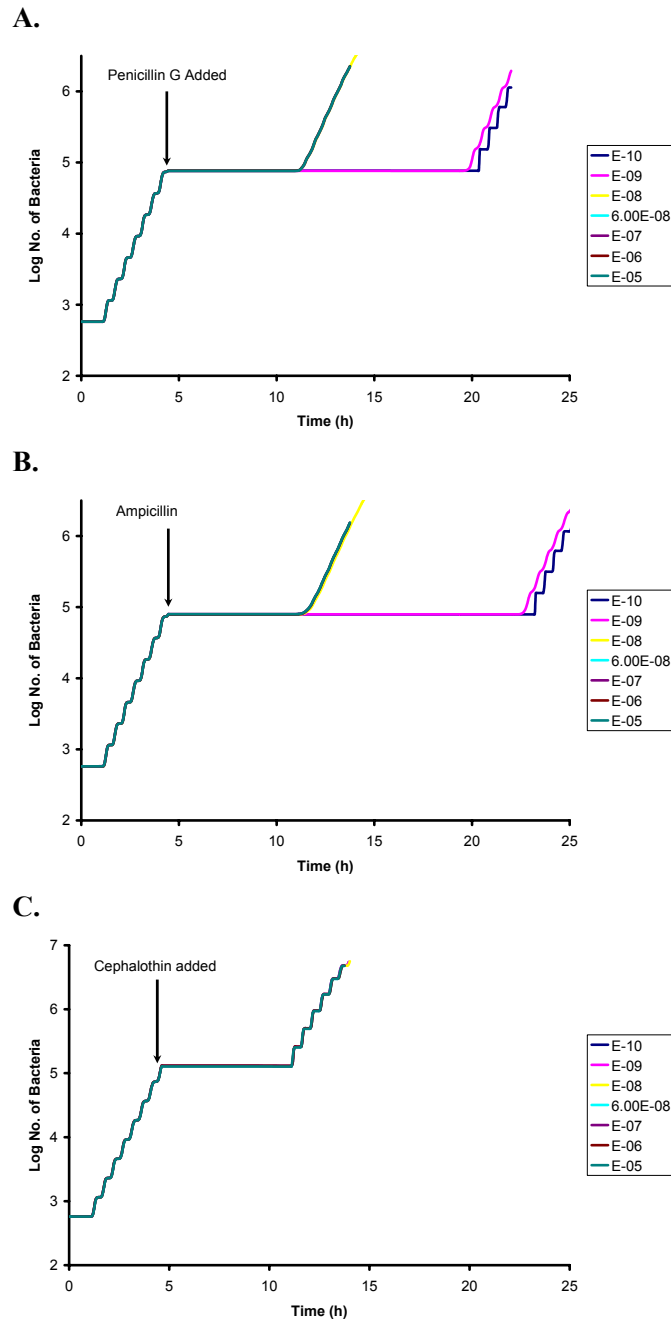


Figure 4.5: Effect of antibiotic intake rate on log growth curves of simulated MRSA bacterial agents grown under simulated *in vitro* culture conditions. The antibiotic intake rate was varied over the range 10^{-10} - 10^{-5} $\mu\text{M loop}^{-1}$ to examine its impact on the length of time bacterial growth is inhibited by the antibiotic. 71.9 $\mu\text{g/ml}$ of Penicillin G (A), 62.9 $\mu\text{g/ml}$ of Ampicillin (B) or 119 $\mu\text{g/ml}$ of Cephalothin (C) were added after 4.4 hours of growth, when the simulated bacterial colonies were in the exponential phase of growth.

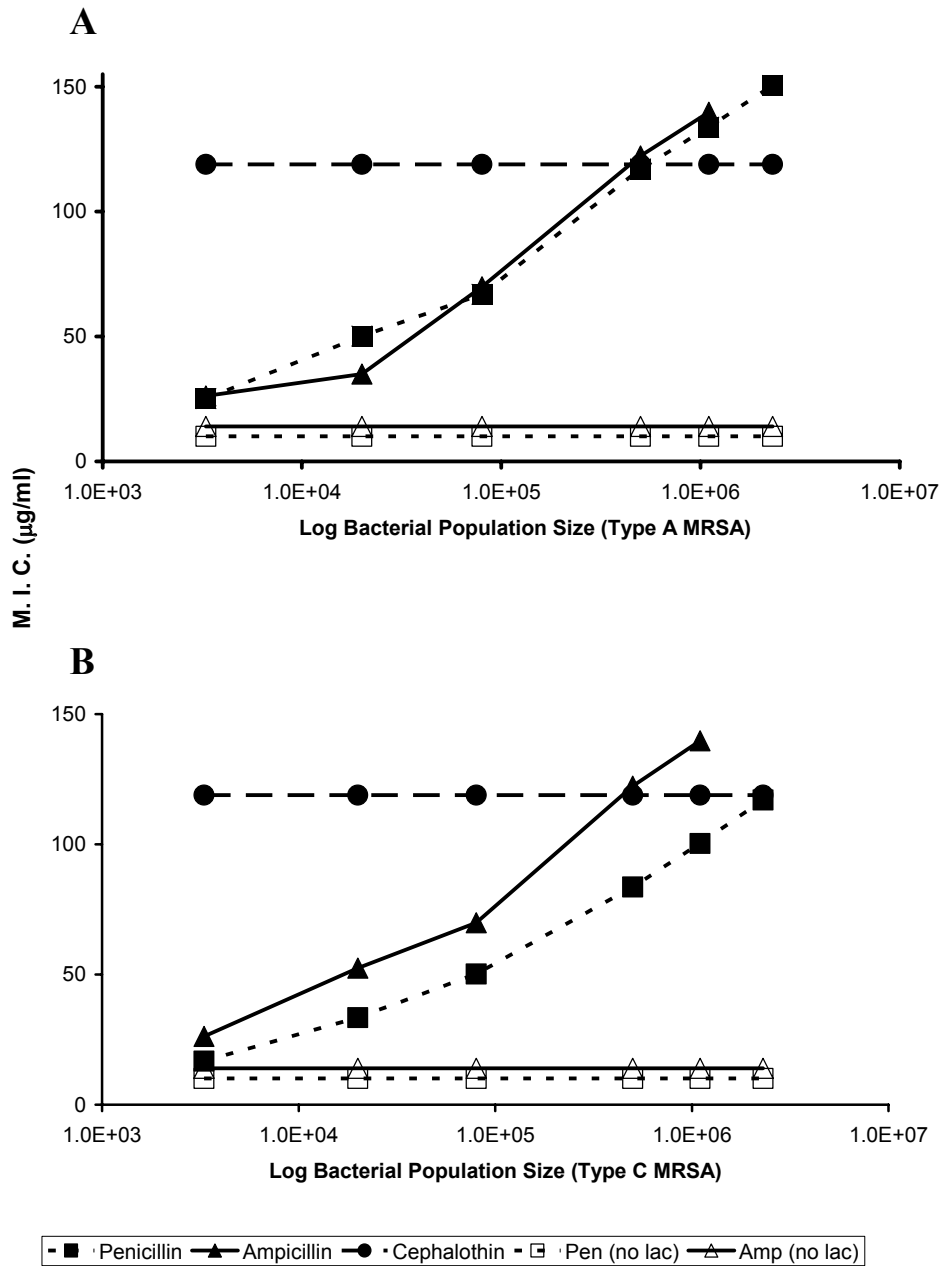


Figure 4.6: The effect of the bacterial population size (“inoculum effect”) on the Minimum Inhibitory Concentrations (MICs) of penicillin G (Pen), ampicillin (Amp) and cephalothin (Ceph) against MRSA. Antibiotic was added (time=4.4 hours) during the exponential phase of bacterial growth, and environment size was 1200^2 patches. Results from β -lactamase-negative MRSA (no lac) included as control. Cellular and kinetic input parameters are listed in Chapter 3. (A) Type A β -lactamase-producing MRSA. (B) Type C β -lactamase-producing MRSA.

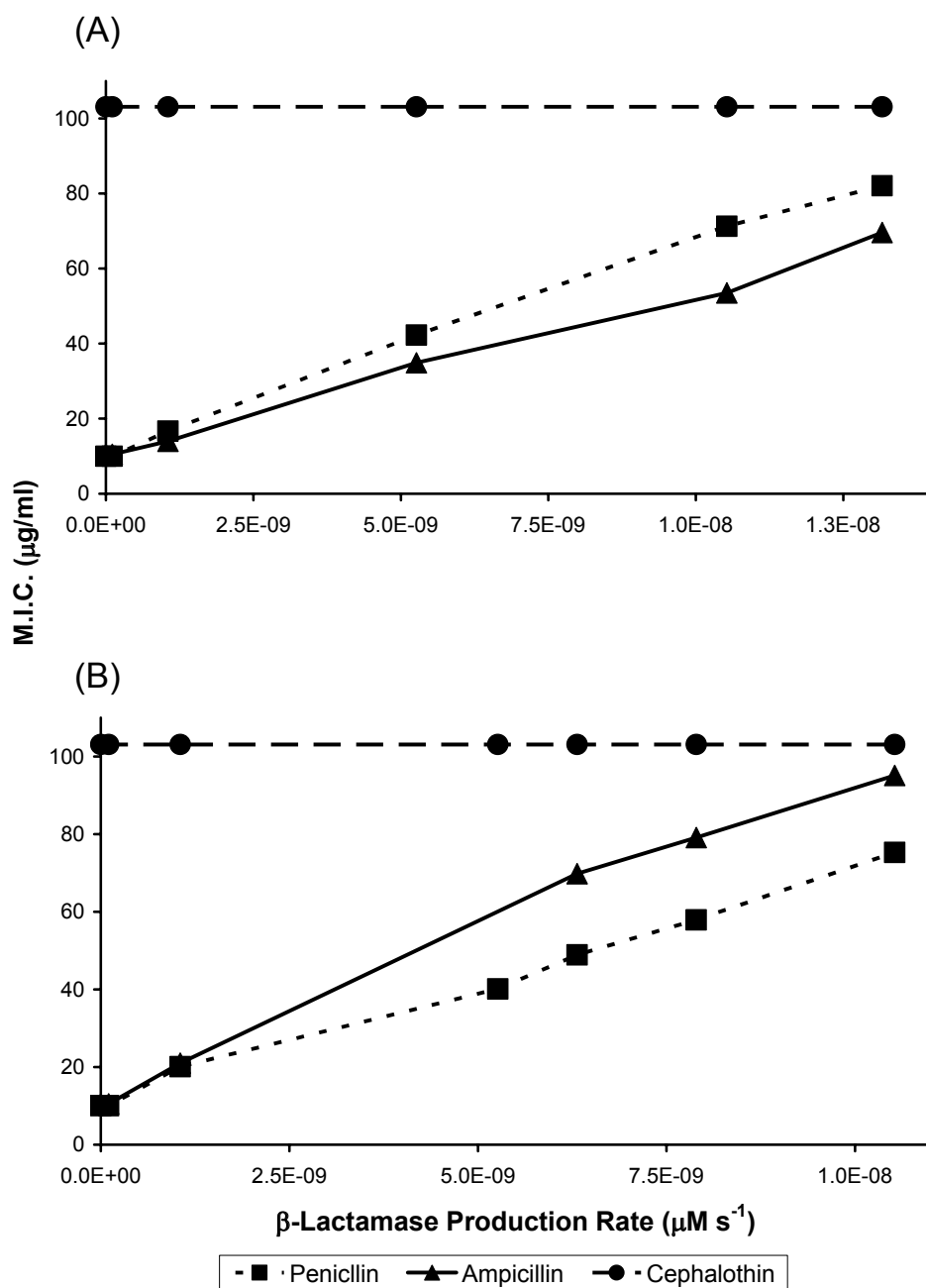


Figure 4.7: Predicted Minimum Inhibitory Concentrations (M.I.C.) for penicillin G, ampicillin and cephalothin from Micro-Gen model over a range of different β -lactamase production rates for Type A (A) and Type C (B) β -lactamase-producing MRSA bacteria. This data was used to estimate the β -lactamase production rate for each bacterial strain by cross-referencing with the experimentally determined MICs of penicillin G (Type A MRSA = 72.1 $\mu\text{g/ml}$, Type C MRSA = 47.9 $\mu\text{g/ml}$) [1].

CHAPTER 5

KINETIC STUDIES

5.1 Overview

This chapter documents the results of integrating antibiotic resistance mechanisms into the bacterial agents, representing MRSA, and analyzing the system dynamics of their interactions with some common β -lactam antibiotics. The aim of these tests is to quantify the effects of the principal pharmacokinetic parameters of β -lactam antibiotics on treatment outcome, and assess their impact in terms of some common high-level measures of antibiotic efficacy such as the minimum inhibitory concentration (MIC).

The complex relationship between the kinetics of drugs and emergent pharmacodynamic parameters, such as the MIC, is an important area to explore for the rational development of drug treatment regimens [69]. This provides a basis for understanding the dynamics involved in the development of antibiotic resistance, and help to develop strategies to limit its expansion. Micro-Gen represents a good theoretical framework for analysing the *in vitro* dynamics of antibiotics interacting with bacteria, though further work could involve extending the model to represent the more complex dynamics found in the *in vivo* clinical setting.

A set of input parameters, summarized in Table 5.3, are configured to represent the attributes of the bacterial agents and the culture environment. For this study, the model was configured to represent MRSA bacteria growing in agar plate culture. Parameters applicable to three types of MRSA bacteria were used, which are differentiated by their β -lactamase status: type A MRSA and type C MRSA are named because they produce β -lactamase enzymes of these respective types. A β -lactamase-negative strain was also included.

Type A and Type C β -lactamase enzymes are distinguished by their kinetic parameters (k_{cat}/K_M) which are derived from experimental literature (see Table 5.3). They were chosen for this study because they are the most common types of β -lactamase found in MRSA bacteria. A study by Norris *et al.* (1994) found that among 50 β -lactamase-producing MRSA isolates taken from nine locations across the U.S.A., 80% expressed type A β -lactamase and the remainder expressed type C. Type B and type D β -lactamases are thought to be less common among MRSA strains [1].

5.2 Minimum Inhibitory Concentration

5.2.1 Overview

Figure 5.1 shows the simulated growth curve of an MRSA bacterial colony in Micro-Gen. The effect of adding an inhibitory dose (103.1 $\mu\text{g}/\text{ml}$) of cephalothin antibiotic after 3.5 hours of incubation on the growth curve is also shown. The control culture of MRSA, where no antibiotic is added, displays the characteristic standard growth curve of bacteria grown in nutrient-limited culture conditions (see chapter 4). The addition of antibiotic during the exponential phase of growth

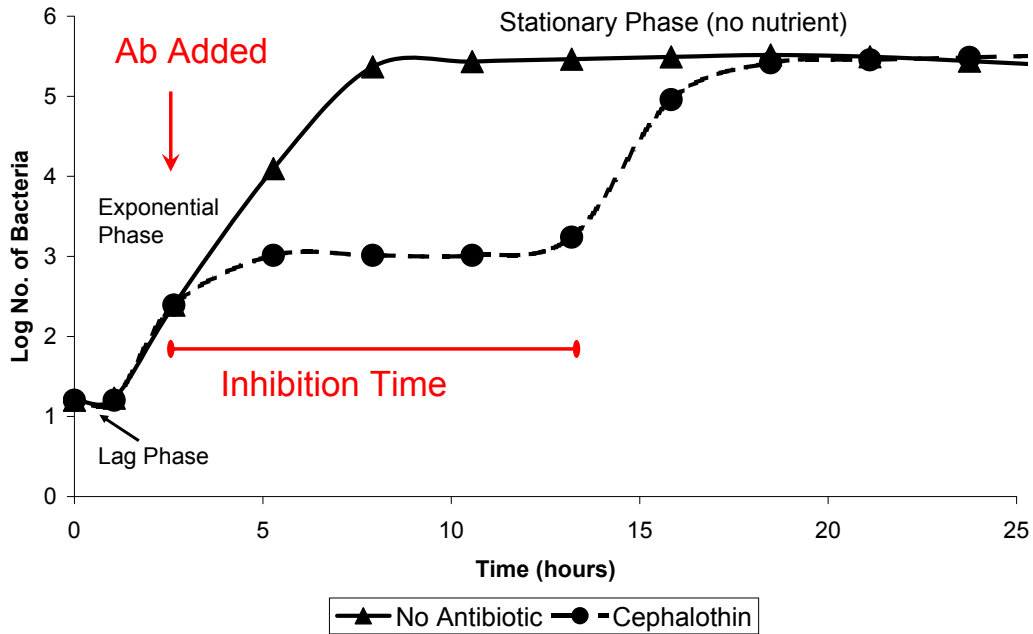


Figure 5.1: Effect of antibiotic exposure on simulated log growth curve of MRSA bacteria in nutrient-limited culture conditions. Cephalothin antibiotic ($103.1 \mu\text{g/ml}$) added after 3.5 hours of incubation, during the exponential phase of colony growth. This results in inhibition of colony growth for a period of time (inhibition time) until depletion of antibiotic according to its natural half-life, or hydrolysis by enzymes such as β -lactamases, allows growth to resume.

causes inhibition of growth for a limited period of time. The length of time bacterial growth is inhibited is important as it determines the recommended dosage regimen for an antibiotic. It is affected by factors such as the half-life of the antibiotic, and the action of bacterial enzymes, such as β -lactamases, which degrade the antibiotic molecules.

The Minimum Inhibitory Concentration (MIC) was calculated from the model for a number of common β -lactam antibiotics against MRSA, and compared with real-world results. The MICs are estimated from the model in an analogous way to the broth dilution test carried out in the experimental environment: a series of simulations are carried out with varying concentrations of antibiotic applied. The

minimum concentration of antibiotic that results in complete inhibition of bacterial growth for a pre-determined length of time is recorded as the MIC.

Prior to carrying out a simulation to predict the antibiotic MIC against a specific strain of bacteria, the β -lactamase production rate per second per bacterial agent must first be estimated by calibrating with a known MIC of an antibiotic (in this case penicillin G was used for calibration). The process involves predicting the MIC of penicillin G from the model over a range of β -lactamase production rates. The production rate that gives an MIC equivalent to the experimentally determined value for penicillin G (in this case Type A MRSA = 72.1 $\mu\text{g/ml}$, Type C MRSA = 47.9 $\mu\text{g/ml}$) is then used in all future simulations for that particular strain [1]. The β -lactamase production rate must be estimated on a strain by strain basis due to potential significant variation between strains. For this study, the estimated β -lactamase production rate for Type A MRSA was $3.28 \times 10^{-7} \mu\text{M s}^{-1}$ per bacterial agent and for Type C it was estimated to be $1.62 \times 10^{-7} \mu\text{M s}^{-1}$ per agent.

5.2.2 Predicted MICs

Figure 5.2 contains the predicted MIC values for a number of common antibiotics compared with results from experimental studies published in the scientific literature (table 5.1) [2, 1]. The MICs of the antibiotics were calculated for three different types of MRSA bacteria: β -lactamase producing strains (Type A, Type C), and a β -lactamase negative strain. All other parameters, including the PBP2a kinetic parameters, were maintained constant across the three types of bacteria. Overall, there is a good correspondence between the predicted values from Micro-Gen and the real-world situation.

The most notable deviation between the predicted and experimentally deter-

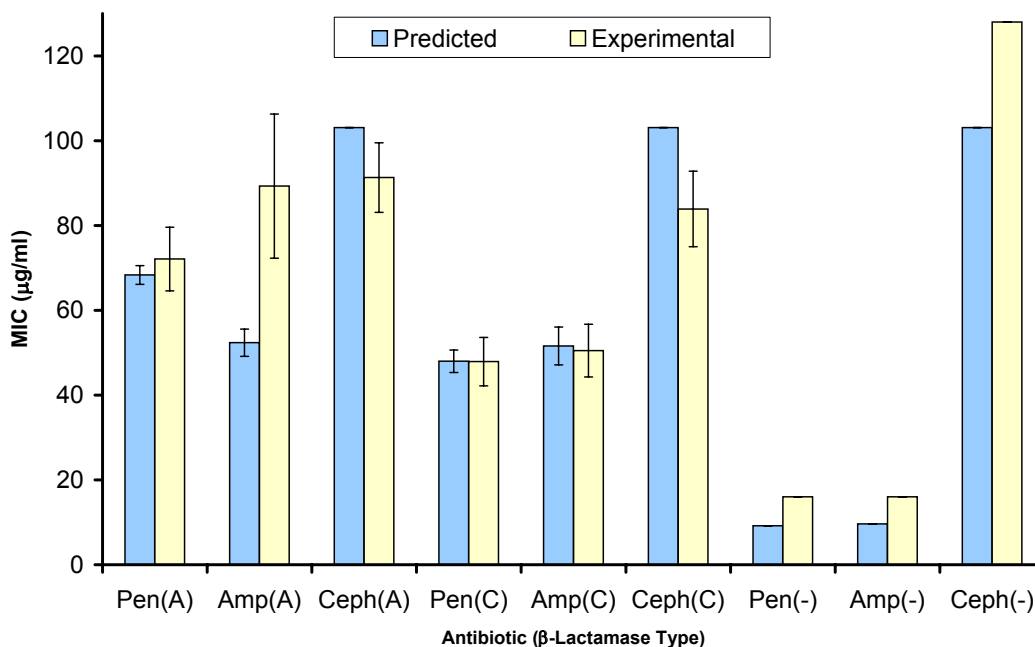


Figure 5.2: Predicted versus experimentally determined geometric mean MIC \pm SEM ($\mu\text{g/ml}$) of penicillin G, ampicillin and cephalothin antibiotics against three different types of MRSA. Experimentally determined MICs for β -lactamase-positive (Type A and C) strains are from Norris *et al.* (1994). Experimentally determined MICs for β -lactamase-negative strains are from Malouin *et al.* (2003). Predicted MICs are derived from triplicate simulations with the geometric mean MIC \pm SEM ($\mu\text{g/ml}$) displayed. Where SEM = 0, no error bar is displayed. (A) = Type A β -lactamase producing MRSA; (C) = Type C β -lactamase producing MRSA; (-) = β -lactamase-negative MRSA.

mined MIC values is when comparing the results for ampicillin antibiotic against Type A β -lactamase producing bacteria ($53.5 \pm 2.3 \mu\text{g/ml}$ versus $89.3 \pm 17.0 \mu\text{g/ml}$, respectively). This may be due to intra-species variation in the kinetic parameters for MRSA or differences in experimental methods for obtaining these values. The second order rate constant for the PBP2a-ampicillin reaction ($9.0 \text{ M}^{-1} \text{ s}^{-1}$) used in the model was derived from experimental tests by Graves-Woodward & Pratt (1998). However, another study by Fuda *et al.* (2004) has calculated the value to be $5.0 \text{ M}^{-1} \text{ s}^{-1}$ for ampicillin. When the rate constant from Fuda *et al.* for ampicillin

Table 5.1: Results from comparison of predicted versus experimentally determined MICs of penicillin G, ampicillin and cephalothin antibiotics (Ab) against three different types of MRSA. Geometric mean MIC \pm SEM ($\mu\text{g/ml}$) given. Experimentally determined MICs are from Norris *et al.* (1994) and Malouin *et al.* (2003) [1, 2].

Ab	Type A		Type C		No Lac	
	Pred	Exp	Pred	Exp	Pred	Exp
<i>PEN</i>	68.3 \pm 2.2	72.1 \pm 7.5	48.0 \pm 2.7	47.9 \pm 5.7	9.2 \pm 0.0	16 \pm 0.0
<i>AMP</i>	52.4 \pm 3.2	89.3 \pm 17	51.6 \pm 4.7	50.5 \pm 6.2	9.6 \pm 0.0	16 \pm 0.0
<i>CEPH</i>	103.1 \pm 0.0	91.3 \pm 8.2	103.1 \pm 0.0	83.9 \pm 8.9	103.1 \pm 0.0	128 \pm 0.0

was used into the model instead, it outputted a predicted MIC of 96.0 \pm 3.9 $\mu\text{g/ml}$, which is closer to that recorded by Norris (89.3 \pm 17.0 $\mu\text{g/ml}$).

Figure 5.3 show how the predicted MIC of an antibiotic depends greatly on the experimental estimates of the low-level kinetic parameters. This illustrates how variation in parameters at the molecular level can have a significant impact on overall treatment response. It is therefore important to obtain reliable, accurate estimates of the pharmacokinetic parameters for the antibiotics and bacterial strains being investigated, in order to make conclusions about the emergent dynamics of the system. There also may be significant natural variation between bacterial isolates recovered from different locations or under different conditions.

The second-order rate constants calculated by Graves-Woodward & Pratt (1998) were chosen over Fuda *et al.* (2004) because rate constants for all three antibiotics used in this study were available, while Fuda's paper did not contain kinetic values for penicillin or cephalothin. Due to variation in experimental techniques between different studies it is important to obtain parameter estimates from a single source for consistency.

Figure 5.4 contains the results from a broader analysis of the MICs of a number

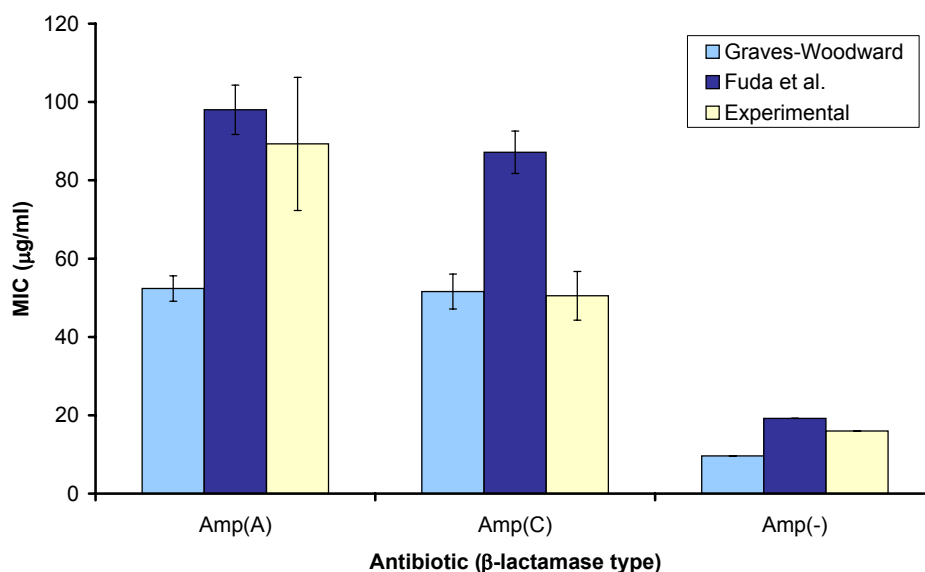


Figure 5.3: Comparison of predicted MICs of ampicillin using kinetic parameters derived from a study by Graves-Woodward & Pratt (1998) or a study by Fuda *et al.* (2004). Experimentally determined MICs are from Norris *et al.* (1994) and Malouin *et al.* (2003). Predicted MICs are derived from triplicate simulations with the geometric mean MIC \pm SEM ($\mu\text{g/ml}$) displayed. (A) = Type A β -lactamase-producing MRSA; (C) = Type C β -lactamase producing MRSA; (-) = β -lactamase-negative MRSA.

of antibiotics compared with experimental estimates of MICs from the biological literature (table 5.2) [1 - 8]. For these antibiotics, kinetic parameters were only available for the PBP2a-antibiotic binding reaction and not for the β -lactamase reaction. Therefore, only a β -lactamase-negative MRSA strain could be represented in the simulations. Nonetheless, it is useful to be able to compare the predicted MICs with those from the literature to assess the validity of the model across a broader range of antibiotics.

The predicted MICs from Micro-Gen match closely the experimental MICs across a wide selection of β -lactam antibiotics, comprising cephalosporins and penicillins, including methicillin, and imipenem, a carbapenem (β -lactam) antibi-

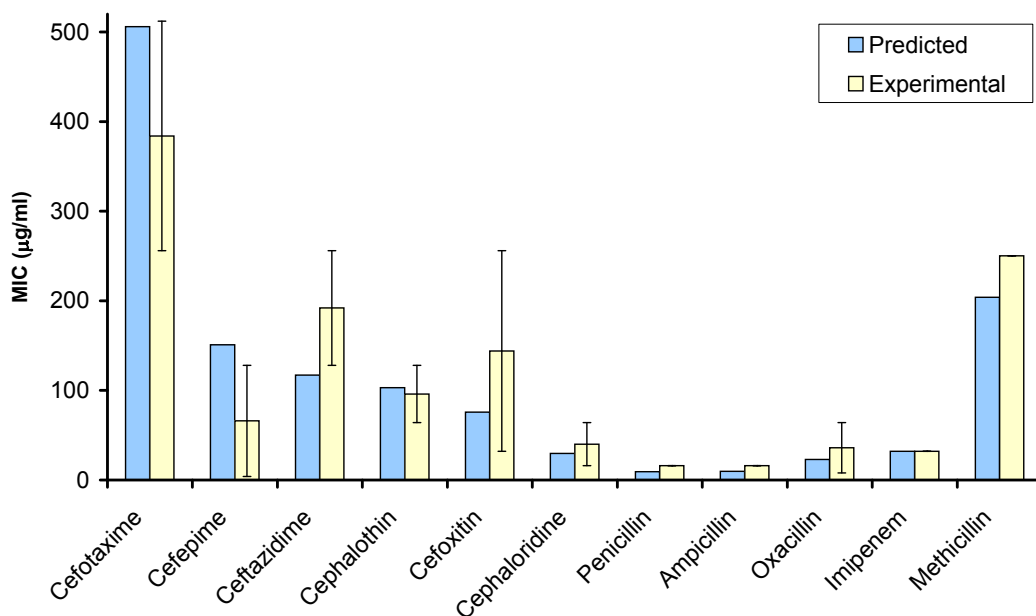


Figure 5.4: Comparison of predicted MICs and experimentally determined MICs for eleven common β -lactam antibiotics versus β -lactamase-negative MRSA bacteria. The experimental values represent the arithmetic means (\pm SEM) of the minimum and maximum MIC values found in the literature [1 - 8]. Where SEM = 0, no error bar is displayed.

otic. There is some degree of natural variation in the experimentally estimated MICs, particularly for the cephalosporins, but overall there is a clear trend in the data that matches closely with the predictions from Micro-Gen. The experimental MICs were chosen from strains of MRSA that were shown to be β -lactamase-negative or where a β -lactamase inhibitor had been administered in conjunction with the antibiotic.

5.2.3 Discussion

The results indicate that the model represents a robust tool for predicting the MIC of an antibiotic against various different strains of bacteria based on low-level bio-

Table 5.2: Results from comparison of predicted MICs and experimentally determined MICs for eleven common β -lactam antibiotics versus β -lactamase-negative MRSA bacteria. The minimum and maximum MIC values found in a review of a subset of the experimental literature are recorded [1, 2, 3, 4, 5, 6, 7, 8].

Antibiotic	Predicted MIC	Exp MIC	
		Min	Max
<i>Cefotaxime</i>	506	256	512
<i>Cefepime</i>	151	4	128
<i>Ceftazidime</i>	117	128	256
<i>Cephalothin</i>	103	64	128
<i>Cefoxitin</i>	75.7	32	256
<i>Cephaloridine</i>	29.6	16	64
<i>Penicillin</i>	9.2	16	16
<i>Ampicillin</i>	9.61	16	16
<i>Oxacillin</i>	22.9	8	64
<i>Imipenem</i>	32.1	32	32
<i>Methicillin</i>	204	250	250

chemical/kinetic data about the antibiotic [77, 78, 20, 19]. Some degree of variation from the experimental results is to be expected due to differences in the methods and conditions used in the experimental studies to calculate the MICs and the kinetic parameters for the bacteria. Also, it must be noted that the experimental results were derived from cultures grown suspended in three-dimensional liquid medium, whereas Micro-Gen represents cultures growing in two-dimensional space. This may also contribute to some of the variation between the predicted and experimentally determined results.

Nevertheless, taking these factors into account, the high degree of correspondence between the predicted and experimental MIC results is encouraging. These results were obtained without attempting to ‘fit’ the kinetic input parameters to the MIC results. The only parameter, which influences the kinetics of the bacterial

agents, that required to be fitted was the β -lactamase production rate. However, the results in figure 5.4 represent a β -lactamase-negative strain, and thus the fitting step did not have to be carried out in this case. Therefore, the predicted MICs were purely an emergent property of the inputted kinetic parameters for the PBP2a-antibiotic binding reaction. There was still a close quantitative agreement between the experimental and simulation results even in this scenario.

The Minimum Inhibitory Concentration (MIC) of an antibiotic is a common high-level measurement for assessing and comparing the efficacies of different antibiotics during the rational development of treatment regimens. These results indicate that a global parameter (MIC) for a bacterial colony can be successfully predicted by inputting parameters at the cellular/molecular level. This affords a different perspective on the factors that lead to a particular MIC being associated with an antibiotic against a specific strain of bacteria. The MIC can be de-constructed to investigate the contributions of different cellular parameters on it.

It must also be noted that the method for calculating the MICs of antibiotics experimentally is limited in its precision compared to computational predictions. For example, the experimental MICs derived from Norris *et al.* (1994) were calculated by testing two-fold dilutions of antibiotics ranging from 2 - 2,048 $\mu\text{g/ml}$ and calculating geometric means from triplicate tests [1]. This necessarily constrains the precision of the results, which may lead to some of the variation between the predicted MICs and the experimental results. The level of precision of the MicroGen model's predicted MICs can be controlled by the user by choosing the amount of different antibiotic concentrations to test. In the case of this study, incremental antibiotic concentration increases of 20% were used. Although greater precision can be obtained from experimental results by similarly testing more concentrations of antibiotic, due to logistical constraints often only two-fold dilution steps are used

in the broth dilution process.

5.3 Kinetic Parameters

The pharmacokinetic parameters dictating the interactions of the antibiotic molecules with β -lactamase enzymes in the environment and with penicillin-binding protein 2a in the bacterial cell are the key determinants of antibiotic efficacy in the model. In order to explore the impact of these parameters on treatment outcome, a number of simulations were carried out over a range of parameter values. Figure 5.5 gives a general overview of how the Minimum Inhibitory Concentration of a drug is influenced by the kinetic parameters.

It can be seen that the k_2/K_d ratio, which is a measure of the antibiotic efficacy at inhibiting PBP2a function, has the most pronounced impact on the MIC of an antibiotic. The relative contribution of the β -lactamase reaction is less pronounced. It does have a significant impact at higher values of k_{cat}/K_M higher than 10^7 . However, in nature the catalytic efficiencies of β -lactamase enzymes have generally been found to be $<10^7$. For example, the k_{cat}/K_M values for type A MRSA β -lactamase range from $3.3 \times 10^6 \text{ M}^{-1} \text{ s}^{-1}$ against penicillin G to $2.2 \times 10^3 \text{ M}^{-1} \text{ s}^{-1}$ against cephalothin. There may be some biological/physical constraints that limit the development of more catalytically efficient β -lactamase enzymes, despite the clear fitness advantage they would produce in the presence of β -lactam antibiotics.

The results in Figure 5.5 indicate that there would be a strong selective advantage for the evolution of PBP2a variants with reduced k_2/K_d values, when exposed to antibiotics over prolonged periods of time. To a certain extent this has been the case, such as in the case of methicillin antibiotic which has been shown to have a k_2/K_d value as low as 0.39 versus PBP2a [78]. However, in the case of the β -

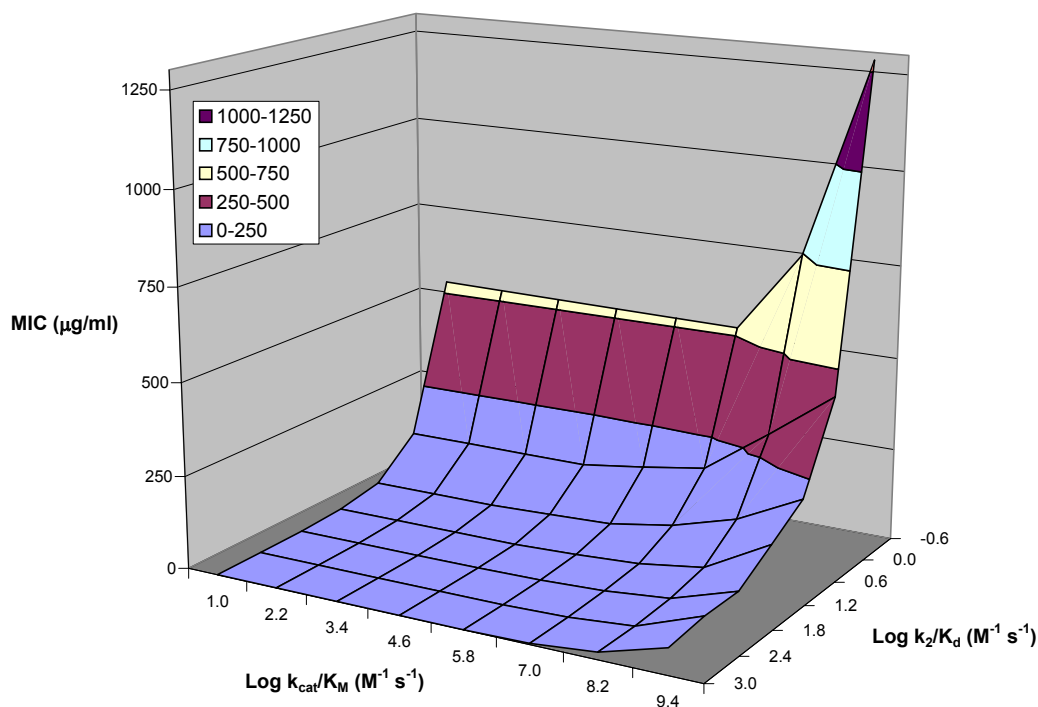


Figure 5.5: Surface plot of predicted Minimum Inhibitory Concentrations of β -lactam antibiotics over range of values for k_{cat}/K_M and k_2/K_d . k_{cat}/K_M is a measure of the catalytic efficiency of β -lactamase enzyme at cleaving antibiotic molecules. k_2/K_d is a measure of antibiotic efficacy at inhibiting PBP2a function.

lactamase-sensitive antibiotic penicillin G this value is 12.0 [78]. These differences may be due again to different biological constraints on the evolution of resistance and/or differences in the patterns of exposure to the antibiotics.

Figure 5.6 represents another way of viewing the data recorded in figure 5.5. In order to more clearly visualise the impact of the β -lactamase reaction kinetics on the MIC, the data has been normalised to represent the relative MICs at different values of k_{cat}/K_M . It can be seen that bacterial strains with a lower k_2/K_d value respond poorly to increases in the k_{cat}/K_M . For example, with a k_2/K_d value of < 0.24 , there is no visible increase in the MIC over the range of k_{cat}/K_M values tested. Examples of antibiotics which might exhibit this behaviour are the cephalosporin antibiotics,

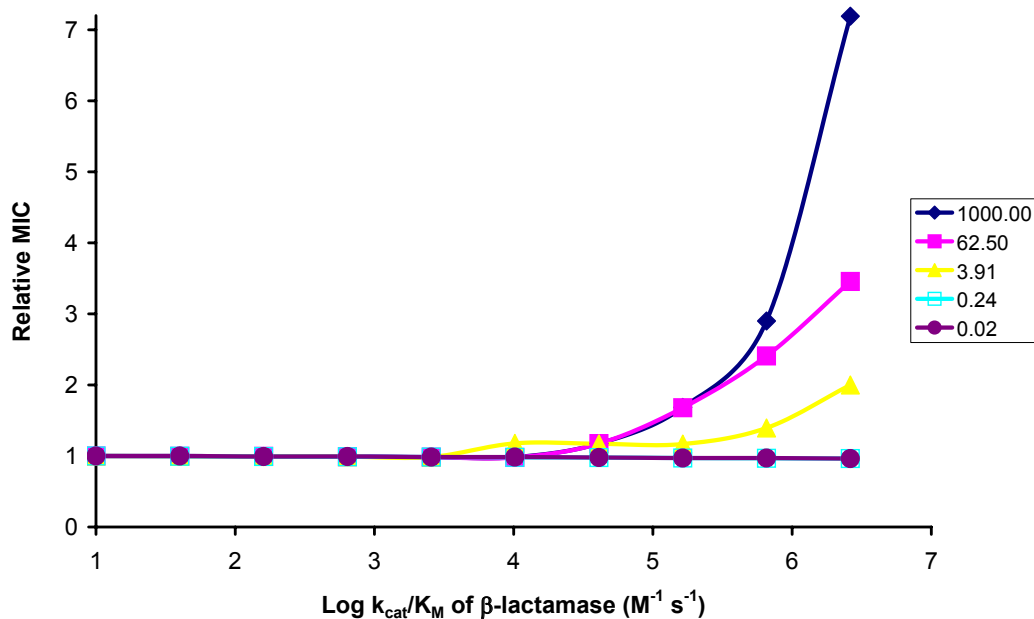


Figure 5.6: Effect of varying catalytic efficiency (k_{cat}/K_M) of β -lactamase enzyme on minimum inhibitory concentration of antibiotic with different k_2/K_d values (0.02 - 1000.0).

as well as imipenem and methicillin.

This indicates that there would not be significant selective pressure to evolve more efficient β -lactamases when the k_2/K_d value for the PBP2a reaction is low. This agrees with experimental studies of several types of β -lactamase enzymes from MRSA bacteria that have been shown to cleave cephalosporin antibiotics (low k_2/K_d) poorly relative to penicillin G [19]. The fact that they have not evolved greater specificities for cephalosporin antibiotics may be because there would be little or no significant fitness advantage conferred. On the other hand, there would be a clear selective advantage for strains of MRSA with higher catalytic efficiencies against penicillin G.

The results in figure 5.7 display the impact of changing k_2/K_d on the MIC output. There is a clear linear relationship between the log k_2/K_d and the log relative MIC,

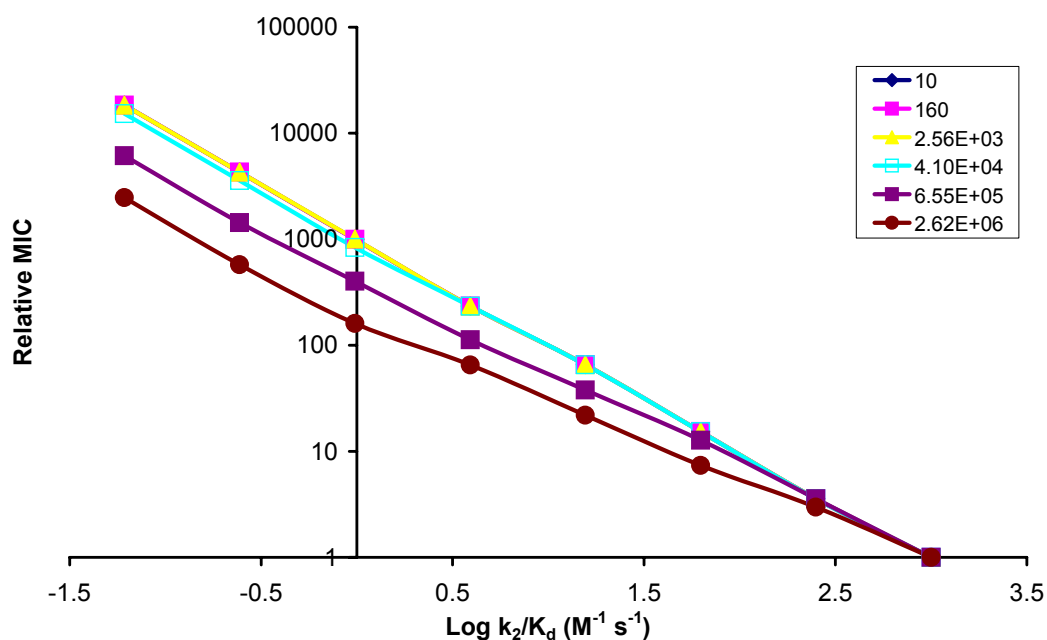


Figure 5.7: Effect of varying second order rate constant (k_2/K_d) of PBP2a-antibiotic reaction on minimum inhibitory concentration of antibiotic with different k_{cat}/K_M values ($10.0 - 2.62 \times 10^6$).

with the k_{cat}/K_M parameters influencing the slope of the line. This indicates that there is selective pressure to evolve PBPs with a lower k_2/K_d value in the presence of β -lactam antibiotics. This is to be expected since the PBP2a binding reaction is crucial for the mode of action of β -lactam antibiotics. The change in the MIC is inversely proportional to the change in the k_2/K_d when the value of k_{cat}/K_M is $< 10^5$. For example, with a k_{cat}/K_M value of 1.64×10^5 , reducing the k_2/K_d value from 1000.0 to 0.06 (16,393-fold decrease) results in a 15,319-fold increase in the MIC.

In the following sections, a more detailed examination of the effect of the kinetic parameters on survival in the presence of antibiotics will be carried out with reference to the antibiotics penicillin G, ampicillin and cephalothin, for which detailed experimental estimates of their kinetic parameters versus PBP2a and two important

types of β -lactamase are available.

5.3.1 Catalytic Efficiency of β -lactamase

The effects of Type A and Type C β -lactamases on the efficacies of penicillin G, ampicillin and cephalothin were examined by exploring the relationship between the length of time growth was inhibited by the antibiotics and the catalytic efficiency (k_{cat}/K_M) of the enzyme at hydrolytically cleaving the β -lactam ring (Fig. 5.8). The inhibition time of an antibiotic is a convenient measure of antibiotic efficacy.

The catalytic efficiencies of the β -lactamase enzymes were varied over the range $10^2 - 10^{10} \text{ M}^{-1} \text{ s}^{-1}$ and the relative length of time growth was inhibited by each antibiotic plotted. The length of time growth is inhibited by an antibiotic is displayed relative to its inhibition time when the default (experimentally estimated) kinetic parameter values are used as input (Fig. 5.8). There are strong negative correlations between $\log \beta$ -lactamase efficiency (k_{cat}/K_M) and inhibition time for both penicillin G and ampicillin ($r < -0.9$, $p < 0.01$), and a weaker but still significant ($p < 0.01$) correlation with cephalothin inhibition time (Type A: $r = -0.803$, Type C: $r = -0.774$). Correlation analyses to calculate the Pearson correlation coefficient (r) and two-tailed significance level (P) were carried out using SPSS statistical analysis software v11.0 (SPSS Inc., Chicago, IL, USA).

When correlation analyses are restricted to the smaller, but more biologically realistic, range of catalytic frequencies $10^2 - 10^6 \text{ M}^{-1} \text{ s}^{-1}$ there is no correlation between inhibition time and $\log k_{cat}/K_M$ for cephalothin over this range ($r = 0.0$). On the other hand, for penicillin G and ampicillin there are still significant negative correlations present ($r < -0.85$, $p < 0.01$). These results agree qualitatively with tests comparing antibiotic administered on its own and in conjunction with a

β -lactamase inhibitor sulbactam [1]. The inhibitor sulbactam competes with antibiotic molecules for binding to β -lactamase, effectively reducing the rate of hydrolytic activity of the enzyme against the antibiotic molecules (i.e. equivalent to a reduced k_{cat}/K_M). Norris *et al.* (1994) recorded a significant increase in antibiotic efficacy for penicillin and ampicillin in the presence of β -lactamase inhibitor, whereas cephalothin was unaffected.

5.3.2 PBP2a Interactions

The other major mechanism of resistance characteristic of MRSA bacteria is the expression of PBP2a protein in the cell membrane, which has decreased binding affinity for β -lactam antibiotics. The role of PBP2a binding efficiency in influencing the outcome of treatment was also investigated across the three different types of MRSA strains. The second order rate constant (a measure of inhibition efficiency) for the reaction between antibiotic and PBP2a in MRSA was varied over a range of several orders of magnitude for the antibiotics (Fig. 5.9).

There is a strong positive correlation between the binding efficiency of PBP2a and the inhibition time for all the antibiotics against the three types of MRSA ($r < 0.9$ and $p < 0.01$). However, there is a steeper increase in the inhibition time of cephalothin relative to penicillin G and ampicillin when treating the Type A and Type C β -lactamase producing strains (up to 4-fold difference in slope of fitted linear regression lines). This difference is much less pronounced in the case of the β -lactamase-negative strain (< 2-fold difference in slope).

Once again, these results are in qualitative agreement with experimental findings comparing MRSA bacterial strains (low k_2/K_d) with methicillin-susceptible *S. aureus* (MSSA) strains (high k_2/K_d) [3, 2]. Miller *et al.* (2005) showed a signifi-

cant increase in cephalothin efficacy between the MRSA and MSSA strains which agrees with the results from Figure 5.9. The results from Malouin *et al.* (2003) showed no significant difference in the antibiotic efficacies for penicillin/ampicillin when comparing β -lactamase-positive MRSA and MSSA strains, but there was a significant increase when comparing β -lactamase-negative strains. This is also in agreement with Micro-Gen's predictions from Figure 5.9. The model didn't show a notable increase in penicillin/ampicillin efficacy for β -lactamase-positive strains unless k_2/K_d was increased $>10^4$ -fold over their experimentally estimated natural values [78].

5.3.3 Discussion

For both type A and type C β -lactamases, if the catalytic efficiency against cephalothin is varied by up to three orders of magnitude over the current natural level, there is little discernible difference to the inhibition time ($<1\%$ difference). This could indicate why both Type A and Type C β -lactamases have relatively low rates of hydrolysis of cephalothin, compared to penicillin G: bacterial cells expressing more efficient β -lactamase against cephalothin would not have a significant evolutionary fitness advantage. By contrast, for penicillin G and ampicillin, over the same range of catalytic efficiencies, there is a steep decrease in the inhibition times that strongly correlates with the catalytic efficiency. This suggests there would be positive selective pressure for MRSA strains expressing more catalytically efficient β -lactamases when exposed to penicillin G or ampicillin over extended periods of time.

Figure 5.9 displays the results of varying the second order rate constant (k_2/K_d) of the reaction between antibiotic and PBP2a in the cell membrane. As this value

is increased, the inhibition times of the antibiotics also increase, as expected since the damage they inflict on the bacterial cell is proportional to their ability to bind to and inhibit PBP2a function. However, the slope of the curve for cephalothin is significantly steeper than either penicillin G or ampicillin when strains of MRSA expressing either Type A or Type C β -lactamase are tested.

This indicates that the PBP2a status of a bacterial cell may have a more marked impact on the clinical outcome of cephalothin treatment than penicillin G or ampicillin treatment, in β -lactamase expressing strains. This agrees with experimental studies which have shown that the MICs for penicillin/ampicillin are the same in either MRSA (PBP2a-positive, low k_2/K_d) or MSSA (PBP2a-negative, high k_2/K_d) strains of β -lactamase-producing bacteria. By contrast, there is a marked difference recorded experimentally (>100 -fold) in the MIC of cephalothin between PBP2a-positive and PBP2a-negative strains [3].

When a β -lactamase-negative strain of MRSA is tested, on the other hand, the profiles of penicillin G and ampicillin match cephalothin more closely, i.e. efficacy is inversely proportional to PBP2a binding affinity. This is because the β -lactamase enzyme is not present to limit the efficacies of the antibiotics. Since the β -lactamase status and production rate can vary considerably across different strains of MRSA, it is important to be able to predict quantitatively how these differences will affect the treatment response in a particular infection.

5.4 Conclusions and Future Work

Traditional methods of measuring antibiotic efficacy such as the Minimum Inhibitory Concentration are insufficient for understanding the complex dynamics that lead to the rapid development and spread of antibiotic resistance within bacterial

populations. However, the ability to investigate the relationship between individual molecular components of the system and the overall treatment outcome can lead to a better understanding of how to optimize antibiotic performance and predict treatment outcome. Micro-Gen can also be used to indicate evolutionary pathways or dead-ends that may exist for bacteria in response to antibiotic exposure.

Future work will include using the model to investigate the system dynamics of combination therapy with multiple classes of antibiotic. It can also be used to test hypothetical scenarios by varying the parameters of existing antibiotics to explore how potential novel compounds might act. It is a useful tool for the rapid screening of drug compounds against a diverse range of *S. aureus* strains in simulated culture conditions. The agent-based approach is also suitable for modelling the evolution of antibiotic resistance over time by incorporating genetic components into the bacterial agents. This would allow both the temporal and spatial dynamics of antibiotic resistance development to be examined.

Another important future aim of the Micro-Gen project is to model β -lactamase-dependent pro-drug delivery systems. Under these systems, a substrate-like pro-drug molecule containing the β -lactam ring structure undergoes therapeutic activation catalysed by β -lactamases to achieve selective release of a cytotoxic antimicrobial agent [79, 80]. Micro-Gen would be a useful tool to examine the dynamics of this system of activation and assess its therapeutic potential from a theoretical standpoint. This will be the subject of the next chapter of this thesis.

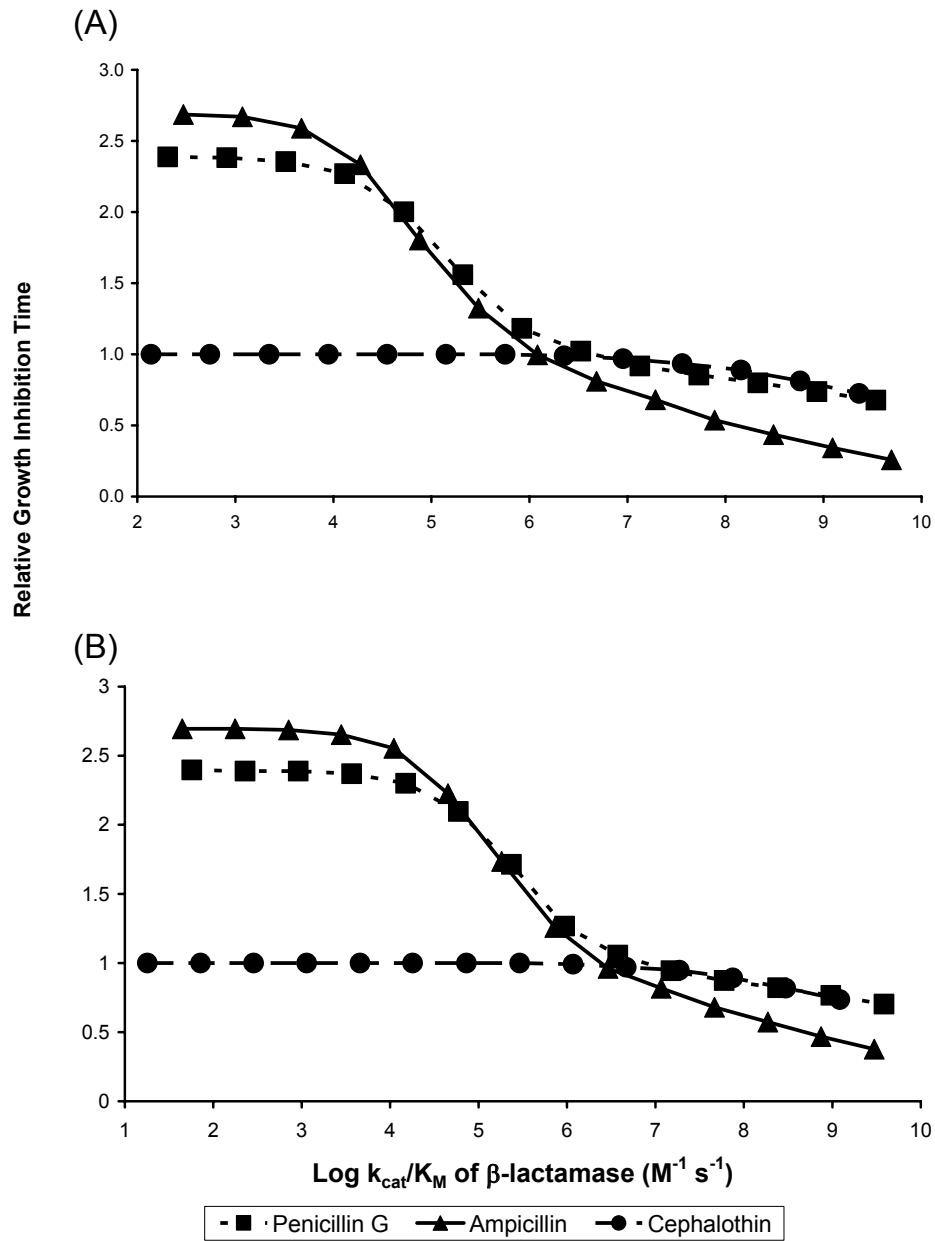


Figure 5.8: Predicted effects of varying catalytic efficiencies (k_{cat}/K_M) of Type A (A) and Type C (B) β -lactamases on relative inhibition times of antibiotics. Inhibition times expressed relative to results when naturally occurring k_{cat}/K_M values used (see Table 5.3). Data points represent means of three replicate simulations. Dosage: Pen = 71.3 $\mu\text{g/ml}$; Amp = 53.5 $\mu\text{g/ml}$; Ceph = 103.1 $\mu\text{g/ml}$.

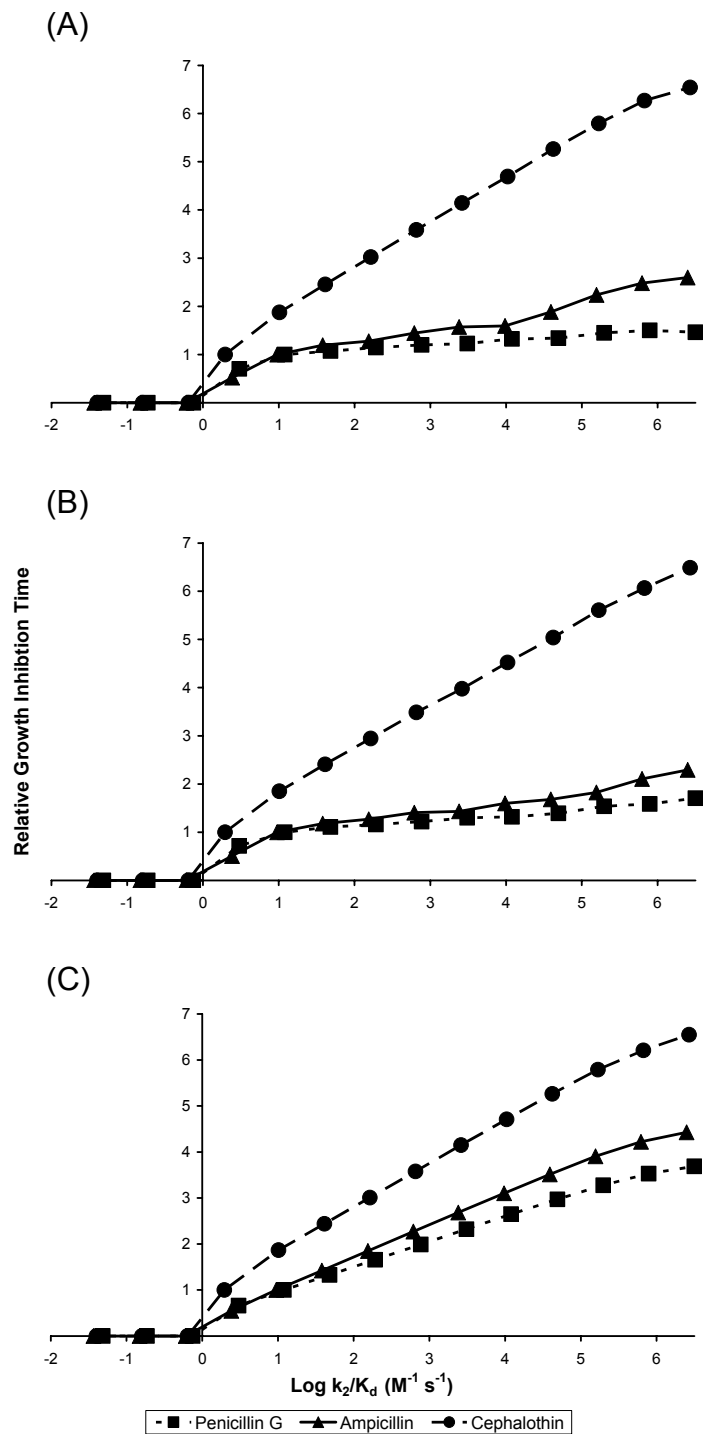


Figure 5.9: Predicted effects of varying second order rate constant (k_2/K_d) of PBP2a-Antibiotic reaction on relative inhibition times for Type A (A), Type C (B) and β -lactamase-negative (C) MRSA strains. Inhibition times expressed relative to result when naturally occurring k_2/K_d value used (see Table 5.3). Data points represent means of three replicate simulations. Dosage: Pen = 71.3 $\mu\text{g/ml}$; Amp = 53.5 $\mu\text{g/ml}$; Ceph = 103.1 $\mu\text{g/ml}$.¹⁰⁶

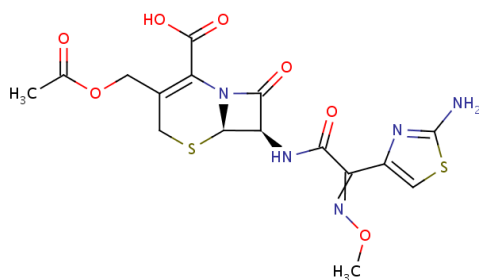
Table 5.3: Inputted parameter values for simulations of antibiotic interactions with MRSA bacteria in Micro-Gen model. *b.u.* = biomass units; *loop* = program loop (~ 2 s in real time)

Type of Entity	Parameters (units)	Input Value
Environment	Patch area (<i>b.u.</i>)	20000
	Patch nutrient level (<i>b.u.</i>)	80000
	Diffusion co-efficient	0.1
Bacterial Cell	Generation time (<i>min</i>)	29
	Threshold for division (<i>b.u.</i>)	10000
	Nutrient intake (<i>b.u. loop</i> ⁻¹)	10.0
	Survival cost (<i>b.u. loop</i> ⁻¹)	0.2
	Stationary phase relative metabolic rate	0.2
	Lag phase length (<i>min</i>)	63
	β -lactamase production rate ($\mu M s^{-1}$):	
	Type A	3.28×10^{-7}
	Type C	1.62×10^{-7}
β -lactamase production cost (<i>b.u.</i>)	0.1	
β -lactamase	Molecular weight (<i>Da</i>)	30000
	Half-life (<i>s</i>)	53640
	k_{cat} (<i>s</i> ⁻¹):	<i>Type A</i> <i>Type C</i>
	Penicillin G	171.0 210.0
	Ampicillin	308.0 355.0
	Cephalothin	0.015 0.095
	K_M (μM):	<i>Type A</i> <i>Type C</i>
	Penicillin G	51.1 55.9
	Ampicillin	255.0 122.0
	Cephalothin	6.8 5.2

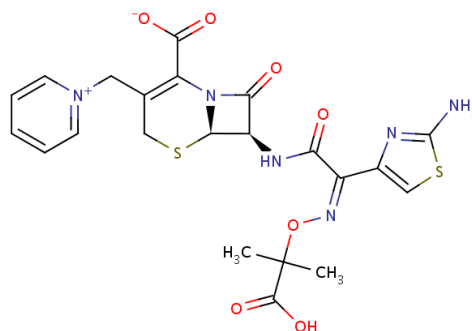
Table 5.4: Inputted kinetic parameter values (k_2 , K_d), molecular weight (M_R) and half-life parameters for simulations of antibiotic interactions with penicillin-binding protein 2a (PBP2a) in MRSA bacteria [1 - 8]. For diagrams of the chemical structures of these antibiotics see figures 5.10 & 5.11

Antibiotic	k_2 (s^{-1})	K_d (μM)	M_R (Da)	Half-life (s)
Cefotaxime	0.00035	586	455.47	3600
Ceftazidime	0.001	671	546.58	6840
Cephalothin	0.00115	586	396.44	1800
Cefoxitin	0.001162	586	427.45	2520
Cefepime	0.0015	1618	480.56	7200
Cephaloridine	0.0024	586	415	3660
Oxacillin	0.0016	180	401.44	1800
Ampicillin	0.0047	495	349.41	3600
Methicillin	0.0083	16900	380.42	3600
Penicillin G	0.185	15400	334.39	2520
Imipenem	0.0017	603	299.35	3600

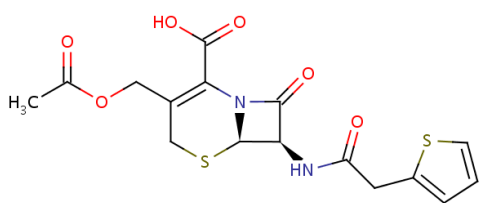
A. Cefotaxime



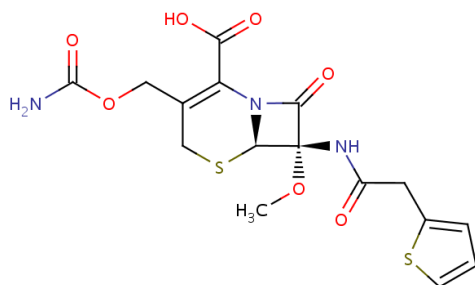
B. Ceftazidime



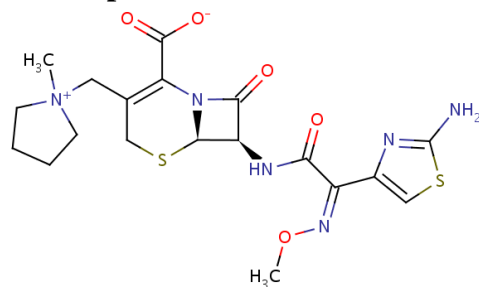
C. Cephalothin



D. Cefoxitin



E. Cefepime



D. Cephaloridine

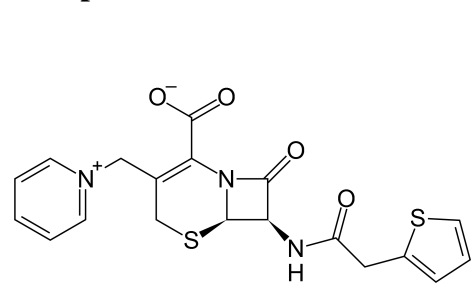
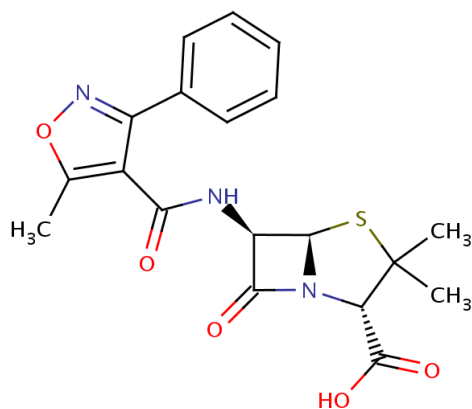
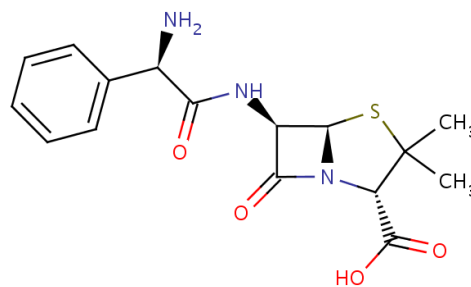


Figure 5.10: Diagrams of the chemical structures of the cephalosporin antibiotics listed in Table 5.4. Structures derived from the on-line cheminformatics database DrugBank [57].

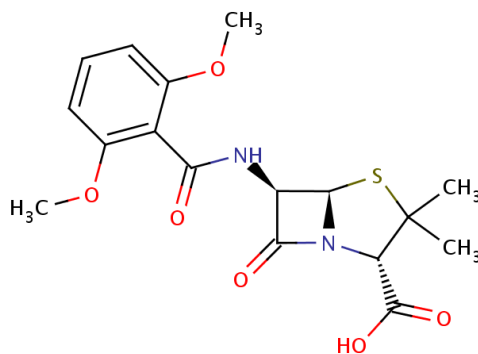
A. Oxacillin



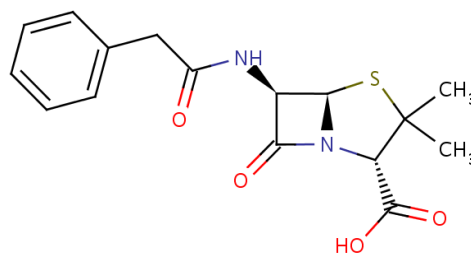
B. Ampicillin



C. Methicillin



D. Penicillin G



E. Imipenem

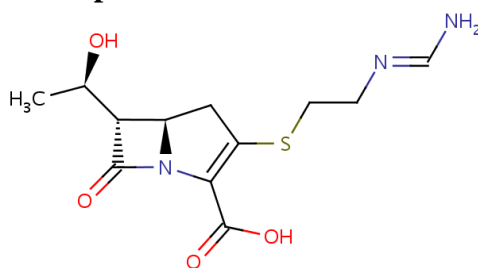


Figure 5.11: Diagrams of the chemical structures of the penicillin antibiotics, oxacillin, ampicillin, penicillin G and methicillin, and the carbapenem antibiotic, imipenem (see Table 5.4). Structures derived from the on-line cheminformatics database DrugBank [57].

CHAPTER 6

PRO-DRUG DELIVERY SYSTEM

6.1 Overview

One of the strengths of the computational approach towards studying bacteria-drug interactions is the ability to model hypothetical scenarios and explore how potential novel compounds might act. For example, there has been recent interest in alternative drug delivery systems to improve the specificity and efficacy of anti-microbial drugs. One such example, is the β -lactamase dependent enzyme-catalysed therapeutic activation (ECTA) pro-drug delivery system. This approach attempts to exploit the presence of β -lactamase enzymes in many species of pathogenic bacteria to deliver inactive precursors of harmful anti-microbial agents which specifically target these bacteria.

The basic premise of this approach is that a substrate-like pro-drug molecule containing a β -lactam promoiety structure is administered to treat an infection [91]. When it comes into contact with β -lactamase producing bacteria, it undergoes therapeutic activation by cleavage of its β -lactam ring which causes selective release of a cytotoxic anti-microbial agent [80, 79, 92]. Therefore, the presence of β -lactamase enzymes effectively decreases the survival chances of bacterial cells,

resulting in negative selective pressure for expression of these genes. This contrasts with the current situation where many common β -lactam drugs are rendered ineffective by the action of β -lactamases.

The theory of a β -lactamase dependent pro-drug delivery system represents a potentially promising approach for treating β -lactamase-producing bacterial infections. However, there are complex system dynamics involved that influence the effectiveness of this technique. For this reason, it is useful to carry out computational investigations to understand how factors such as the kinetics of the β -lactamase/pro-drug interaction influence treatment outcome.

Micro-Gen is well suited for such investigations as it incorporates a model of the kinetics of β -lactam ring cleavage in antibiotic molecules. By reversing the effect of this reaction, whereby the drug is rendered active (not inactive) by this interaction, some interesting preliminary insights can be made into the type of system dynamics that would be expected to take place in a pro-drug delivery system.

6.2 System Dynamics of Pro-Drug Delivery System

The pro-drug delivery system differs from the traditional method of applying a relatively high dose of an active anti-microbial agent. Traditional antibiotics such as penicillin G or cephalothin are administered in a pharmacologically active form, which then degrades over time according to its natural half-life or is inactivated by enzymes such as β -lactamases. A pro-drug, on the other hand, can be a relatively inert molecule which only becomes pharmacologically active after a specific activation event takes place.

It is possible that the pro-drug could have some pharmacological activity itself. For example, in a β -lactamase-dependent pro-drug delivery system, the β -lactam

ring structure in the pro-drug could interact with the penicillin-binding proteins in the bacterial cell to inhibit cell growth. However, for the simulations carried out here, the pro-drug is assumed to be in an inert, pharmacologically inactive form. This is in order to assess the effectiveness of this delivery system without introducing any ambiguities into the system due to direct antimicrobial activity. The simulated pro-drug only becomes active after interaction and successful cleavage by a β -lactamase enzyme.

As a result of this, when the pro-drug is added to the system there is initially no active anti-microbial agent present (no contamination through non-selective activation, such as chemical hydrolysis, is assumed). As described in chapter 3, when a bacterial cell interacts with a β -lactam ring-containing molecule, β -lactamase enzyme production is triggered. This starts at a low rate which increases exponentially until the full production rate is reached after about 80 minutes [59]. During this period, there is a gradual increase in the concentration of activated antimicrobial agents in the vicinity of the bacteria. When the concentration of active drug exceeds a threshold for activity then bacterial growth is inhibited. There is therefore a time delay between the addition of a pro-drug and the accumulation of sufficient activated drug molecules to inhibit growth. This does not occur with traditional antibiotics, which immediately bind to bacterial cells upon first contact according to their kinetic rules.

Figure 6.1 shows a sample concentration curve for activated anti-microbial agent when it is added in pro-drug form to a simulated colony of MRSA (input parameters listed in Table 6.2). There is a gradual increase in the active drug compound until it crosses a certain threshold to cause inhibition of bacterial growth (0.6-0.8 $\mu\text{g/ml}$). Figure 6.1 also shows the effect of adding the active antimicrobial agent directly (not in pro-drug form) at a concentration (0.8 $\mu\text{g/ml}$) that is

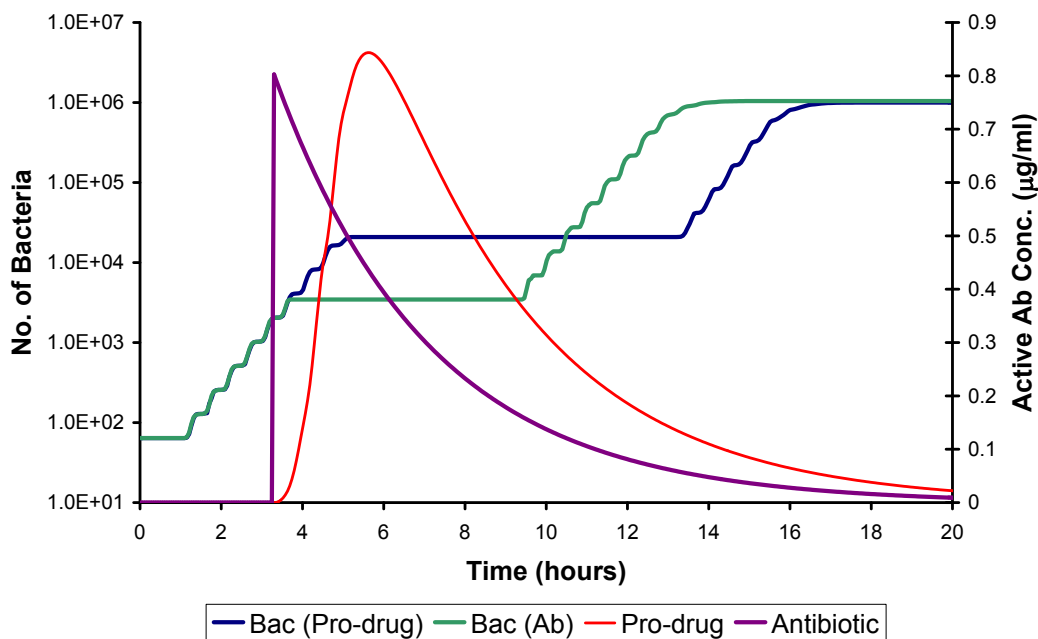


Figure 6.1: Comparison of activities of hypothetical active antibiotic applied directly or in pro-drug form. Two simulations were carried out: one with 1.8 $\mu\text{g/ml}$ of pro-drug administered at time = 3.3 hours, and the other with 0.8 $\mu\text{g/ml}$ of pre-activated anti-microbial agent (antibiotic) added at time = 3.3 hours. There is a clear delay in inhibition of bacterial growth by the pro-drug due to the requirement of a β -lactamase-mediated activation step.

above the threshold for inhibition of bacterial growth. There is a threshold in the concentration of the active drug compound that must be reached to inhibit bacterial growth, which is dependent on the pharmacological properties of the activated drug molecule. This results in a delay, due to the β -lactamase-mediated activation step, between administration of the pro-drug and inhibition of bacterial growth when there is a sufficient concentration of activated drug available.

6.2.1 Kinetics Studies

The speed and efficiency of activation of the pro-drug is an important factor for determining the efficacy of a pro-drug delivery system. A number of simulations were carried out to examine the effects of several different parameters on the activation of the pro-drug and inhibition of bacterial growth by the activated product. The same cellular parameters for representing β -lactamase-producing MRSA that were used in previous chapters were applied in the simulations here (Table 6.2). A hypothetical penicillin-based pro-drug was simulated, i.e. the kinetic parameter values (k_{cat}/K_M) for penicillin G were used to define the interaction between β -lactamases and the pro-drug molecules. The kinetic values for penicillin G were chosen because this represents a situation where the β -lactamase enzymes have a high catalytic efficiency versus the sample pro-drug. This represents an optimal situation in order to assess the potential of this approach.

The active drug agent that arises from cleavage of the hypothetical penicillin-based pro-drug has kinetic parameters (k_2/K_d) which determine the rate of binding to the bacterial cell (Table 6.2). Although the same parameters (k_2/K_d) that were used to represent binding of a β -lactam antibiotic to PBP2a in the bacterial cell are used, this does not mean that the activated antimicrobial agent represents a β -lactam

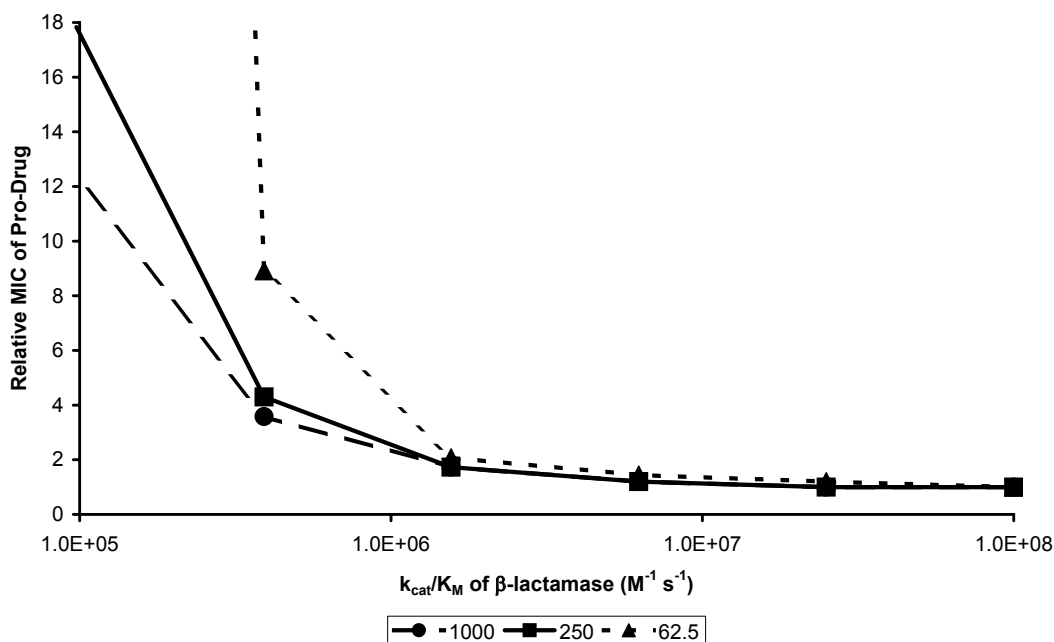


Figure 6.2: Effect of catalytic efficiency (k_{cat}/K_M) of β -lactamase enzyme on minimum inhibitory concentration (MIC) of pro-drug. Three different pro-drugs are graphed which differ by the rate of binding of their activated anti-microbial agent to the bacterial cell (k_2/K_d of activated anti-microbial agent varied between 62.5 and 1000 $M^{-1} s^{-1}$).

antibiotic. These parameters are simply used because they are a convenient way of carrying out initial modelling experiments and visualise their outcomes. The specific target of the active drug is not specified. For the purposes of this investigation this is sufficient since the aim of the study is to assess the pro-drug delivery system rather than obtain a quantitative estimate of the efficacy of a specific pro-drug. This would require the availability of the kinetic parameters related to the interaction of the activated antimicrobial agent with its specific target in the bacterial cell. Please note that since the activated drug is assumed to lack the β -lactam ring structure, it is not subject to cleavage and re-inactivation by β -lactamases.

Figure 6.2 shows the results of experiments investigating the effect of the ki-

netic parameters on the minimum inhibitory concentration (MIC) of the penicillin-based pro-drug. Three hypothetical variations of the pro-drug were investigated, which differed by the rate of binding of the activated anti-microbial agent to the bacterial cell ($k_2/K_d = 62.5, 250, \text{ or } 1000 M^{-1} s^{-1}$). The catalytic efficiency of the β -lactamase enzyme (k_{cat}/K_M) at cleaving and activating the pro-drug was assessed by varying over a range of $10^5 - 10^8$ for each pro-drug variant. As would be expected, higher values for the catalytic efficiency result in a lower MIC for the pro-drug.

The pattern in Figure 6.2 is the reverse of the trend seen in Figure 5.6 for traditional β -lactam antibiotics. This is one of the reasons why there is interest in the β -lactamase-dependent pro-drug delivery system. It would be expected that administration of β -lactamase-dependent pro-drugs could lead to evolutionary selective pressure opposed to the current selective pressure exerted by β -lactam drugs.

However, it must be noted that for high catalytic efficiencies there is a leveling of the rate of decrease in the MIC (Fig. 6.2). This fitness “plateau” could negate the selective advantage of bacteria producing β -lactamases with lower catalytic efficiencies. For example, in Figure 6.2, there is a less than 50% decrease in the MIC above a k_{cat}/K_M value of approximately 10^6 . On the other hand, Figure 5.6 shows that increasing the k_{cat}/K_M above 10^6 for active β -lactam antibiotics (non pro-drugs) results in a significant fitness advantage (up to 7-fold increase in MIC).

The dynamics between the negative selective pressure from pro-drugs and positive selective pressure from β -lactam antibiotics would be an important factor to consider when assessing the possible evolution of drug resistance in bacteria in response to these two therapeutic strategies. However, the complex interplay of biophysical, pharmacokinetic, pharmacological and epidemiological factors which would contribute to this are beyond the scope of this study. Nevertheless, this modelling approach is useful for developing theories about how molecular parameters

may contribute to the dynamics observed.

6.2.2 Half-Life

One of the most important parameters that limits the efficacy of both traditional antibiotics and novel drug candidates such as pro-drugs, is the half-life of the molecule. However, as demonstrated in Chapter 4, the impact of this parameter can vary substantially depending on the type of antibiotic used. For example, the efficacy of penicillin G was predicted to be relatively resistant to changes in its half-life compared to cephalothin (Fig. 4.2). Since the half-life of a molecule can vary dramatically depending on local environmental conditions, it is important to determine its influence in order to attempt to predict treatment success.

For this reason, computational analyses were carried out to predict the impact of this parameter on the pro-drug delivery system (Fig. 6.3). The half-life for the penicillin-based hypothetical pro-drug was varied between 16 minutes and 2.8 hours, and the growth curve of the bacterial population plotted along with the concentration curve of activated anti-microbial agent. As can be seen in the graphs, there is a certain threshold above which the concentration of activated drug must cross before inhibition of bacterial growth is observed (in this case, the threshold is approximately $0.8 \mu\text{g/ml}$).

With a half-life of ≤ 16 minutes, the concentration of activated anti-microbial agent never exceeds the threshold required for growth inhibition (Fig. 6.3A-B). Therefore, the bacterial population follows the standard growth curve, eventually entering the stationary phase due to nutrient limitations. However, when the half-life of the pro-drug is increased to 1.4 hours or greater, then the required concentration of active drug compound is reached and the length of time growth is inhibited

is determined by the rate at which this compound degrades over time.

The half-life of a pro-drug is therefore a very important parameter when determining its efficacy against β -lactamase-producing *S. aureus* bacteria. This system is particularly sensitive to the half-life parameter because of the time delay between administration of the pro-drug and activation of sufficient quantities of active agent to inhibit growth. The length of time that the drug inhibits bacterial growth is also directly influenced by the activated drug's own half-life.

6.2.3 Diffusion Rate

The impact of diffusion on the activity and dynamics of the pro-drug delivery system was also investigated. This is an important parameter to assess because the pro-drug delivery system depends on the targeted release of active anti-microbial agents in the close vicinity of bacterial cells. Micro-Gen does not represent the complex flow dynamics experienced in the *in vivo* situation. However, the implementation of an algorithm based on Fick's First Law of diffusion allows some insights to be obtained on the role of diffusion dynamics in the system (see chapter 3).

Figure 6.5 shows the impact of varying the rate of diffusion in the environment on the activation and efficacy of a penicillin-based pro-drug. The rate of diffusion was varied by modifying the user-defined diffusion coefficient (D) for Fick's First Law of diffusion (see Fig. 3.1). This is a system-level parameter that alters the rates of diffusion of all the molecules (pro-drug, active drug, β -lactamase and nutrients) in the environment, see Chap. 3. Higher values correspond to a more fluid/dynamic environment whereas lower values result in a more viscous/inert environment. The results from these simulations indicate that the rate of diffusion has an important influence on the availability of activated pro-drug in the vicinity of the bacterial

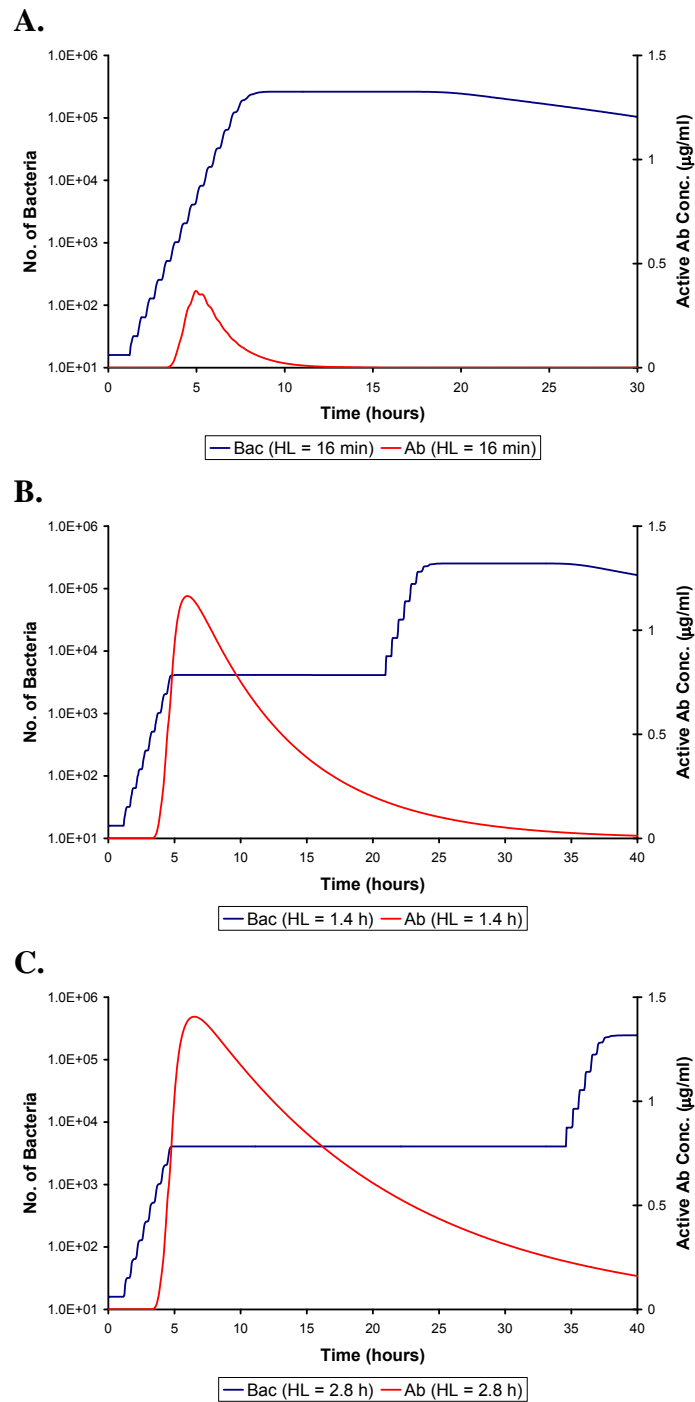


Figure 6.3: Effect of varying the half-life parameter for a penicillin-based pro-drug on the inhibition of β -lactamase-producing *S. aureus* bacterial growth. The graphs display the simulated log bacterial growth curve along with the concentration of activated drug molecules ($\mu\text{g/ml}$). $1.8 \mu\text{g/ml}$ pro-drug added at time = 3.3 hours. **A.** Half-life = 16 min; **B.** Half-life = 1.4 h; **C.** Half-life = 2.8 h;

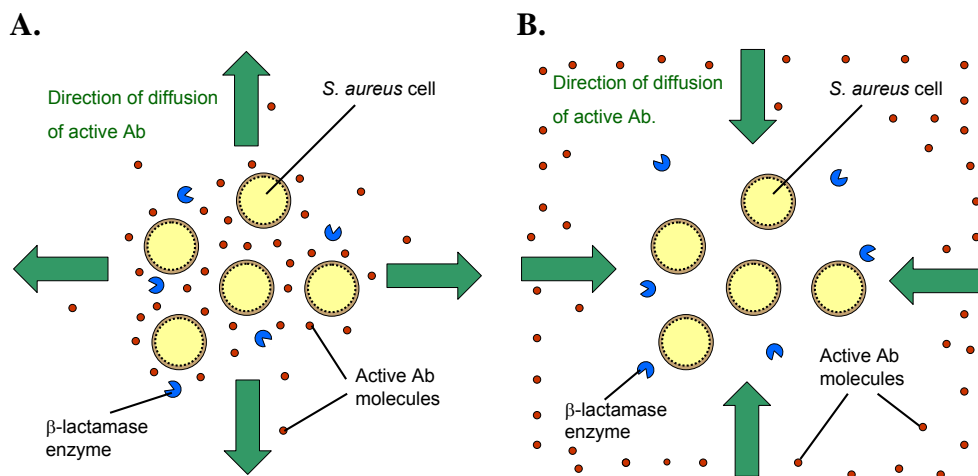


Figure 6.4: Comparison of the local diffusion gradients of active antimicrobial agents in the local environment of β -lactamase producing *S. aureus* cells for pro-drug (A) and traditional β -lactam antibiotics (B). **A.** When administered in pro-drug form the active antimicrobial agent concentration is highest in the vicinity of the bacterial cells due to β -lactamase-mediated activation. **B.** For traditional β -lactam antibiotics the concentration of active agent is depleted in the vicinity of the bacterial cells due to inactivation by the β -lactamases.

cells as measured by the height of the peak in the concentration of activated antimicrobial agent (Fig. 6.5).

With a lower diffusion rate, the concentration of activated anti-microbial agents in the local vicinity of the bacterial cells increased more rapidly. This may be explained by the fact that with higher diffusion rates, the rate of clearance of the activated drug molecules from the vicinity of the bacterial cells would be quicker (Fig. 6.4A). This type of behaviour would also be expected to occur in environments where there is a high flow rate. The efficacy of the activated antimicrobial agents depends on their ability to stay long enough in the vicinity of the bacterial cells to bind to and inhibit growth.

The pro-drug delivery system results in higher concentrations of activated drug molecules in the direct vicinity of the bacterial cells. The system is therefore sensitive to any forces, such as diffusion or flow forces, that may result in dispersal of

the activated compounds. It is important, therefore, to take this into account when designing pro-drugs and try to take measures to minimize this such as, for example, designing molecules that have a greater binding affinity or are electrostatically attracted to the bacterial cells.

This problem is not so evident with traditional antibiotic approaches because they usually involve the administration of relatively high doses of active antimicrobial agent that are not specifically targeted to the local vicinity of the bacterial cells. In fact for some types of β -lactam antibiotic, such as penicillin G, increasing the diffusion rate results in increased antibiotic efficacy (Fig. 4.4). This could be due to the fact that higher rates of diffusion results in dispersal of β -lactamase-inactivated penicillin G in the vicinity of the bacterial cells and replacement by active penicillin G from elsewhere in the environment - the reverse situation to the pro-drug system (Fig. 6.4B).

6.2.4 β -lactamase Production Rate

It is clear that the β -lactamase production rate of the bacterial cells is an important parameter to be considered when investigating the β -lactamase-dependent pro-drug delivery system. The production rate can vary considerably between different bacterial strains, and this must be factored in when assessing the usefulness of this drug delivery system. Figure 6.6 shows the growth dynamics of a bacterial population when exposed to a penicillin-based pro-drug ($1.8 \mu\text{g/ml}$), with the β -lactamase production rate varied between 10^{-7} - $10^{-5} \mu\text{M s}^{-1} \text{ agent}^{-1}$. For reference, the β -lactamase production rate for naturally occurring Type A MRSA under these simulation conditions was estimated to be $3.28 \times 10^{-7} \mu\text{M s}^{-1} \text{ agent}^{-1}$ (see chapter 3).

The results confirm the important role that the β -lactamase production rate has

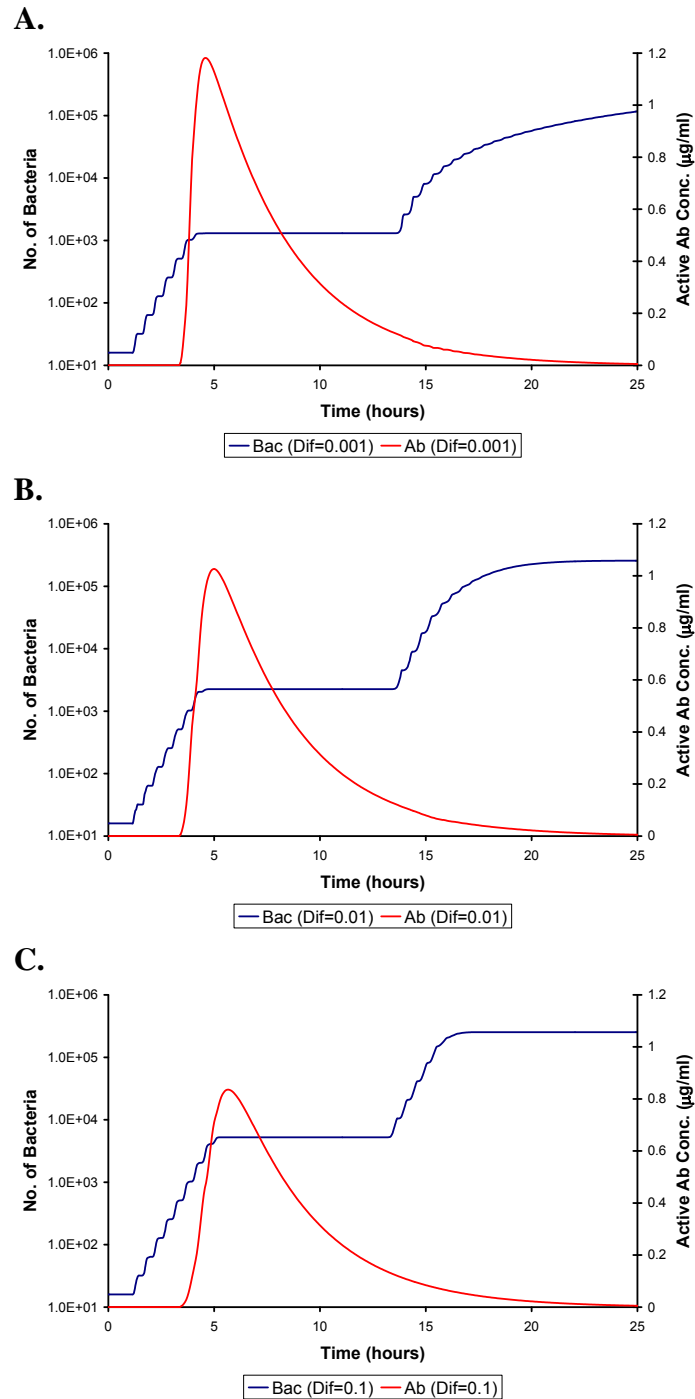


Figure 6.5: Effect of varying the user-defined diffusion parameter (D) for Fick's First Law of diffusion on the inhibition of β -lactamase-producing *S. aureus* bacterial growth by a penicillin-based pro-drug. The graphs display the simulated log bacterial growth curve along with the concentration of activated drug molecules ($\mu\text{g/ml}$). $1.8 \mu\text{g/ml}$ of pro-drug added at time = 3.3 hours. **A.** $D=0.001$; **B.** $D=0.01$; **C.** $D=0.1$.

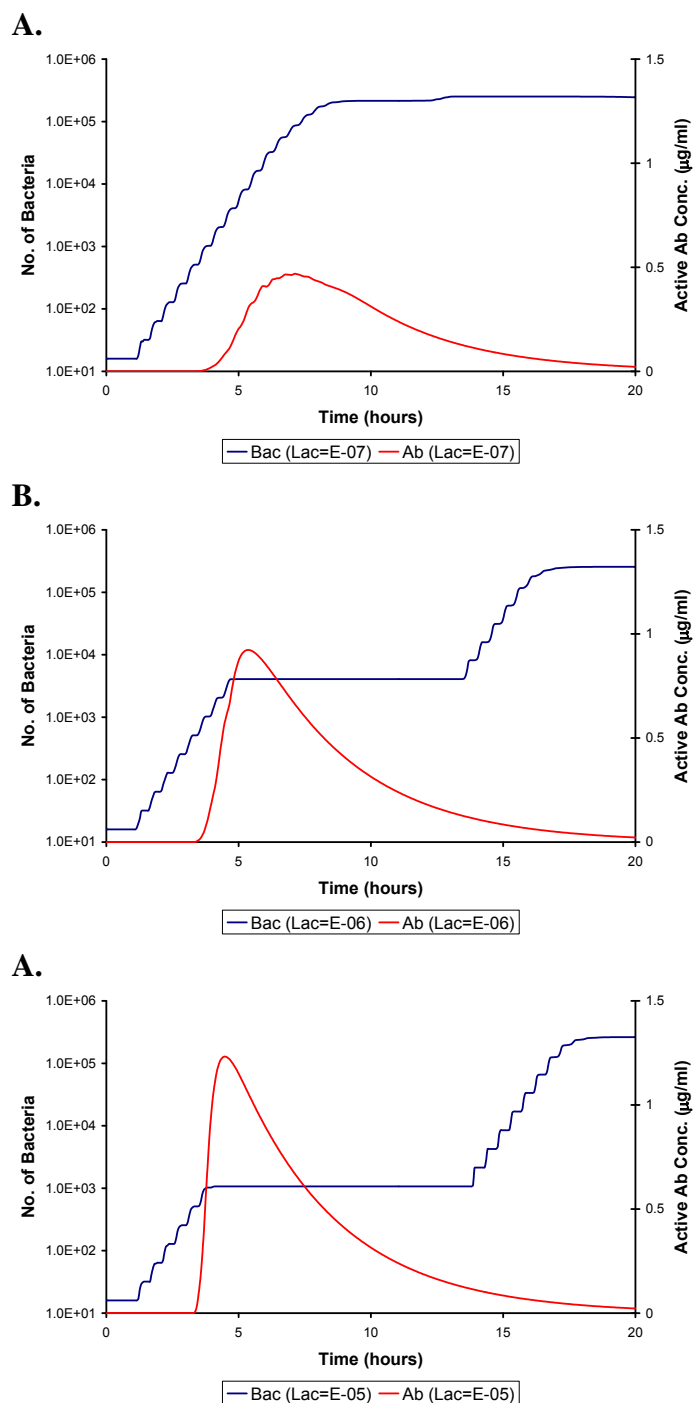


Figure 6.6: Effect of varying the β -lactamase production rate on the inhibition of β -lactamase-producing *S. aureus* bacterial growth by a penicillin-based pro-drug. The graphs display the simulated log bacterial growth curve along with the concentration of activated drug molecules ($\mu\text{g/ml}$). $1.8 \mu\text{g/ml}$ of pro-drug added at time = 3.3 hours. **A.** Production Rate = $10^{-7} \mu\text{M s}^{-1} \text{agent}^{-1}$; **B.** Production Rate = $10^{-6} \mu\text{M s}^{-1} \text{agent}^{-1}$; **C.** Production Rate = $10^{-5} \mu\text{M s}^{-1} \text{agent}^{-1}$.

on the efficacy of the β -lactamase dependent pro-drug delivery system. For these simulations, it is assumed that there is no contamination or spontaneous activation of the active anti-microbial agent apart from activation by β -lactamase. In real life, there may be some contamination with active compound that would lead to positive results even when treating β -lactamase-negative strains of bacteria. However, this ambiguity can lead to problems when assessing the true effectiveness of the approach.

The active drug concentration threshold required for inhibition of growth is approximately $0.8 \mu\text{g/ml}$. This threshold is determined by the minimum inhibitory concentration of the activated antimicrobial agent. It is noteworthy however, that even at high β -lactamase production rates (e.g. Fig. 6.6E) where the active drug concentration remains above the threshold of inhibition for a longer period of time, the length of time growth is inhibited is not significantly longer than at lower production rates (Fig. 6.6C). The length of time growth is inhibited seems to be limited by the half-life (2520 s) of the drug in this case (see Fig. 6.3).

6.3 Case Study: NB2001 & NB2030

In recent years, there has been increased interest in developing novel pro-drug compounds for treating antibiotic resistant bacteria. Two compounds, called NB2001 and NB2030, were recently developed that exploit the β -lactamase dependent enzyme-catalysed therapeutic activation (ECTA) pro-drug strategy [8, 80]. The general structure of these compounds consists of a cephalosporin backbone (cephalothin derivative for NB2001 and cefazolin derivative for NB2030) with an antibacterial agent (triclosan) in pro-drug form at the 3' position of the cephem nucleus (Fig. 6.7) [8]. The antibacterial agent is released by β -lactamase-mediated

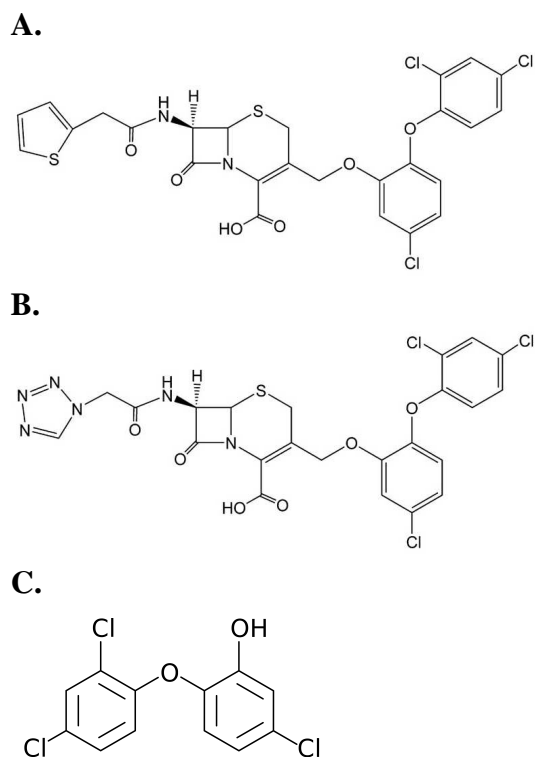


Figure 6.7: Chemical structures of NB2001 (**A**), NB2030 (**B**) and triclosan (**C**). They consist of a cephalosporin side chain (NB2001 = cephalothin, NB2030 = cefazolin) at position C-7, along with the enoyl reductase inhibitor triclosan at the C-3 position of the cephem nucleus [80].

hydrolysis of the β -lactam ring in the pro-drug structure.

The active antibacterial agent released from NB2001 and NB2030 is triclosan, which possesses broad-spectrum antimicrobial activity against both gram-positive and negative bacteria [93]. It is commonly used in health-care products such as handwash, toothpaste and surgical scrubs [94]. Triclosan has been shown to have potent activity against *S. aureus* bacteria by binding to the enoyl-[acyl-carrier-protein] reductase (FabI) enzyme involved in the bacterial fatty acid synthesis cycle [81]. However, the complex interactions that triclosan has with the bacterial cell which lead to its lethality have still not been fully elucidated [93].

In order to explore Micro-Gen's usefulness as a tool for investigating the ef-

fectiveness of the pro-drug strategy, information from the experimental studies of NB2001 and NB2030 were used to develop a pro-drug model of their interactions with *S. aureus* bacteria. The bacterial cellular parameters were maintained the same as those used to represent Type A β -lactamase-producing MRSA in the previous chapters, including the β -lactamase-production rate which was estimated in chapter 3. The kinetic parameters for the interaction between Type A β -lactamase and the pro-drug compounds NB2001/NB2030 were derived from the experimental literature (see Table 6.2) [80].

The mechanism of action of triclosan is less well understood than the traditional β -lactam antibiotics. The main cellular target of triclosan is believed to be the FabI enzyme of the fatty acid biosynthetic pathway (see above). Therefore, an abstract representation of triclosan is incorporated in the model by using the pre-steady state reaction kinetic parameters (k_2/K_d) to describe the binding of triclosan in the bacterial cell to FabI enzyme and concomitant inhibition of bacterial growth (equation 3.1). This is a simplistic but reasonable representation of the mode of action of triclosan for the objectives of this study aiming at evaluating the pro-drug delivery system.

The kinetic parameter values (k_2/K_d) that determined triclosan's interaction with the bacterial cell were estimated by fitting the values to the experimental MIC estimates determined from the literature [80]. These were maintained constant across all the simulations carried out in order to assess the effects of changes to the pro-drug delivery system.

6.3.1 MIC Test Results

The *in vitro* activities of NB2001 and NB2030 (as well as the active antimicrobial agent triclosan on its own and a cephalosporin antibiotic cephalothin) against *S. aureus* bacteria from the experimental literature were compared with predicted values from Micro-Gen (Table 6.1) [80]. Predicted values where a specified percentage of contamination with free triclosan was assumed were also included. The percentage of contamination was derived from the experimental results of high-pressure liquid chromatography (HPLC) tests documented in the original experimental study [80].

Table 6.1: Comparison of predicted MICs (with and without contamination with free triclosan) from Micro-Gen model and experimentally determined MICs for the pro-drugs NB2001 and NB2030, as well as triclosan and cephalothin, versus Type A β -lactamase-producing MRSA bacteria. Percentage contamination with free triclosan: NB2001 = 4 %, NB2030 = 1 %.

Antimicrobial Drug	Pred MIC ($\mu\text{g/ml}$)	Pred (Contam) MIC ($\mu\text{g/ml}$)	Exp MIC ($\mu\text{g/ml}$)
NB2001	0.0014	0.001	0.0002 - 0.002
NB2030	0.0003	0.0003	0.0002 - 0.004
Triclosan	0.0001	NA	≤ 0.0002
Cephalothin	103.1	NA	64

The experimental estimates of the MICs for NB2001 and NB2030 vary greatly between different strains of *S. aureus*, which makes it difficult to verify the experimental predictions with a high degree of accuracy. In particular, the β -lactamase production rates for the strains used in the experimental analysis were only qualitatively estimated by a colourimetric test with nitrocefin [80]. However, given these limitations, it is still encouraging that the predicted MICs for NB2001 and NB2030 were within the range of values recorded in the experimental study.

The model also provided a means to assess the impact of potential contamina-

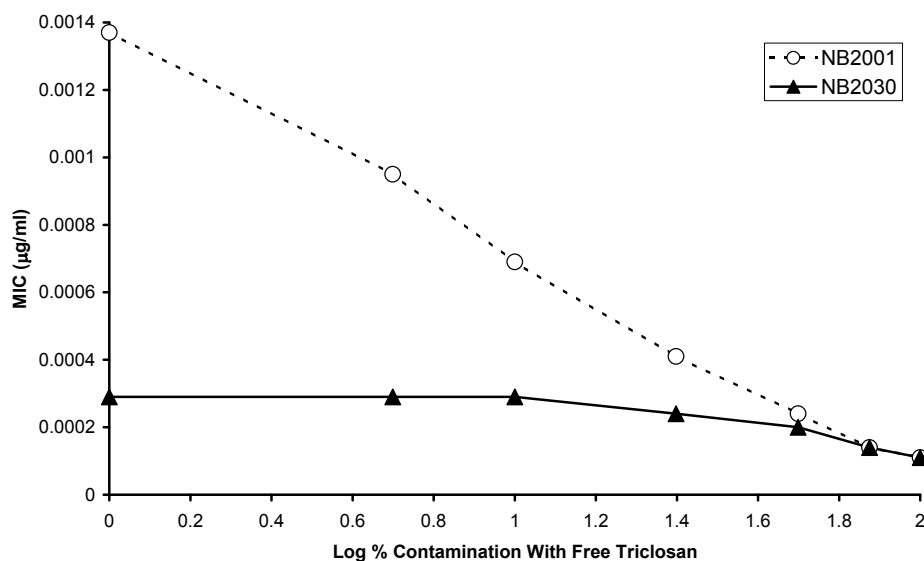


Figure 6.8: Predicted effect of varying percentage contamination with free triclosan (0% = pure pro-drug, 100% = pure triclosan) on Minimum Inhibitory Concentrations (MICs) of NB2001 and NB2030 versus Type A β -lactamase-producing MRSA bacteria. Simulated drug compounds were added after 3.3 hours of incubation, during the exponential phase of bacterial growth.

tion with free triclosan on the MICs of the pro-drugs. For example, the level of contamination in NB2001 was estimated experimentally to be 4%. The Micro-Gen model predicts that this level of contamination would account for approximately a 30% decrease in the MIC compared to pure NB2001 (0.0010 versus 0.0014 $\mu\text{g/ml}$). On the other hand, the 1% contamination found in NB2030 was predicted to not have a detectable effect on its MIC.

Due to the inherent problem of contamination in pro-drug preparations it is useful to be able to quantify how this might distort MIC determinations. Theoretical modelling of the drug compounds can provide a means to estimate this effect. Figure 6.8 shows the effect of varying the percentage of free triclosan contamination between 1 - 100%, where 100% represents pure triclosan. Since triclosan has very potent antibacterial activity ($\text{MIC} \leq 0.0002 \mu\text{g/ml}$), the results of MIC de-

terminations for the pro-drugs can be sensitive to contamination or β -lactamase-independent hydrolysis.

In the case of NB2001, there is a strong negative correlation between the MIC and the proportion of contamination with free triclosan ($r = -0.997$, $p < 0.01$). However, the MIC of NB2030 is less sensitive to distortion by the presence of free triclosan, although there is still a significant negative correlation ($r = -0.868$, $p = 0.011$) This is because the catalytic efficiency (k_{cat}/K_M) of the β -lactamase enzyme versus NB2030 is ten-fold higher than NB2001, and therefore the availability of activated triclosan is less of a limiting factor on the efficacy.

If there is a high amount of contamination, then this can lead to misleading results. For example, NB2001 and NB2030 were found to have lower experimental MICs ($0.0002 \mu\text{g/ml}$) against *S. aureus* strain 29213 than strain PC1 (NB2001 = $0.002 \mu\text{g/ml}$; NB2001 = $0.004 \mu\text{g/ml}$) [80]. This was in spite of the fact that strain PC1 had a higher β -lactamase production rate, and therefore would be expected to have a lower MIC. Differences in the level of contamination with free triclosan (or non- β -lactamase-mediated activation) could not be ruled out as a cause for this behaviour, and it highlights the importance of contamination studies when assessing the efficacy of a pro-drug treatment strategy.

6.3.2 Sensitivity Analyses

The β -lactamase enzyme catalysed therapeutic activation (ECTA) pro-drug strategy employed by NB2001 and NB2030 means that their efficacy is strongly dependent on the β -lactamase status of the bacterial cells being treated. This approach is designed to be particularly effective against β -lactamase over-expressing cells. This dependence on the β -lactamase status of the cells is illustrated in Figure 6.9

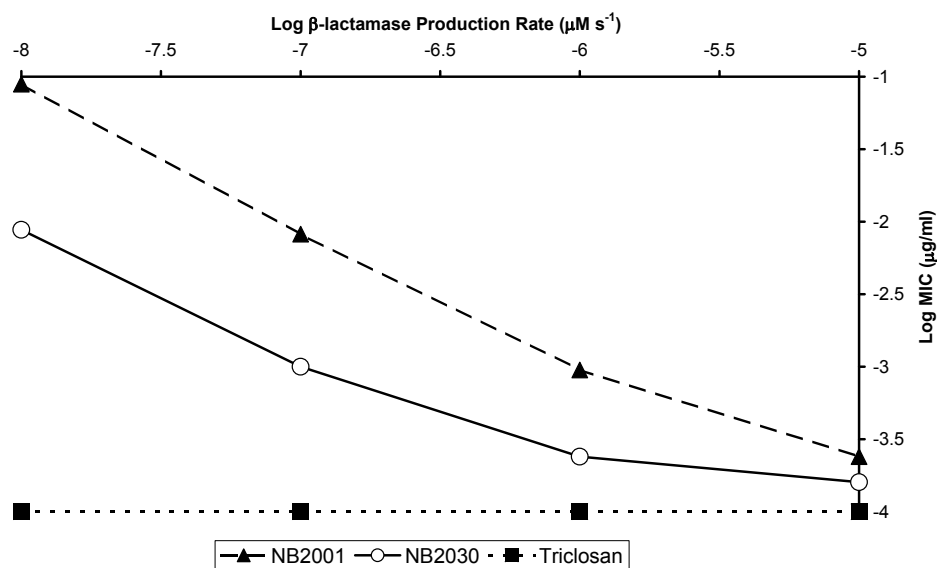


Figure 6.9: Predicted effect of β -lactamase production rate on minimum inhibitory concentrations (MIC) of NB2001 and NB2030 versus simulated β -lactamase-producing *S. aureus* bacteria. Free triclosan (which is unaffected by β -lactamase) is included as a control. Drug compounds were added after 3.3 hours of incubation, during the exponential phase of bacterial growth.

where the simulated log MIC of each pro-drug is graphed against a range of different β -lactamase production rate values. There is a significant negative correlation between the β -lactamase production rate and the MICs in the results (NB2001: $r = -0.993$, $p = 0.007$; NB2030: $r = -0.959$, $p = 0.041$). This is to be expected given the mechanism of activation is β -lactamase-dependent.

Variation between the graphs of NB2001 and NB2030 are due to differences in the kinetic parameters of the enzymatic cleavage of the β -lactam ring. The catalytic efficiency (k_{cat}/K_M) of Staphylococcal Type A β -lactamase with NB2030 is approximately ten-fold higher than with NB2001. As a result, the MIC for NB2030 is lower than NB2001 at any given β -lactamase production rate. However, at very high production rates (e.g. $>10^{-5} \mu\text{M s}^{-1} \text{ agent}^{-1}$) the MIC of NB2030 begins to be limited by the efficacy of the activated triclosan, and the graphs of the two

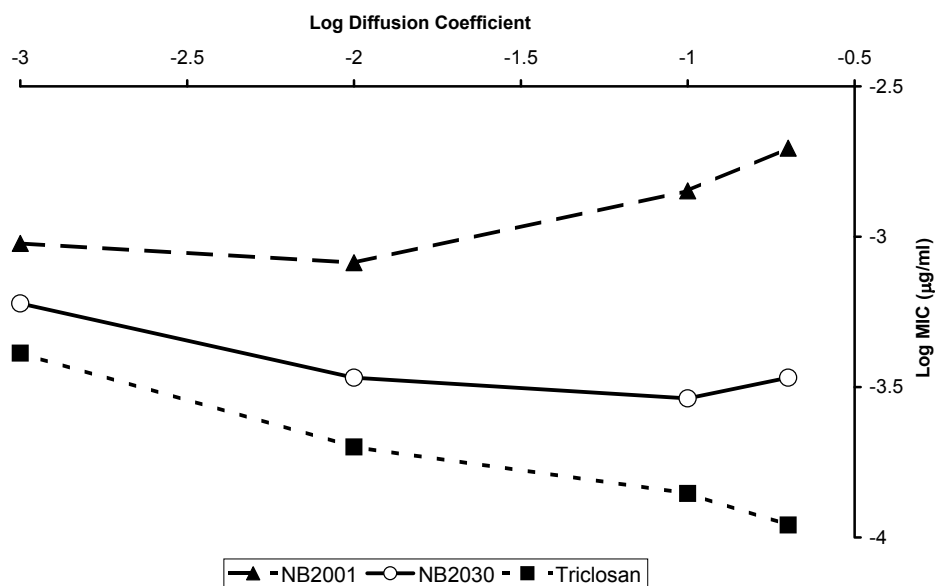


Figure 6.10: The user-defined diffusion coefficient for Fick's first law of diffusion was varied over the range 0.001 - 0.2 to assess the relative impact of diffusion rate on the minimum inhibitory concentration (MICs) of NB2001, NB2030 and triclosan against β -lactamase-producing *S. aureus* bacteria. Drug compounds added after 3.3 hours of incubation, during the exponential phase of bacterial growth.

pro-drugs start to converge.

Another important factor that can influence pro-drug activity is the diffusion rate in the environment. As discussed above, for the hypothetical penicillin-based pro-drug, this can have an important impact on pro-drug efficacy. Figure 6.10 shows the results of investigations on the effect it has on the MICs of the pro-drugs NB2001 and NB2030. For free triclosan, there is a significant negative correlation between the MIC and the diffusion coefficient of Fick's first law of diffusion ($r = -0.989$, $p = 0.011$). This is probably due to faster transport of antibiotic via diffusion processes to the interior of the colony resulting in better drug efficacy, or lower MIC (see Fig. 6.4B).

However, when triclosan is administered in pro-drug form (NB2001 and NB2030), there is no longer a significant negative correlation between the diffu-

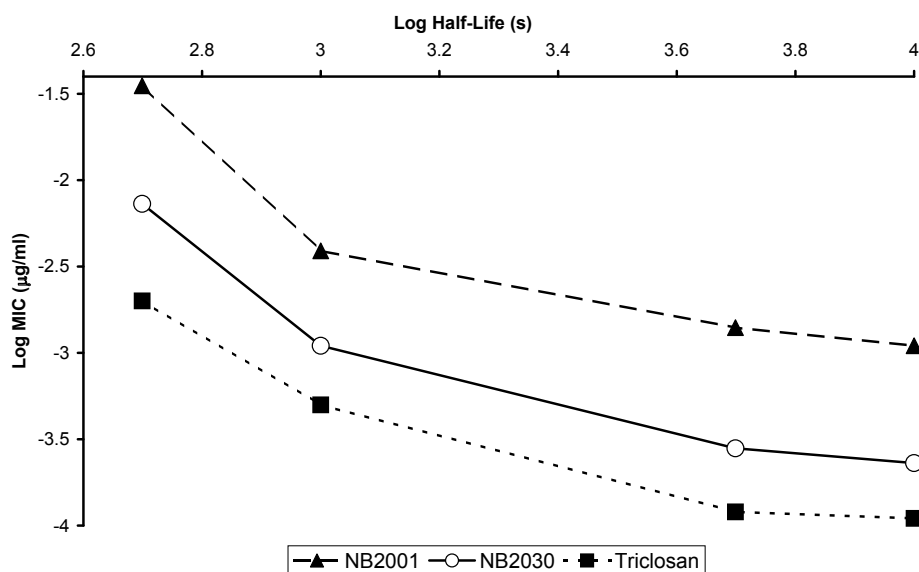


Figure 6.11: Predicted effect of varying the half-life on the minimum inhibitory concentrations (MICs) of NB2001 and NB2030, and triclosan against simulated β -lactamase-producing *S. aureus* bacteria in culture. Drug compounds were added after 3.3 hours of incubation, during the exponential phase of bacterial growth.

sion coefficient and the MIC (NB2001: $r=0.829$, $p=0.171$; NB2030: $r=-0.860$, $p=0.140$). In fact, for NB2001 there is evidence of a positive correlation, although it is not statistically significant. This may be because the increased diffusion rate results in dispersal of the activated antimicrobial agent from the vicinity of the bacterial cells (see Fig. 6.4A). The rate of β -lactamase-mediated activation of the pro-drugs in the vicinity of the colony could also be a limiting factor in this case. This is particularly evident with NB2001 because of the lower catalytic efficiency (compared to NB2030) of the β -lactamase enzyme at cleaving it.

Finally, the impact of the half-life on the efficacy of the pro-drugs was also investigated. For free triclosan, there is a significant negative correlation between the half-life and the MIC of the drug ($r=-0.961$, $p=0.039$). There is also a negative correlation between the half-lives of NB2001 and NB2030 and their MICs but it is

not statistically significant over the range of values tested (NB2001: $r = -0.914$, $p = 0.086$; NB2030: $r = -0.945$, $p = 0.055$). When the half-life of the pro-drug is below a certain threshold (in this case, approximately 1000 s), the pro-drug degrades before the concentration of activated antimicrobial agent can reach the minimum threshold for inhibition of growth (see Fig. 6.3). This threshold is influenced by the time it takes for induction of β -lactamase expression in the bacterial cells to take place.

6.4 Conclusions

The results presented here provide preliminary examinations of the pro-drug delivery system and how it influences the dynamics of bacterial growth and interactions with drug molecules. These initial investigations show that the enzyme-catalysed therapeutic activation (ECTA) pro-drug strategy represents a promising alternative approach for treating β -lactamase expressing resistant pathogens. There are distinct characteristics about the pro-drug system which distinguish it from the traditional antibiotic approach, and it is worthwhile to explore these differences in order to compare the strengths and weaknesses of each approach.

The dynamics of this system differ from the traditional β -lactam treatment strategy and therefore could result in contrasting selective pressure on the bacteria (i.e. selection against β -lactamase-producing strains of bacteria). However, a good theoretical understanding of the complex interactions involved must be developed in order to prevent rapid development of resistance to these new types of drugs as has occurred with many traditional antibiotics. This will require studies at various levels, from high level population-based mathematical studies to low-level agent-based models. However, as is the case for other antibiotics, these models require detailed

biological information about the cellular and molecular components of the system in order to correctly address the questions of how to optimize for treatment success.

Table 6.2: Inputted parameter values for simulations of pro-drug interactions with β -lactamase-producing *S. aureus* bacteria in Micro-Gen model. *b.u.* = biomass units; *loop* = program loop (~ 2 s in real time)

Type of Entity	Parameters (units)	Input Value
Environment	Patch area (<i>b.u.</i>)	20000
	Patch nutrient level (<i>b.u.</i>)	80000
	Diffusion co-efficient	0.1
Bacterial Cell	Generation time (<i>min</i>)	29
	Threshold for division (<i>b.u.</i>)	10000
	Nutrient intake (<i>b.u. loop</i> ⁻¹)	10.0
	Survival cost (<i>b.u. loop</i> ⁻¹)	0.2
	Stationary phase relative metabolic rate	0.2
	Lag phase length (<i>min</i>)	63
	β -lactamase production rate ($\mu M s^{-1}$):	
	Type A	3.28×10^{-7}
Type C	1.62×10^{-7}	
β -lactamase	β -lactamase production cost (<i>b.u.</i>)	0.1
	Molecular weight (<i>Da</i>)	30000
	Half-life (<i>s</i>)	53640
	k_{cat} (s^{-1}):	
	Penicillin-based pro-drug	171.0
	NB2001	1.01
	NB2030	30.8
	K_M (μM):	
	Penicillin G-based pro-drug	51.1
NB2001	6.3	
NB2030	20.0	
Activated Pro-Drugs	Half-life (<i>s</i>)	
	Hypothetical compound	2520
	Triclosan-equivalent	3600
	k_2 (s^{-1}):	
	Hypothetical compound	0.185
	Triclosan-equivalent	10.0
	K_d (μM):	
Hypothetical compound	1540	
Triclosan-equivalent	10.0	

CHAPTER 7

CONCLUSIONS AND FUTURE WORK

7.1 Summary and Conclusions

An agent-based model of bacteria-antibiotic interactions has been developed, which incorporates the antibiotic resistance mechanisms of MRSA bacteria. The model, called the Micro-Gen Bacterial Simulator, uses information about the cell biology of bacteria to produce global information about population growth in different environmental conditions (Chap. 3). It facilitates a detailed systems-level investigation of the dynamics involved in bacteria-antibiotic interactions and a means to relate this information to traditional high-level properties such as the Minimum Inhibitory Concentration (MIC) of an antibiotic (Chaps. 4 - 5).

The individual bacteria are represented by software agents that store physical traits of the cells as well as behavioural rules associated with them. The culture environment is represented by a discrete, two-dimensional grid containing diffusible elements such as nutrients, enzymes and antibiotics. Micro-Gen is also designed to take advantage of high performance computing resources by including an implementation of the Message Passing Interface (MPI) for running in parallel on multiple computers.

The model is highly adaptable and capable of being scaled up from lightweight portable devices to high performance parallel computing machines. The user can input parameters applicable to different species of bacteria by modifying low-level cellular attributes such as size, growth rate, motility etc. However, as shown here, it can also be adapted to incorporate detailed representations of specific antibiotic-resistance strategies such as those employed by MRSA.

The two main resistance strategies against β -lactam antibiotics employed by MRSA were incorporated into the model: β -lactamase enzymes which hydrolytically cleave antibiotic molecules, and penicillin-binding proteins (PBP2a) with reduced binding affinities for antibiotics. In order to quantify the efficacy of the antibiotics at inhibiting cell division, kinetic parameters describing the reactions between antibiotics and PBP2a in the cell and β -lactamase cleavage of antibiotics were derived from biological literature.

Tests with common β -lactam antibiotics indicate that the model can be used to generate quantitatively accurate predictions of dosage requirements for antibiotics against different strains of MRSA from basic cellular and biochemical information. Furthermore, by varying key parameters in the model the relative impact of different kinetic parameters associated with the two resistance mechanisms to β -lactam antibiotics were investigated. The model has also been used to investigate the system dynamics taking place within a population of bacteria. By varying properties such as the diffusion rate, population size, β -lactamase production rate or antibiotic half-life, the effects of these parameters on treatment response could be examined.

Traditional methods of measuring antibiotic efficacy such as the Minimum Inhibitory Concentration are insufficient for understanding the complex dynamics that lead to the rapid development and spread of antibiotic resistance within bacterial populations. However, the ability to investigate the relationship between individ-

ual molecular components of the system and the overall treatment outcome can lead to a better understanding of how to optimize antibiotic performance and predict treatment outcome. The agent-based modelling approach represents another computational tool set, in addition to existing pharmacokinetic-pharmacodynamic mathematical models, for assessing the efficacy of novel drug compounds. Micro-Gen can also be used to indicate evolutionary pathways or dead-ends that may exist for bacteria in response to antibiotic exposure.

The model can also be extended to represent new classes of antimicrobial agents and strategies for treating resistant bacteria. For example, the model has been used to examine the system dynamics involved in the enzyme-catalysed therapeutic activation (ECTA) pro-drug strategy for treating antibiotic resistant bacteria (Chap. 6). This involves the application of a substrate-like pro-drug molecule containing the β -lactam ring structure, which undergoes therapeutic activation catalysed by β -lactamase enzymes to achieve selective release of a cytotoxic antimicrobial agent. The model was used to examine the dynamics of this system of activation and assess its therapeutic potential from a theoretical standpoint.

7.2 Future Work

Micro-Gen can be used to test hypothetical scenarios by varying the parameters of existing antibiotics to explore how potential novel compounds might act. It is a useful tool for the rapid screening of drug compounds against a diverse range of *S. aureus* strains in simulated culture conditions. Future work could also include using the model to investigate the system dynamics of combination therapy with multiple classes of antibiotic. The agent-based approach is also suitable for modelling the evolution of antibiotic resistance over time by incorporating genetic components

into the bacterial agents. This would allow both the temporal and spatial dynamics of antibiotic resistance development to be examined.

Another important development of the model would be to expand the environment to represent three-dimensional space in order to model more complex spatially structured microbial communities such as biofilms. Biofilms are complex aggregations of microbial cells that are characterised by their genetic diversity, structural heterogeneity and complex cellular interactions. In these structured communities, there can be highly heterogeneous localised niches where the chemistry varies dramatically over small distances. The agent-based approach is a powerful tool for modelling interactions within a heterogeneous environment since the parameters for the simulation are defined at the individual level.

Bacteria communicate with one another within biofilms in a process known as quorum sensing, using chemical signalling molecules called auto-inducers. This cell-to-cell communication allows a population of bacteria to coordinate the gene expression, and therefore the behaviour, of the group. When bacteria exist in spatially structured communities, the cell numbers can reach sufficiently high numbers to induce a quorum sensing response. In the case of *S. aureus* bacteria, the change from a commensal, non-invasive state to a pathogenic state is mediated by signalling peptides that are part of the quorum sensing response.

The concentration of signals in a community is influenced by the production rate and half-life of the signal molecule, the diffusion properties of the signal and external hydrodynamic conditions. Micro-Gen already has systems to model these properties with respect to free molecules (e.g. nutrients, enzymes, antibiotics) in the environment. A diffusion algorithm implementing Fick's First Law of diffusion dictates the movement of molecules in the simulated environment. This will need to be adapted and expanded to represent the more complex dynamics within the highly

structured organisation of a biofilm community. This could be achieved by incorporating a more complex hydrodynamics algorithm to represent the flow of nutrients and other molecules within the colony. The model represents a robust foundation on which to build more complex models of real-world microbial communities such as these.

BIBLIOGRAPHY

- [1] S. R. Norris, C. W. Stratton, and D. S. Kernodle, "Production of a and c variants of staphylococcal beta-lactamase by methicillin-resistant strains of *Staphylococcus aureus*," *Antimicrobial Agents and Chemotherapy*, vol. 38, no. 7, pp. 1649–1650, Jul 1994.
- [2] F. Malouin, J. Blais, S. Chamberland, M. Hoang, C. Park, C. Chan, K. Mathias, S. Hakem, K. Dupree, E. Liu, T. Nguyen, and M. N. Dudley, "Rwj-54428 (mc-02,479), a new cephalosporin with high affinity for penicillin-binding proteins, including pbp 2a, and stability to staphylococcal beta-lactamases," *Antimicrobial Agents and Chemotherapy*, vol. 47, no. 2, pp. 658–664, Feb 2003.
- [3] K. Miller, C. Storey, W. J. Stubbings, A. M. Hoyle, J. K. Hobbs, and I. Chopra, "Antistaphylococcal activity of the novel cephalosporin cb-181963 (cab-175)," *The Journal of Antimicrobial Chemotherapy*, vol. 55, no. 4, pp. 579–582, Apr 2005.
- [4] D. J. Diekema, S. L. Coffman, S. A. Marshall, M. L. Beach, K. V. Rolston, and R. N. Jones, "Comparison of activities of broad-spectrum beta-lactam compounds against 1,128 gram-positive cocci recently isolated in cancer treatment centers," *Antimicrobial Agents and Chemotherapy*, vol. 43, no. 4, pp. 940–943, Apr 1999.

- [5] A. Lozniewski, C. Lion, F. Mory, and M. Weber, "In vitro synergy between cefepime and vancomycin against methicillin-susceptible and -resistant *Staphylococcus aureus* and *Staphylococcus epidermidis*," *The Journal of Antimicrobial Chemotherapy*, vol. 47, no. 1, pp. 83–86, Jan 2001.
- [6] P. C. Fuchs, A. L. Barry, and S. D. Brown, "Comparative in vitro antimicrobial activity of a new carbapenem, e1010, and tentative disc diffusion test interpretative criteria," *The Journal of Antimicrobial Chemotherapy*, vol. 48, no. 1, pp. 23–28, Jul 2001.
- [7] C. J. Fernandes, L. A. Fernandes, P. Collignon, and A. G. on Antimicrobial Resistance, "Cefoxitin resistance as a surrogate marker for the detection of methicillin-resistant *Staphylococcus aureus*," *The Journal of Antimicrobial Chemotherapy*, vol. 55, no. 4, pp. 506–510, Apr 2005.
- [8] Q. Li, J. Y. Lee, R. Castillo, M. S. Hixon, C. Pujol, V. R. Doppalapudi, H. M. Shepard, G. M. Wahl, T. J. Lobl, and M. F. Chan, "Nb2001, a novel antibacterial agent with broad-spectrum activity and enhanced potency against beta-lactamase-producing strains," *Antimicrobial Agents and Chemotherapy*, vol. 46, no. 5, pp. 1262–1268, May 2002.
- [9] D. Skinner and C. S. Keefer, "Significance of bacteremia caused by *Staphylococcus aureus*," *Archives of Internal Medicine*, vol. 68, pp. 851–875, 1941.
- [10] E. Chain, H. W. Florey, M. B. Adelaide, A. D. Gardner, N. G. Heatley, M. A. Jennings, J. Orr-Ewing, and A. G. Sanders, "Penicillin as a chemotherapeutic agent. 1940," *Clinical Orthopaedics and Related Research*, vol. 295, pp. 3–7, Oct 1993.

- [11] S. B. Levy and B. Marshall, “Antibacterial resistance worldwide: causes, challenges and responses,” *Nature Medicine*, vol. 10, no. 12 Suppl, pp. S122–9, Dec 2004.
- [12] H. C. Neu, “The crisis in antibiotic resistance,” *Science*, vol. 257, no. 5073, pp. 1064–1073, Aug 21 1992.
- [13] P. G. Ambrose, S. M. Bhavnani, C. M. Rubino, A. Louie, T. Gumbo, A. Forrest, and G. L. Drusano, “Pharmacokinetics-pharmacodynamics of antimicrobial therapy: it’s not just for mice anymore,” *Clinical Infectious Diseases*, vol. 44, no. 1, pp. 79–86, Jan 1 2007.
- [14] A. M. Lacasta, I. R. Cantalapiedra, C. E. Auguet, A. Penaranda, and L. Ramirez-Piscina, “Modeling of spatiotemporal patterns in bacterial colonies,” *Physical Review. E, Statistical Physics, Plasmas, Fluids, and Related Interdisciplinary Topics*, vol. 59, no. 6, pp. 7036–7041, Jun 1999.
- [15] D. A. Devine, “Cationic antimicrobial peptides in regulation of commensal and pathogenic microbial populations,” *Mammalian Host Defense Peptides*, pp. 9–39, 2004.
- [16] R. Walshe, “Modelling bacterial growth patterns in the presence of antibiotic,” in *Proceedings of the 11th IEEE International Conference on Engineering of Complex Computer Systems*. Washington, DC, USA: IEEE Computer Society, 15-17 August 2006, pp. 177–188.
- [17] J. T. Murphy and R. Walshe, “Micro-gen: An agent-based model of bacteria-antibiotic interactions in batch culture,” in *Proceedings of the 20th Annual European Simulation and Modelling Conference*. Eurosis-ETI, October 23-25, 2006 2006, pp. 239–242.

- [18] J. T. Murphy, R. Walshe, and M. Devocelle, “Agent-based model of methicillin-resistant *Staphylococcus aureus* and antibiotics in batch culture,” in *Proceedings of 21st Annual European Simulation and Modelling Conference*. Eurosis-ETI, October 20-22, 2007 2007, pp. 409–414.
- [19] D. J. Zygmunt, C. W. Stratton, and D. S. Kernodle, “Characterization of four beta-lactamases produced by *Staphylococcus aureus*,” *Antimicrobial Agents and Chemotherapy*, vol. 36, no. 2, pp. 440–445, Feb 1992.
- [20] W. P. Lu, Y. Sun, M. D. Bauer, S. Paule, P. M. Koenigs, and W. G. Kraft, “Penicillin-binding protein 2a from methicillin-resistant *Staphylococcus aureus*: kinetic characterization of its interactions with beta-lactams using electrospray mass spectrometry,” *Biochemistry*, vol. 38, no. 20, pp. 6537–6546, May 18 1999.
- [21] H. Kitano, “Computational systems biology,” *Nature (Lond.)*, vol. 420, no. 6912, pp. 206–210, Nov 14 2002.
- [22] V. Grimm, “Ten years of individual-based modelling in ecology: what have we learned and what could we learn in the future?” *Ecological Modelling*, vol. 115, no. 2-3, pp. 129–148, 2/15 1999.
- [23] W. Materi and D. S. Wishart, “Computational systems biology in drug discovery and development: methods and applications,” *Drug Discovery Today*, vol. 12, no. 7-8, pp. 295–303, Apr 2007.
- [24] M. J. Grimson and G. C. Barker, “Continuum model for the spatiotemporal growth of bacterial colonies,” *Physical Review. E, Statistical Physics, Plasmas, Fluids, and Related Interdisciplinary Topics*, vol. 49, no. 2, pp. 1680–1684, Feb 1994.

- [25] M. Peleg, D. Rubin, and R. B. Altman, "Using petri net tools to study properties and dynamics of biological systems," *Journal of the American Medical Informatics Association*, vol. 12, no. 2, pp. 181–199, Mar-Apr 2005.
- [26] M. Gardner, "Mathematical games: The fantastic combinations of john conways new solitaire game life," *Scientific American*, vol. 223, no. 4, pp. 120–123, 1970.
- [27] D. S. Wishart, R. Yang, D. Arndt, P. Tang, and J. Cruz, "Dynamic cellular automata: an alternative approach to cellular simulation," *In Silico Biology*, vol. 5, no. 2, pp. 139–161, 2005.
- [28] L. B. Kier, C. K. Cheng, B. Testa, and P. A. Carrupt, "A cellular automata model of enzyme kinetics," *Journal of Molecular Graphics*, vol. 14, no. 4, pp. 227–31, 226, Aug 1996.
- [29] R. M. Z. dos Santos and S. Coutinho, "Dynamics of hiv infection: a cellular automata approach," *Physical Review Letters*, vol. 87, no. 16, p. 168102, Oct 15 2001.
- [30] E. Ben-Jacob, O. Schochet, A. Tenenbaum, I. Cohen, A. Czirok, and T. Vicsek, "Generic modelling of cooperative growth patterns in bacterial colonies," *Nature (Lond.)*, vol. 368, no. 6466, pp. 46–49, Mar 3 1994.
- [31] M. Ginovart, D. Lopez, and J. Valls, "Indisim, an individual-based discrete simulation model to study bacterial cultures," *Journal of Theoretical Biology*, vol. 214, no. 2, pp. 305–319, Jan 21 2002.

- [32] J. U. Kreft, G. Booth, and J. W. Wimpenny, “Bacsim, a simulator for individual-based modelling of bacterial colony growth,” *Microbiology*, vol. 144, no. 12, pp. 3275–3287, Dec 1998.
- [33] S. J. Pirt, “A kinetic study of the mode of growth of surface colonies of bacteria and fungi,” *Journal of General Microbiology*, vol. 47, no. 2, pp. 181–197, May 1967.
- [34] J. U. Kreft, C. Picioreanu, J. W. Wimpenny, and M. C. van Loosdrecht, “Individual-based modelling of biofilms,” *Microbiology*, vol. 147, no. 11, pp. 2897–2912, Nov 2001.
- [35] C. Picioreanu, M. C. van Loosdrecht, and J. J. Heijnen, “A new combined differential-discrete cellular automaton approach for biofilm modeling: application for growth in gel beads,” *Biotechnology and Bioengineering*, vol. 57, no. 6, pp. 718–731, Mar 20 1998.
- [36] K. Grijspeerdt, J. U. Kreft, and W. Messens, “Individual-based modelling of growth and migration of salmonella enteritidis in hens’ eggs,” *International Journal of Food Microbiology*, vol. 100, no. 1-3, pp. 323–333, Apr 15 2005.
- [37] E. J. Dens, K. Bernaerts, A. R. Standaert, and J. F. V. Impe, “Cell division theory and individual-based modeling of microbial lag: part i. the theory of cell division,” *International Journal of Food Microbiology*, vol. 101, no. 3, pp. 303–318, Jun 15 2005.
- [38] E. J. Dens, K. Bernaerts, A. R. Standaert, J. U. Kreft, and J. F. V. Impe, “Cell division theory and individual-based modeling of microbial lag: part ii. modeling lag phenomena induced by temperature shifts,” *International Journal of Food Microbiology*, vol. 101, no. 3, pp. 319–332, Jun 15 2005.

- [39] M. Ginovart, D. Lopez, J. Valls, and M. Silbert, "Individual based simulations of bacterial growth on agar plates," *Physica A: Statistical Mechanics and its Applications*, vol. 305, no. 3-4, pp. 604–618, 3/15 2002.
- [40] C. Prats, D. Lopez, A. Giro, J. Ferrer, and J. Valls, "Individual-based modelling of bacterial cultures to study the microscopic causes of the lag phase," *Journal of Theoretical Biology*, vol. 241, no. 4, pp. 939–953, Aug 21 2006.
- [41] C. Prats, A. Giro, J. Ferrer, D. Lopez, and J. Vives-Rego, "Analysis and ibm simulation of the stages in bacterial lag phase: Basis for an updated definition," *Journal of Theoretical Biology*, Jan 31 2008.
- [42] M. Ginovart, D. Lopez, and A. Gras, "Individual-based modelling of microbial activity to study mineralization of c and n and nitrification process in soil," *Nonlinear Analysis: Real World Applications*, vol. 6, no. 4, pp. 773–795, 9 2005.
- [43] R. Gregory, J. R. Saunders, and V. A. Saunders, "The paton individual-based model legacy," *Bio Systems*, vol. 85, no. 1, pp. 46–54, Jul 2006.
- [44] C. Vlachos, R. Gregory, R. C. Paton, J. R. Saunders, and Q. H. Wu, "Individual-based modelling of bacterial ecologies and evolution," *Comparative and Functional Genomics*, vol. 5, no. 1, pp. 100–104, 2004.
- [45] R. Paton, R. Gregory, C. Vlachos, J. Saunders, and H. Wu, "Evolvable social agents for bacterial systems modeling," *IEEE Trans. Nanobioscience*, vol. 3, no. 3, pp. 208–216, Sep 2004.

- [46] L. R. Johnson, "Microcolony and biofilm formation as a survival strategy for bacteria," *Journal of Theoretical Biology*, vol. 251, no. 1, pp. 24–34, Mar 7 2008.
- [47] W. M. M. Kirby, "Extraction of a highly potent penicillin inactivator from penicillin resistant staphylococci," *Science*, vol. 99, no. 2579, pp. 452–453, June 2 1944.
- [48] C. C. Fuda, J. F. Fisher, and S. Mobashery, "Beta-lactam resistance in *Staphylococcus aureus*: the adaptive resistance of a plastic genome," *Cellular and Molecular Life Sciences*, vol. 62, no. 22, pp. 2617–2633, Nov 2005.
- [49] P. Giesbrecht, T. Kersten, H. Maidhof, and J. Wecke, "Staphylococcal cell wall: morphogenesis and fatal variations in the presence of penicillin," *Microbiology and Molecular Biology Reviews*, vol. 62, no. 4, pp. 1371–1414, Dec 1998.
- [50] G. J. Moran, A. Krishnadasan, R. J. Gorwitz, G. E. Fosheim, L. K. McDougal, R. B. Carey, D. A. Talan, and E. I. N. S. Group, "Methicillin-resistant *S. aureus* infections among patients in the emergency department," *The New England Journal of Medicine*, vol. 355, no. 7, pp. 666–674, Aug 17 2006.
- [51] E. Y. Furuya and F. D. Lowy, "Antimicrobial-resistant bacteria in the community setting," *Nature Reviews Microbiology*, vol. 4, no. 1, pp. 36–45, Jan 2006.
- [52] G. D. Wright, "The antibiotic resistome: the nexus of chemical and genetic diversity," *Nature Reviews Microbiology*, vol. 5, no. 3, pp. 175–186, Mar 2007.

- [53] C. Walsh, "Molecular mechanisms that confer antibacterial drug resistance," *Nature (Lond.)*, vol. 406, no. 6797, pp. 775–781, Aug 17 2000.
- [54] J. F. Fisher, S. O. Meroueh, and S. Mobashery, "Bacterial resistance to beta-lactam antibiotics: compelling opportunism, compelling opportunity," *Chemical Reviews*, vol. 105, no. 2, pp. 395–424, Feb 2005.
- [55] E. P. Abraham and E. Chain, "An enzyme from bacteria able to destroy penicillin," *Nature (Lond.)*, vol. 146, p. 837, 1940.
- [56] A. Bondi and C. C. Dietz, "Penicillin resistant staphylococci," *Proceedings of the Society for Experimental Biology and Medicine*, vol. 60, no. 1, pp. 55–58, 1945.
- [57] D. S. Wishart, C. Knox, A. C. Guo, S. Shrivastava, M. Hassanali, P. Stothard, Z. Chang, and J. Woolsey, "Drugbank: a comprehensive resource for in silico drug discovery and exploration," *Nucleic Acids Research*, vol. 34, no. Database issue, pp. D668–72, Jan 1 2006.
- [58] R. P. Ambler, "The amino acid sequence of *Staphylococcus aureus* penicillinase," *The Biochemical Journal*, vol. 151, no. 2, pp. 197–218, Nov 1975.
- [59] R. A. Lewis, S. P. Curnock, and K. G. Dyke, "Proteolytic cleavage of the repressor (blai) of beta-lactamase synthesis in *Staphylococcus aureus*," *FEMS Microbiology Letters*, vol. 178, no. 2, pp. 271–275, Sep 15 1999.
- [60] J. B. Nielsen and J. O. Lampen, "Membrane-bound penicillinases in gram-positive bacteria," *The Journal of Biological Chemistry*, vol. 257, no. 8, pp. 4490–4495, Apr 25 1982.

- [61] H. Z. Zhang, C. J. Hackbarth, K. M. Chansky, and H. F. Chambers, "A proteolytic transmembrane signaling pathway and resistance to beta-lactams in staphylococci," *Science*, vol. 291, no. 5510, pp. 1962–1965, Mar 9 2001.
- [62] B. G. Hall, "Predicting the evolution of antibiotic resistance genes," *Nature Reviews Microbiology*, vol. 2, no. 5, pp. 430–435, May 2004.
- [63] K. R. Eriksen, "Celbenin-resistant staphylococci." *Ugeskrift for laeger*, vol. 123, pp. 384–386, Mar 17 1961.
- [64] Y. Katayama, T. Ito, and K. Hiramatsu, "A new class of genetic element, staphylococcus cassette chromosome mec, encodes methicillin resistance in *Staphylococcus aureus*," *Antimicrobial Agents and Chemotherapy*, vol. 44, no. 6, pp. 1549–1555, Jun 2000.
- [65] T. Ito, X. X. Ma, F. Takeuchi, K. Okuma, H. Yuzawa, and K. Hiramatsu, "Novel type v staphylococcal cassette chromosome mec driven by a novel cassette chromosome recombinase, ccrc," *Antimicrobial Agents and Chemotherapy*, vol. 48, no. 7, pp. 2637–2651, Jul 2004.
- [66] D. A. Robinson and M. C. Enright, "Evolutionary models of the emergence of methicillin-resistant *Staphylococcus aureus*," *Antimicrobial Agents and Chemotherapy*, vol. 47, no. 12, pp. 3926–3934, Dec 2003.
- [67] K. Okuma, K. Iwakawa, J. D. Turnidge, W. B. Grubb, J. M. Bell, F. G. O'Brien, G. W. Coombs, J. W. Pearman, F. C. Tenover, M. Kapi, C. Tiensasitorn, T. Ito, and K. Hiramatsu, "Dissemination of new methicillin-resistant *Staphylococcus aureus* clones in the community," *Journal of Clinical Microbiology*, vol. 40, no. 11, pp. 4289–4294, Nov 2002.

- [68] W. A. Craig, "Pharmacokinetic/pharmacodynamic parameters: rationale for antibacterial dosing of mice and men," *Clinical Infectious Diseases*, vol. 26, no. 1, pp. 1–10; quiz 11–2, Jan 1998.
- [69] R. R. Regoes, C. Wiuff, R. M. Zappala, K. N. Garner, F. Baquero, and B. R. Levin, "Pharmacodynamic functions: a multiparameter approach to the design of antibiotic treatment regimens," *Antimicrobial Agents and Chemotherapy*, vol. 48, no. 10, pp. 3670–3676, Oct 2004.
- [70] S. Dutta, Y. Matsumoto, and W. F. Ebling, "Is it possible to estimate the parameters of the sigmoid emax model with truncated data typical of clinical studies?" *Journal of Pharmaceutical Sciences*, vol. 85, no. 2, pp. 232–239, Feb 1996.
- [71] N. H. Holford and L. B. Sheiner, "Pharmacokinetic and pharmacodynamic modeling in vivo," *Critical Reviews in Bioengineering*, vol. 5, no. 4, pp. 273–322, 1981.
- [72] D. Czock and F. Keller, "Mechanism-based pharmacokinetic-pharmacodynamic modeling of antimicrobial drug effects," *Journal of Pharmacokinetics and Pharmacodynamics*, vol. 34, no. 6, pp. 727–751, Dec 2007.
- [73] M. Ender, N. McCallum, R. Adhikari, and B. Berger-Bachi, "Fitness cost of sccmec and methicillin resistance levels in *Staphylococcus aureus*," *Antimicrobial Agents and Chemotherapy*, vol. 48, no. 6, pp. 2295–2297, Jun 2004.
- [74] J. G. Mitchell and K. Kogure, "Bacterial motility: links to the environment and a driving force for microbial physics," *FEMS Microbiology Ecology*, vol. 55, no. 1, pp. 3–16, Jan 2006.

- [75] J. E. Segall, S. M. Block, and H. C. Berg, "Temporal comparisons in bacterial chemotaxis," *Proceedings of the National Academy of Sciences of the United States of America*, vol. 83, no. 23, pp. 8987–8991, Dec 1986.
- [76] H. F. Chambers, M. J. Sachdeva, and C. J. Hackbarth, "Kinetics of penicillin binding to penicillin-binding proteins of *Staphylococcus aureus*," *The Biochemical Journal*, vol. 301 (Pt 1), no. Pt 1, pp. 139–144, Jul 1 1994.
- [77] C. Fuda, M. Suvorov, S. B. Vakulenko, and S. Mobashery, "The basis for resistance to beta-lactam antibiotics by penicillin-binding protein 2a of methicillin-resistant *Staphylococcus aureus*," *The Journal of Biological Chemistry*, vol. 279, no. 39, pp. 40 802–40 806, Sep 24 2004.
- [78] K. Graves-Woodward and R. F. Pratt, "Reaction of soluble penicillin-binding protein 2a of methicillin-resistant *Staphylococcus aureus* with beta-lactams and acyclic substrates: kinetics in homogeneous solution," *The Biochemical Journal*, vol. 332, no. 3, pp. 755–761, Jun 15 1998.
- [79] K. Bush, M. Macielag, and M. Weidner-Wells, "Taking inventory: antibacterial agents currently at or beyond phase 1," *Current Opinion in Microbiology*, vol. 7, no. 5, pp. 466–476, Oct 2004.
- [80] G. W. Stone, Q. Zhang, R. Castillo, V. R. Doppalapudi, A. R. Bueno, J. Y. Lee, Q. Li, M. Sergeeva, G. Khambatta, and N. H. Georgopapadakou, "Mechanism of action of nb2001 and nb2030, novel antibacterial agents activated by beta-lactamases," *Antimicrobial Agents and Chemotherapy*, vol. 48, no. 2, pp. 477–483, Feb 2004.
- [81] C. Slater-Radosti, G. V. Aller, R. Greenwood, R. Nicholas, P. M. Keller, W. E. D. Jr, F. Fan, D. J. Payne, and D. D. Jaworski, "Biochemical and ge-

- netic characterization of the action of triclosan on *Staphylococcus aureus*,” *The Journal of Antimicrobial Chemotherapy*, vol. 48, no. 1, pp. 1–6, Jul 2001.
- [82] L. L. Guan and K. Kamino, “Bacterial response to siderophore and quorum-sensing chemical signals in the seawater microbial community,” *BMC Microbiology*, vol. 1, p. 27, 2001.
- [83] I. A. Swinnen, K. Bernaerts, E. J. Dens, A. H. Geeraerd, and J. F. V. Impe, “Predictive modelling of the microbial lag phase: a review,” *International Journal of Food Microbiology*, vol. 94, no. 2, pp. 137–159, Jul 15 2004.
- [84] T. Nystrom, “Not quite dead enough: on bacterial life, culturability, senescence, and death,” *Archives of Microbiology*, vol. 176, no. 3, pp. 159–164, Sep 2001.
- [85] D. A. Siegele and R. Kolter, “Life after log,” *Journal of Bacteriology*, vol. 174, no. 2, pp. 345–348, Jan 1992.
- [86] M. J. Pucci and T. J. Dougherty, “Direct quantitation of the numbers of individual penicillin-binding proteins per cell in *Staphylococcus aureus*,” *Journal of Bacteriology*, vol. 184, no. 2, pp. 588–591, Jan 2002.
- [87] A. R. Horswill, P. Stoodley, P. S. Stewart, and M. R. Parsek, “The effect of the chemical, biological, and physical environment on quorum sensing in structured microbial communities,” *Analytical and Bioanalytical Chemistry*, vol. 387, no. 2, pp. 371–380, Jan 2007.
- [88] J. T. Murphy, R. Walshe, and M. Devocelle, “A computational model of antibiotic-resistance mechanisms in methicillin-resistant *Staphylococcus au-*

reus (MRSA),” *Journal of Theoretical Biology*, vol. 254, no. 2, pp. 284–293, Sep 21 2008.

- [89] J. H. Hewitt and M. T. Parker, “Sensitivity of penicillinase-forming strains of *Staphylococcus aureus* and of their penicillinase-negative variants to cephaloridine, cephalothin, methicillin, and benzylpenicillin,” *Journal of Clinical Pathology*, vol. 21, no. 1, pp. 75–84, Jan 1968.
- [90] L. D. Sabath, C. Garner, C. Wilcox, and M. Finland, “Effect of inoculum and of beta-lactamase on the anti-staphylococcal activity of thirteen penicillins and cephalosporins,” *Antimicrobial Agents and Chemotherapy*, vol. 8, no. 3, pp. 344–349, Sep 1975.
- [91] J. Rautio, H. Kumpulainen, T. Heimbach, R. Oliyai, D. Oh, T. Jarvinen, and J. Savolainen, “Prodrugs: design and clinical applications,” *Nature Reviews Drug discovery*, vol. 7, no. 3, pp. 255–270, Mar 2008.
- [92] T. P. Smyth, M. E. O’Donnell, M. J. O’Connor, and J. O. StLeger, “beta-lactamase-dependent prodrugs recent developments,” *Tetrahedron*, vol. 56, no. 31, pp. 5699–5707, 2000.
- [93] M. G. Escalada, A. D. Russell, J. Y. Maillard, and D. Ochs, “Triclosan-bacteria interactions: single or multiple target sites?” *Letters in Applied Microbiology*, vol. 41, no. 6, pp. 476–481, 2005.
- [94] R. D. Jones, H. B. Jampani, J. L. Newman, and A. S. Lee, “Triclosan: a review of effectiveness and safety in health care settings,” *American Journal of Infection Control*, vol. 28, no. 2, pp. 184–196, Apr 2000.

List of Publications

1. Murphy J.T., Walshe R. and Devocelle M.: “A Computational Model of Antibiotic-Resistance Mechanisms in Methicillin-Resistant *Staphylococcus aureus* (MRSA)”. *J. Theor. Biol.*, vol. 254, no. 2, pp. 284-293 (2008)
2. Murphy J.T., Walshe R. and Devocelle M.: “High-Performance Computing for Modelling Bacterial Communities”. *ERCIM News*, No. 74, pp.37-38 (2008)
3. Murphy J.T., Walshe R. and Devocelle M.: “A Novel Cellular Model of Methicillin-Resistant *S. aureus* (MRSA) for Predicting Antibiotic Susceptibility”. *Genomes 2008 conference* (Poster), April 8-11 2008, Institut Pasteur, Paris, France (2008)
4. Murphy J.T., Walshe R. and Devocelle M.: “An Agent Based Approach to Modelling Microbial Ecosystems”. *ERCIM News*, No. 73, pp.39-40 (2008)
5. Murphy J.T., Walshe R. and Devocelle M.: “Agent-Based Model of Methicillin-Resistant *Staphylococcus aureus* and Antibiotics in Batch Culture”. *Proc. of ESM'07 conference*, Eurosis-ETI, pp.409-414 (2007)
6. Murphy, J., Walshe, R.: “Micro-Gen: An agent-based model of bacteria-antibiotic interactions in batch culture”. *Proc. of 20th ESM'06 conference*, Eurosi-ETI, pp.239-242 (2006)